



**SMART FOOD WASTE RECYCLING SYSTEM
USING BLACK SOLDIER FLY LARVAE**

LIM YING MIN, ALICIA

INNOVATION & DESIGN PROGRAMME

NATIONAL UNIVERSITY OF SINGAPORE

2024

SMART FOOD WASTE RECYCLING SYSTEM

USING BLACK SOLDIER FLY LARVAE

LIM YING MIN, ALICIA

A THESIS SUBMITTED FOR THE DEGREE OF

BACHELOR OF ENGINEERING (MECHANICAL ENGINEERING)

INNOVATION & DESIGN PROGRAMME

NATIONAL UNIVERSITY OF SINGAPORE

DECLARATION

I hereby declare that this thesis is my original work and it has been written by me in its entirety.

I have duly acknowledged all the sources of information which have been used in this thesis.

A handwritten signature in black ink, appearing to read "Alicia".

LIM YING MIN, ALICIA

2 APRIL 2024

Acknowledgements

I would like to express my sincere gratitude to my supervisors, namely Dr. Elliot Law, Ms. Wong Kah Wei and Mr. Adrian Fuhrmann, as well as my fellow group members, whose constructive guidance, sharing of valuable knowledge and insightful suggestions have played a pivotal role throughout the duration of this year-long project.

Additionally, I would like to extend my appreciation to Singapore-ETH Centre for generously granting us access to their laboratory facilities. This access significantly aided my team in gaining a deeper understanding of black soldier flies, their capabilities and the environment requirements necessary for the effective bioconversion of food waste.

Lastly, I wish to thank the workshop staff who were always present to help me in my EG4301 journey. Special thanks to Mr. Hamilton Toh, Mr. Dickson Foo and Mr. Vincent Bay from the Central Workshops, as well as Mrs. Annie Tan and Mr. Alvin Poh from iDP Electronics Workshop, for their continuous guidance and patience which was indispensable for refining my design and prototyping effectively.

Table of Contents

DECLARATION	3
Acknowledgements	4
Summary	1
1 Introduction	2
1.1 Singapore's Food Waste Problem	2
1.2 Current Strategies To Manage Singapore's Food Waste	3
Current Strategy: Waste-To-Energy plant	3
Current Strategy: Homogeneous Food Waste Recycling	5
1.3 Potential Solutions to Manage Singapore's Food Waste	6
Potential Solution: Anaerobic Digestion	6
Potential Solution: Insects Bioconversion	7
1.4 Black Soldier Fly As A Food Waste Management Solution	9
1.4.1 Black Soldier Fly Life Cycle	9
1.4.2 Current Black Soldier Fly Food Waste Solutions	10
1.5 Project Objective	13
2 Our Solution	15
2.1 Food Waste Source	15
2.2 Decentralised Location	15
2.3 User Needs	16
2.4 Concept Design	17
2.5 Overall Design Specifications	21
2.6 Initial Sizing	22
2.6.1 Food waste bioconversion capacity	22
2.7 Scope of Work	24
3 Design Configurations and Simulation of Ventilation System	26
3.1 Design Configurations	28
3.2 Detailed Design of Ventilation System	30
3.2.1 Sizing and Selection of fan	31
3.2.2 Chimney sizing	35
3.3 Simulations	39
3.3.1 Airflow Simulation for Full-fan spacing Configuration	41
3.3.2 Airflow Simulation for Half-fan spacing Configuration	47
3.3.3 Airflow Simulation for Half-fan spacing Configuration with fan tubes	55
3.3.4 Simulation findings	58
4 Fabrication and Testing of Ventilation System	60
4.1 Fabrication of prototype	60

4.1.1 Walls of reactor	60
4.1.2 Chimney	62
4.1.3 Fan tube	63
4.2 Assembly	67
4.2.1 Assembly of full-fan spacing configuration	68
4.2.2 Assembly of half-fan spacing configuration	72
4.2.3 Assembly of half-fan spacing with fan tube configuration	73
4.3 Airflow Testing	74
4.3.1 Chimney outflow	75
4.3.2 Fan test	78
4.3.3 Individual tray airflow distribution	80
4.3.4 Airflow testing conclusion	82
5 Full System Testing	82
5.1 Preparation of Food Waste	83
5.2 Characterisation of food waste	91
5.3 Full System Test Setup	94
5.4 Test results	95
6 Conclusion and Future Work	96
6.1 Conclusion	96
6.2 Future Work	97
References	98
Appendix	102
Appendix A: Comparison between Food and Plastic Carbon emission when landfilled	102
Appendix B: Land Used for Singapore's Waste Management	102
Appendix C: CO ₂ Emission Due to Food Waste Generated	103
Appendix D: Applications of Anaerobic Digesters	104
Appendix E: Food Waste Management Transportation Carbon Emission	105
Appendix F: Concept Generation and Evaluation Matrix Table	109
Appendix G: User Insights and Design Specifications	121
Appendix H: Minimum air exchange capacity required of a food waste bioconversion using BSFL reactor	125
Appendix I: Derivation of Size Constraints	125
Appendix J : Derivations used for Sizing of our reactor	130
Appendix K : Evaluation Matrix Table of Ventilation System's 5 Design Configurations	131
Appendix L: Derivation of the required air exchange rate of our reactor	132
Appendix M: Average velocity of exit airflow for various configurations	133
Appendix N: Ventilation system testing - Chimney outflow results	136

Summary

Food waste is one of the top waste streams in Singapore and the amount of waste generated has been increasing significantly. However, current food waste management solutions deployed to manage Singapore's food waste lack effectiveness and sustainability. Hence, there is a need to devise an effective and sustainable solution to manage Singapore's large amounts of food waste. The use of black soldier fly larvae (BSFL) in managing food waste is a new food waste management method that is being explored. Due to the use of BSFL in food waste management being a new concept, the current work on it is very limited. The Singapore-ETH Centre (SEC) has been researching the use of BSFL in food waste management but is currently still limited to its laboratory scale and setting. Hence our project aims to leverage on SEC's understanding of BSFL in food waste management to design a solution that can potentially manage Singapore's food waste issue effectively and sustainably.

The ventilation system for the environment where BSFL bioconverts food waste is crucial in the success and optimisation of the bioconversion process, hence this report would explore ways to design, manufacture and test a ventilation system that can aid in optimising the bioconversion process.

1 Introduction

1.1 Singapore's Food Waste Problem

Food waste is one of the largest waste streams in Singapore and there has been a significant increase in food waste generated over the past decade [1], [2]. Additionally, the food waste recycling rate is very low [2], [3], [4]. It is considerably lower than Singapore's overall recycling rate as well as those of other top waste sources in Singapore, as shown in FIGURE 1.1 [2], [3], [4]. Moreover, TABLE 1.1 shows that recycling rate for food waste has remained relatively stagnant over the past five years [2], [3].

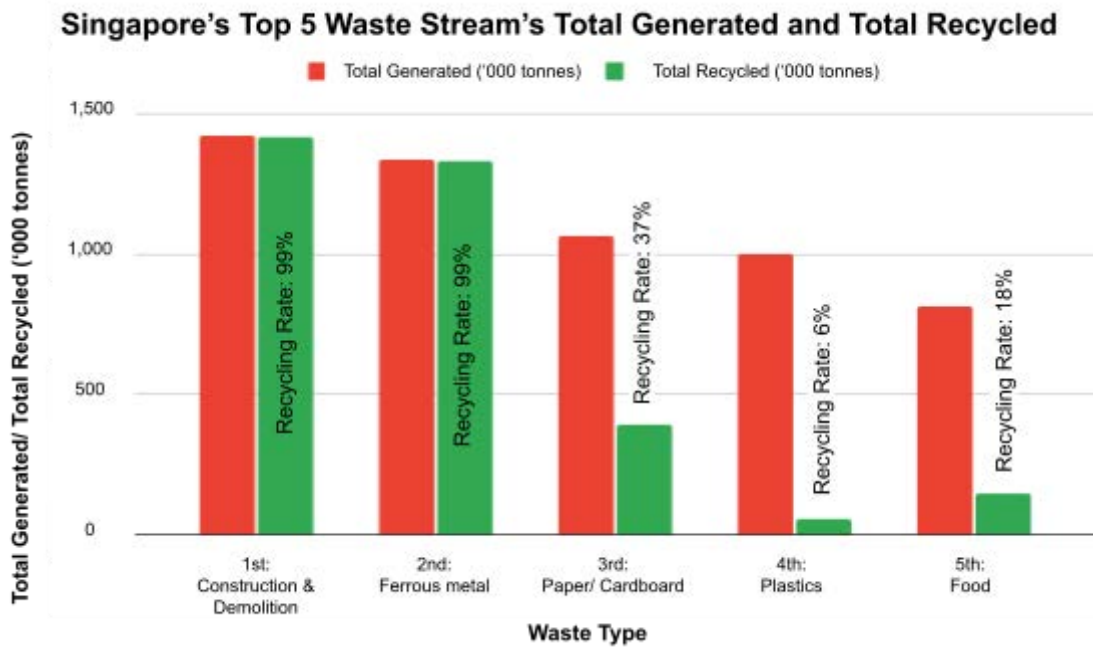


FIGURE 1.1: Singapore's Top 5 Waste Streams' Total Generated and Total Recycled [2]

TABLE 1.1: Singapore's Food Waste Recycling Rate from 2018 to 2022 [3]

Year	Food Waste Recycling Rate
2022	18%
2021	19%
2020	19%
2019	18%
2018	17%

Although FIGURE 1.1 portrays that more plastic waste is generated than food waste and it has an even lower recycling rate compared to food waste, food waste may have more detrimental effects on the environment compared to plastic waste [5]. Landfilling is a common waste management method deployed, and landfilling a kilogram of food waste produces the same carbon emission as landfilling 225kg of plastic bottles (Refer to Appendix A for derivation) [5], [6]. Thus, the large amounts of food waste generated and poor recycling rate of food waste, as well as its severe detrimental effects on the environment, makes food waste a significant problem. Hence it is important to employ effective means to manage Singapore's food waste.

1.2 Current Strategies To Manage Singapore's Food Waste

Currently, the usage of Waste-To-Energy plants to incinerate food waste and the recycling of homogeneous food waste are the two strategies deployed to manage Singapore's food waste.

Current Strategy: Waste-To-Energy plant

Waste-to-energy (WTE) plants, also known as incineration plants, is Singapore's current food waste management strategy that started its operations in 1979 [7]. Waste is collected and transported to WTE plants and then fed into the incinerator. During the incineration process, the heat released during combustion produces electricity. After incineration, the waste is reduced to ash, which is just 10% of its original volume. This ash will then be disposed at Semakau, Singapore's only landfill [8].

However, this measure is limited due to three main factors. Firstly, at the current rate of waste generation the landfill is projected to last only until 2035, earlier than its initial plan to last until 2045 [9]. FIGURE 1.2 shows the rapid rate at which the landfill is filling up.



FIGURE 1.2 Historical Satellite Views of Semakau Since the Start of Operations [10]

Secondly, this strategy occupies large designated lands in Singapore and strains Singapore's limited land resources. The current 374.4 ha of land designated for our four WTE plants and only landfill is equivalent to 524 football fields (Refer to Appendix B for derivation) [11], [12], [13], [14], [15], [16], [17].

Thirdly, WTE plants generate large amounts of carbon dioxide when incinerating food waste. The 2 million tonnes of carbon dioxide that was emitted due to the 813,000 tonnes of food waste generated in 2022 is equivalent to the carbon dioxide emitted to manufacture 363,000 cars (Refer to Appendix C for derivation) [2], [18], [19].

Current Strategy: Homogeneous Food Waste Recycling

Presently, most recycled food waste is homogeneous food waste from food manufacturers, such as spent yeast and grains from beer brewing. This homogeneous waste is sorted at the source and sold to recyclers for conversion to animal feed [20].

While this food waste management strategy may offer a sustainable solution tailored to Singapore's homogeneous waste, a large proportion of food waste generated in Singapore, such as households and food retail establishments, are heterogeneous rather than homogeneous waste. Consequently, only a limited amount of food waste can be managed by homogeneous food waste recycling. Therefore the efficacy of this strategy in addressing Singapore's food waste problem is limited [2], [20].

1.3 Potential Solutions to Manage Singapore's Food Waste

Due to the lack of effectiveness of the current food waste management solutions deployed in Singapore, other means of managing food waste are being explored.

Potential Solution: Anaerobic Digestion

One of the potential solutions is anaerobic digestion. It is a process in which bacteria break down organic materials and produce biogas and digestate, in the absence of oxygen. It occurs naturally, and the biogas produced can be used as an energy source while the digestate can potentially be used as fertilisers [21], [22].

Anaerobic digesters are mainly used in off-site centralised facilities, such as Singapore's developing Integrated Waste Management Facility (IWMF). However, such off-site centralised anaerobic digesters require large designated land allocated for them (Refer to Appendix D for more details) [23, p. 4].

While on-site applications of anaerobic digestion have been explored, they are still limited to pilot studies such as the anaerobic digester at East Coast Lagoon Food Village as shown in FIGURE 1.3 [1], [22], [24]. Although such digesters may be self-sufficient in its energy needs, its effectiveness in contributing to other power sources and the use of its digestate in closing the food waste loop would require further research and testing (Refer to Appendix D for more details) [22].



FIGURE 1.3: The anaerobic digester at the East Coast Lagoon Food Village [22]

Potential Solution: Insects Bioconversion

Another potential solution for food waste management is the use of insects at industrial scale. It is a viable method of closing the urban food system loop by converting otherwise lost nutrients from low-grade food waste back into biomass rich in proteins, fats, vitamins, and minerals [25], [26], [27]. This nutrient-rich biomass can potentially substitute traditional feed ingredients for agriculture, such as soybean and fishmeal, that negatively impact the climate and biodiversity. While the residual excrements from the insect's larvae, known as frass, can be processed into organic fertilisers [25], [26], [27], [28], [29].

Especially in import-reliant Singapore, where more than 90% of our food is imported, Singapore is susceptible to food supply shocks and disruptions [30]. With insects bioconverting food waste, this not only helps in Singapore's food waste management but the nutrient-rich feed and fertiliser can

also substitute imported feed for locally-grown animals and replace imported fertiliser. This reduces Singapore's reliance on imports to meet its nutritional needs and aids Singapore in achieving its 30 by 30 goal, which is to be able to produce 30% of its nutritional needs by 2030 while having less than 1% of land set aside for farming [30].

The most researched and popular insect species to produce animal feed from food waste are black soldier fly larvae (BSFL), house flies, mealworms, and crickets. BSFL is more efficient than other species used for bioconversion [31]. It allows 100% conversion of food waste into higher-value products. One of the two products is the BSFL. It is rich in protein and fats, making it a good animal feed. Moreover, its considerably low cost makes it an extremely profitable feed source compared to traditional animal feed [31], [32]. The other product is the residue that can be converted to organic fertilisers [31].

Given that the use of BSFL is more environmentally and economically-efficient than incineration and anaerobic digestion, and it allows the food system loop to be closed by bioconverting food waste into nutritional animal feed and fertilisers, the use of BSFL for food waste management is a promising solution that is worth investigating [2], [20], [26], [31].

1.4 Black Soldier Fly As A Food Waste Management Solution

For a better understanding of the potential use and effectiveness of using BSFL in Singapore's management of food waste, the black soldier fly life cycle and its applications in managing food waste would be presented in this chapter.

1.4.1 Black Soldier Fly Life Cycle

There are five main stages in a Black Soldier Fly (BSF) Life Cycle - Adult, Egg, Larval, Prepupal and Pupal stages as shown in FIGURE 1.4.1 [33]. When the BSF is in its larval stage, it feeds on waste. Food waste is a type of waste BSFL feeds on. After the feeding, the food waste is bioconverted into residue that has a volume of just 50% to 80% and mass of 80% of the original food waste [34], [35].

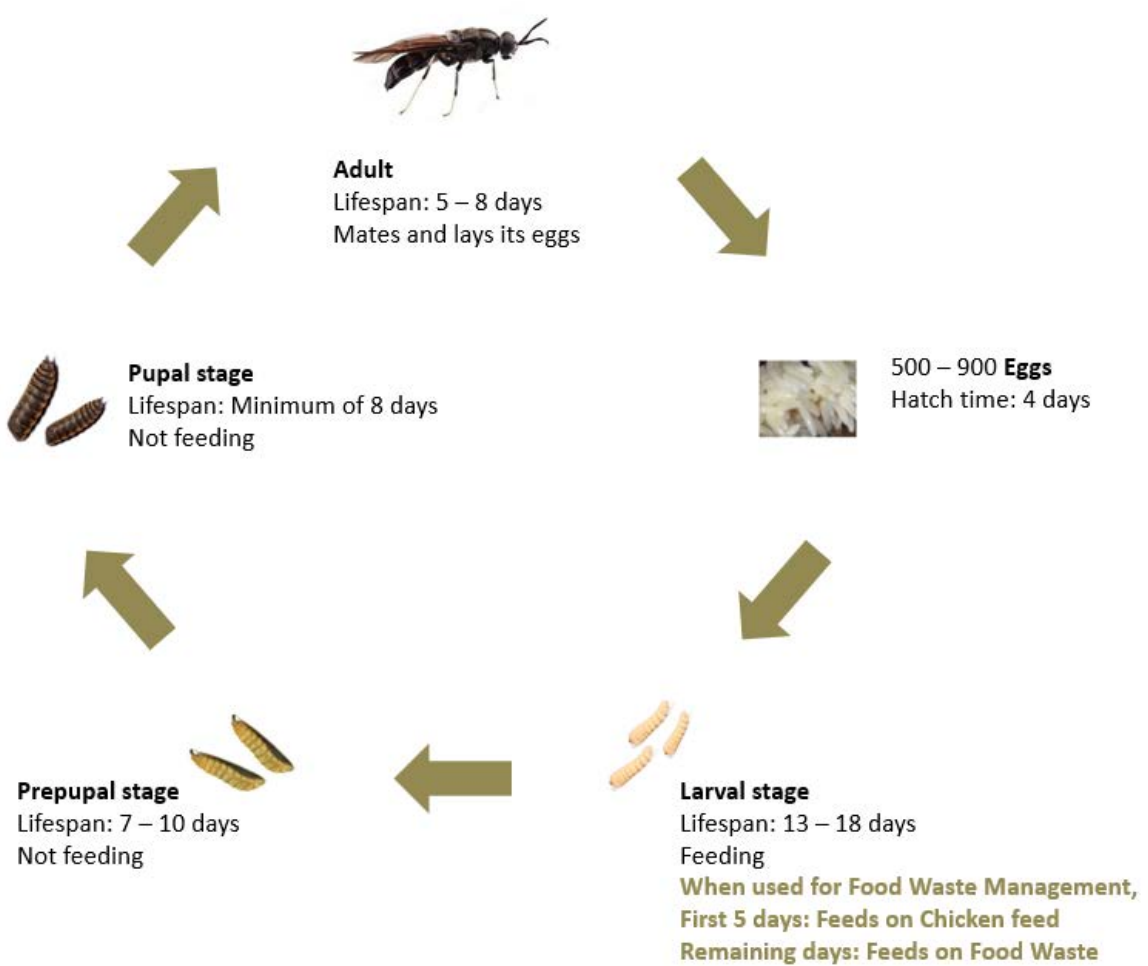


FIGURE 1.4.1: Black Soldier Fly Life Cycle. Adapted from [33]

1.4.2 Current Black Soldier Fly Food Waste Solutions

There are many international and local new-small-scale applications and laboratory research on using BSFL in food waste management including Insectta, TOGO and Singapore ETH Centre.

1. Insectta

Founded in 2018, Insectta is a Singapore startup that developed proprietary technologies to extract high-value biomaterials from the exoskeletons left behind by BSFL after the feeding.

One of the extracted biomaterials is Chitosan which can be used in skincare, biomedical as well as food and beverage industries. Another biomaterial extracted is Melanin, which can be used in organic electronics and biomedical industries [36], [37].

However, Insectta only valorises less than 0.02% of Singapore's food waste generated. Besides that, it only focuses on valorising homogeneous food waste and does not manage Singapore's heterogeneous food waste [2], [38].

2. TOGO

TOGO was established in 2008 in China, it is able to use BSFL to convert pre-consumer food waste into high-value animal feed, organic fertiliser or biofuel [39]. This is done by using a multi-processes large treatment facility as shown in FIGURE 1.4.2a. This measure has limited effectiveness in

managing Singapore's food waste as it specialises only on managing pre-consumer food waste and its ability to manage other food waste such as households' and food and beverage establishments' food wastes is not known.



FIGURE 1.4.2a: TOGO's Multi-Process Large BSFL - Food Waste Treatment Facility [39]

3. The Singapore-ETH Centre (SEC)

Using Black Soldier Flies in Food Waste Management and Sustainable Food Production in Urban Systems is a three-year research project by SEC, National University of Singapore, ETH Zurich and Nanyang Technological University Singapore. It aims to increase feasibility and sustainability of food production in Singapore by capturing value in food waste. The team plans to develop a model to integrate food waste management and sustainable food production in urban settings like Singapore using BSFL [40].

This SEC project does waste sourcing and has the complete BSFL treatment facility similar to the one shown in FIGURE 1.4.2b.

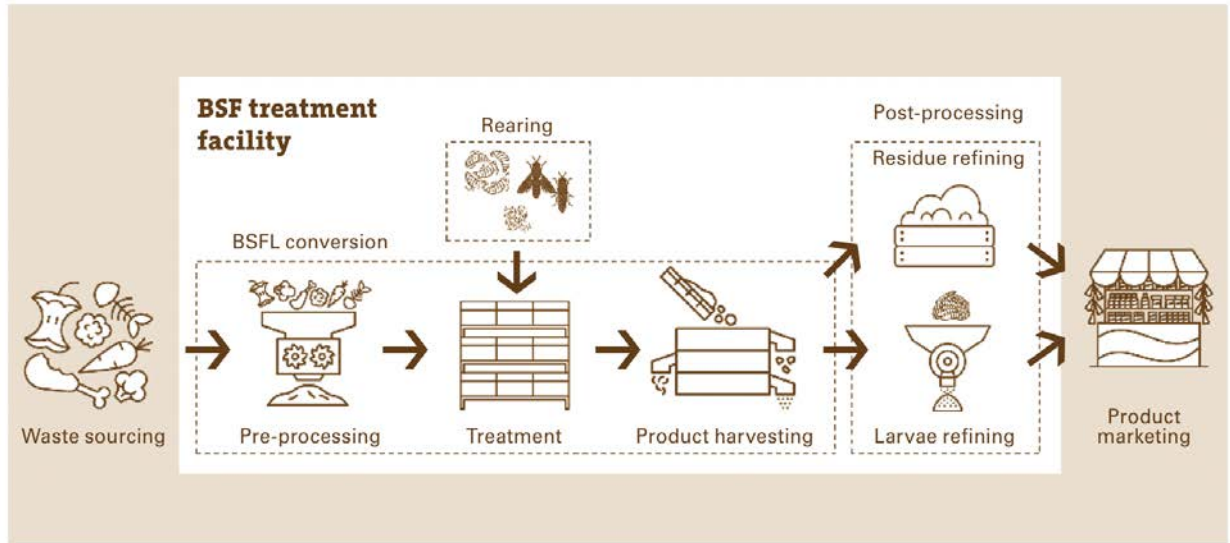


FIGURE 1.4.2b: Flow of Food Waste Management using BSF [35]

Although the SEC project shows a promising use of BSFL in food waste management, SEC has only conducted laboratory-setting investigations to manage 100 kg of food waste per day (A. Fuhrmann, Research student at SEC, personal communication, October 27, 2023) . Hence there is a need to look into issues and systems for the implementation of BSFL in food waste management at a larger scale, to manage the daily 2200 tonnes of food waste generated in Singapore [2].

1.5 Project Objective

Singapore generates both heterogeneous and homogeneous food waste, with the homogeneous food waste being managed by recycling, a sustainable and effective strategy. However, Singapore's heterogeneous food waste is currently managed unsustainably by incineration and landfilling as explained in the earlier sections [8], [20]. Hence, there is a dire need for the development of sustainable and effective food waste management solutions that can handle Singapore's large amounts of heterogeneous food waste.

The lack of effectiveness and sustainability of Singapore's current heterogeneous food waste management strategies, coupled with the potential capability of using BSFL for heterogeneous food waste management and the additional benefit of closing the food resource loop, there is a need to explore the development of an optimised BSFL-food waste management strategy that can handle Singapore's large amounts of heterogeneous food waste generated.

Additionally, the research on the bioconversion of heterogeneous food waste using BSFL that is being conducted by SEC shows the potential efficacy of BSFL in managing Singapore' food waste. However, its current applicability is limited by its laboratory-scale investigations and controlled environmental conditions. Therefore, there is a need to achieve greater success by bridging the gap of bioconverting food waste in laboratory-setting using BSFL to a scale large enough to manage Singapore's excessive amount of food waste.

Hence, our project aims to develop a solution that can manage the large amount of heterogeneous food waste that Singapore generates by collaborating with SEC to scale-up and optimise their current laboratory-setting of bioconversion of food waste using BSFL.

2 Our Solution

2.1 Food Waste Source

Our project will be focusing on heterogeneous food waste from large food establishments as they are one of the key sources of heterogeneous food waste in Singapore.

2.2 Decentralised Location

Larger food establishments with bin centres located near them would enable our solution to be deployed in a decentralised approach, which lowers the carbon footprint and reduces the need for large designated space for our BSFL food waste management solution for Singapore. A decentralised approach enables our solution to deploy a portable reactor that bioconverts food waste using BSFL, and be placed at available spaces in bin centres of food establishments.

Reduction in Carbon Emissions and Cost of Transportation

Decentralising the reactors by locating them near food waste sources would reduce the carbon emissions and cost of transporting food waste. Carbon emissions due to transportation for food waste management can potentially be reduced to a third when our solution is deployed instead of the current WTE strategy (Refer to Appendix E for derivation) [41], [42].

Reduction in need for large designated space

With a decentralised concept, our reactor can be located at spare spaces around the bin centres where food waste is usually disposed, reducing the need for land designated for a centralised food waste management facility in land-scarce Singapore. With a reduced need for designated land, scaling up of the usage of BSFL for food waste management would be more achievable in land-scarce Singapore.

2.3 User Needs

Based on our project objective, literature review and interview with SEC, the following user needs shown in TABLE 2.3 were noted down to help with our concept design.

TABLE 2.3: Our project's user needs

Category of User Needs	User Needs	Demand / Wish
Reactor's internal environmental and substrate conditions	The pH value of the substrate (feed) must be monitored and controlled for the survival of the BSFL and the optimisation of the bioconversion process [43].	Demand
	The moisture content in the substrate must be monitored and controlled for the survival of the BSFL and the optimisation of the bioconversion process [44], [45].	Demand
	The substrate temperature must be monitored and controlled for the survival of the BSFL and the optimisation of the bioconversion process [44].	Demand
	The air temperature in the reactor must be monitored and controlled for the survival of the BSFL and the optimisation of the bioconversion process [32], [46].	Demand
	The relative humidity of the air in the reactor must be monitored and controlled for the survival of the BSFL and the optimisation of the	Demand

	bioconversion process [32].	
	The concentration of CO ₂ , CH ₄ , NH ₃ must be monitored and controlled, excessive buildup of these gases can be toxic and suffocating to the BSFL (A. Fuhrmann, Research student at SEC, personal communication, August 18, 2023).	Demand
	Sufficient air exchange between the air in the reactor and the surrounding air to aid in maintaining suitable conditions for the BSFL survivability and effective bioconversion in the reactor (A. Fuhrmann, Research student at SEC, personal communication, August 18, 2023).	Demand
Mechanical Design	Current methods of loading and unloading of the food waste trays onto and off the bioconversion racks are very strenuous for the SEC researchers (A. Fuhrmann, Research student at SEC, personal communication, August 18, 2023).	Wish
	A portable reactor will enable easier implementation of an on-site reactor for food waste bioconversion using BSFL due to the smaller space each reactor occupies on-site and the ease of transport to the food waste source.	Wish

2.4 Concept Design

The selected concept, shown in FIGURE 2.4a, was selected from seven concepts that were generated based on the user needs and evaluated using an evaluation matrix (Refer to Appendix F for the concepts generated and evaluation matrix table). Our reactor is ventilated using fans that expels the internal air out into the surroundings from the top of the reactor, as shown in FIGURE 2.4a. While the steps to load and unload the food waste are explained in FIGURE 2.4b and FIGURE 2.4c, respectively.

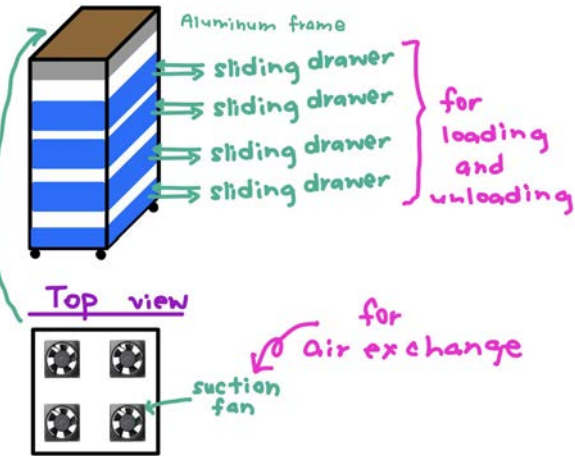


FIGURE 2.4a: Our selected concept

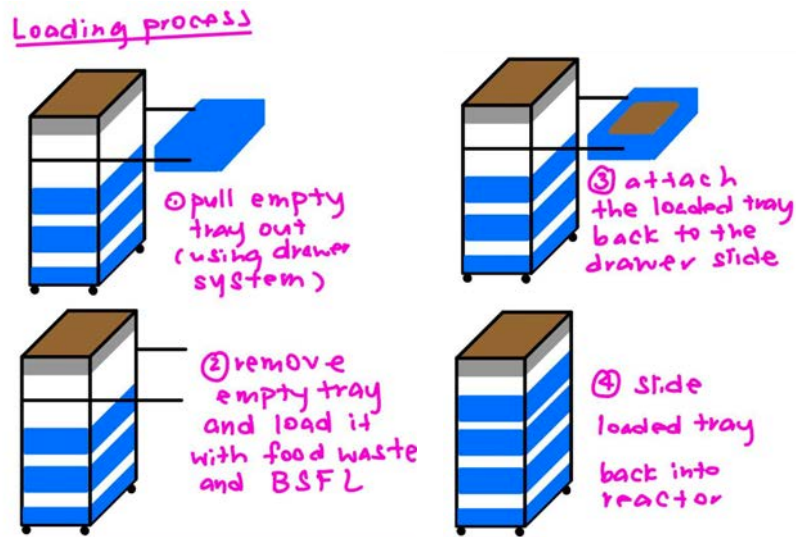


FIGURE 2.4b: Loading process

Unloading process

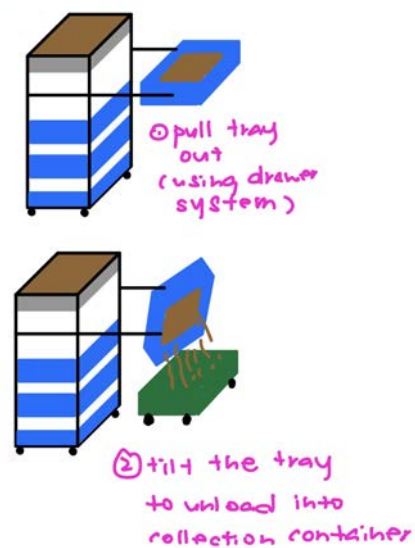


FIGURE 2.4c: Unloading process

Our reactors will be placed on-site as part of our decentralised approach. It will bioconvert heterogeneous food waste from food establishments, using BSFL via an optimised bioconversion process to tackle Singapore's heterogeneous food waste issue. The flow of the integration of our reactor into food establishments' food waste management is illustrated in FIGURE 2.4c.

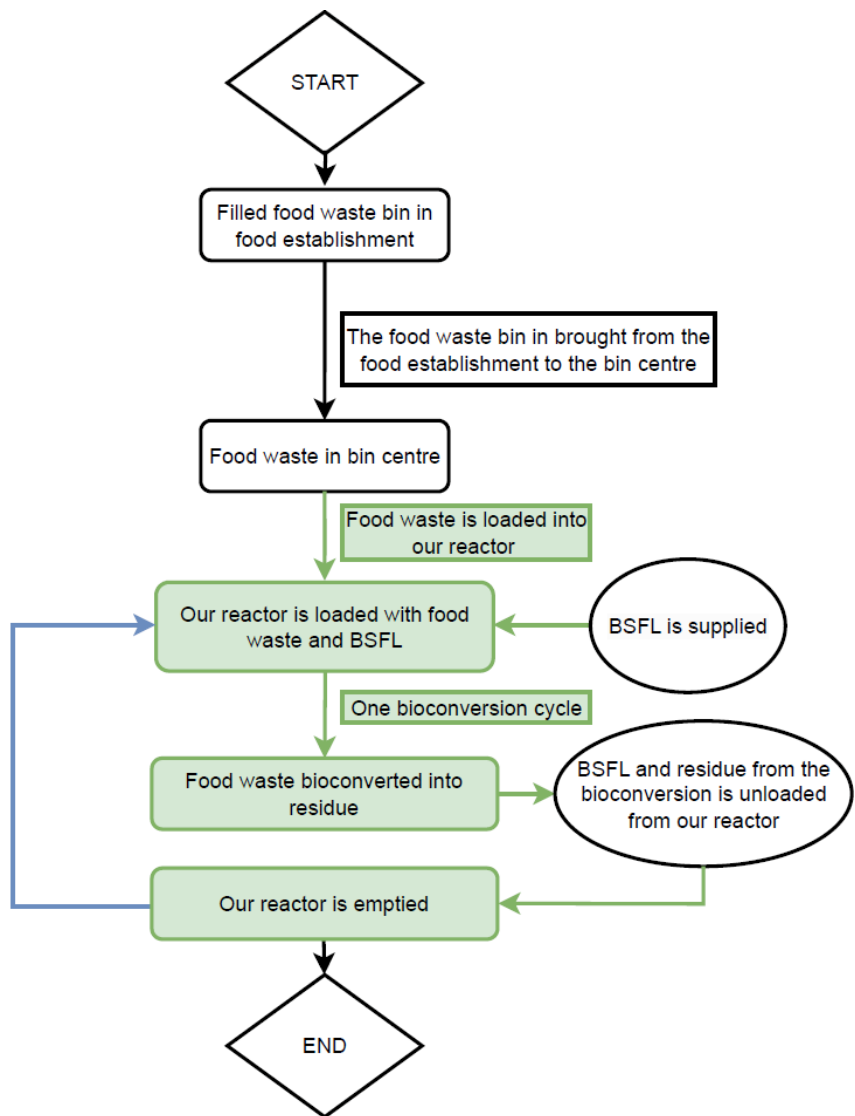


FIGURE 2.4c: Concept Design of Our Solution

2.5 Overall Design Specifications

The overall design specifications of our project is explained in TABLE 2.5 with the mapping to their respective user needs found in Appendix G.

TABLE 2.5: Design Specifications

Design Specification	Demand/ Wish
Ability to maintain the substrate pH level to be from 6 to 10 [43]	Demand
Ability to maintain the substrate moisture level to be from 40% to 80% [44], [45]	Demand
Ability to maintain the substrate temperature to be within 25°C to 47°C [44]	Demand
Ability to maintain the internal air temperature of the reactor to be within 25°C to 35°C [32]	Demand
Ability to maintain the relative humidity in the reactor to be $\geq 40\%$ [32]	Demand
Prevent accumulation of CO ₂	Demand
Prevent accumulation of CH ₄	Demand
Prevent accumulation of NH ₃	Demand
Minimum air exchange capacity of 330m ³ h ⁻¹ for every 1m ³ of internal reactor volume (Derivations can be found in Appendix H)	Demand
Less strenuous loading and unloading of food waste trays onto the bioconversion racks	Wish
Maximum width of 0.85m [47] (Derivations can be found in Appendix I)	Wish
Maximum depth of 1.2m [47] (Derivations can be found in Appendix I)	Wish
Maximum height of 2m [47] (Derivations can be found in Appendix I)	Wish
Maximum mass of 400 kg [48] (Derivations can be found in Appendix I)	Wish

2.6 Initial Sizing

The initial sizing of our prototype that will be based on the selected concept design shown in FIGURE 2.4a.

2.6.1 Food waste bioconversion capacity

Based on interviews conducted with Singapore food court and hawker centre' staff, an average of one food waste bin worth of food waste is generated daily by a food court or hawker centre. This is equivalent to 190 kg of food waste per food court or hawker centre in a day (Refer to Appendix J for derivation) [42].

Additionally, the recommended feed height for a more optimised bioconversion process is 6cm (A. Fuhrmann, Research student at SEC, personal communication, September 4, 2023). With this 6cm food waste height constraint, 190kg of food waste would require a container base area of 2m^2 (Refer to Appendix J for derivation).

Due to the limited fundings and the duration constraint of this year-long project, the scope of this project is to develop a quarter-scale prototype to evaluate our proposed concept design.

The trays used in our reactor was chosen to be those currently used in the SEC laboratory, since it has been proven to work in the conditions of the bioconversion as well as its ability to take on the optimised 8 kg food waste load over the duration of the lengthy bioconversion process.

Since each tray can take on 8 kg of food waste, each of our one quarter-scale prototype, which would have a food waste capacity of 48 kg, would require six trays.

In estimating the vertical height, the chassis structure, height of the six trays, spacing between each stack for ventilation, space for electronics and wheels were considered.

While the estimated width was determined by accounting for the chassis structure, width of the six trays, drawer system and spacing between walls of reactor and trays for ventilation.

As for the estimated depth, the chassis structure, depth of the tray, spacing between walls of the reactor and trays for ventilation were considered.

TABLE 2.6.1: Initial sizing of our reactor

Our reactor	
Food waste bioconversion capacity	48 kg
Number of Trays	6 trays
Dimensions (W x D x H)	900 x 600 x 1900 mm

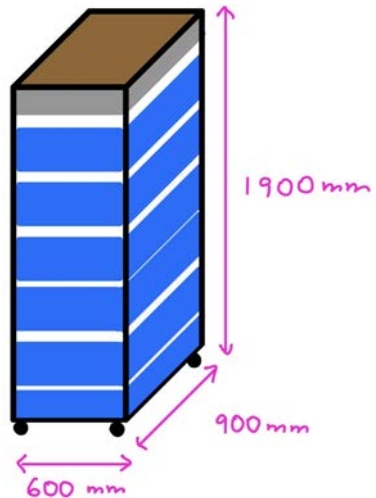


FIGURE 2.6.1: Initial sizing of our reactor

2.7 Scope of Work

Based on our project's design specifications, our solution can be split into two main systems, Electrical and Mechanical. Each main system has been split into various subsystems with work allocated to each group member as shown in TABLE 2.7a as well as the goal each subsystem has which contributes to the accomplishment of our project objective.

TABLE 2.7a: Systems and Work Allocation

Main Systems	Subsystems	Work Allocation
Electrical	Sensors and Data	1. Mok Jia Luo 2. Lee Wai Seng
	Software	
	Power and Integration	
Mechanical	Chassis and Container	1. Ashley Chua 2. Man Chun Hang
	Ventilation	1. Alicia Lim

TABLE 2.7b: The goals of each subsystem and our project objective

Main Systems	Subsystems	Subsystem Goal	Project Objective
Electrical	Sensors and Data	Aims to optimise the environmental conditions within the reactor for the survivability of the BSFL and bioconversion process by monitoring and adjusting the reactor's internal conditions	Our project aims to develop a solution that can manage the large amount of heterogeneous food waste that Singapore generates by collaborating with SEC to scale-up and optimise their current laboratory-setting of bioconversion of food waste using BSFL.
	Software		
	Power and Integration		
Mechanical	Chassis and Tray	Aims to minimise heavy load-bearing movements during the loading and unloading of food waste for bioconversion using BSFL	
	Ventilation	Aims to optimise the choice of components used in the ventilation system as well as their settings and arrangements to aid with achieving the optimal environmental conditions within the reactor for the survivability of the BSFL and bioconversion process	

This thesis is focused on the ventilation system of our reactor, and the purpose of our one quarter-scale prototype for the ventilation subsystem is to enable the optimisation of the ventilation system for the bioconversion of food waste to be studied.

3 Design Configurations and Simulation of Ventilation System

The purpose of the ventilation system is to ensure that the reactor has sufficient air exchange with the surrounding air. According to A. Fuhrmann, a research student at SEC, one of the most important purposes of the ventilation system in the reactor is to promote the drying of the substrate by airflow. The drying of the substrate is important as it aids in speeding up the bioconversion process and enables a drier substrate that is more easily harvested at the end of the bioconversion. While the other factors that the ventilation can influence that would affect the survivability and bioconversion processes such as certain gases that would suffocate the BSFL if there is a build up, air temperature, substrate temperature and relative humidity are more easily controlled within their acceptable ranges.

The SEC laboratory has a 3-tray configuration reactor with one fan used per reactor, as shown in FIGURE 3a and FIGURE 3b. The design of the SEC reactor's ventilation system was considered in the design of the ventilation system of our reactor.



FIGURE 3a: One of the four SEC Reactors has been marked out in red

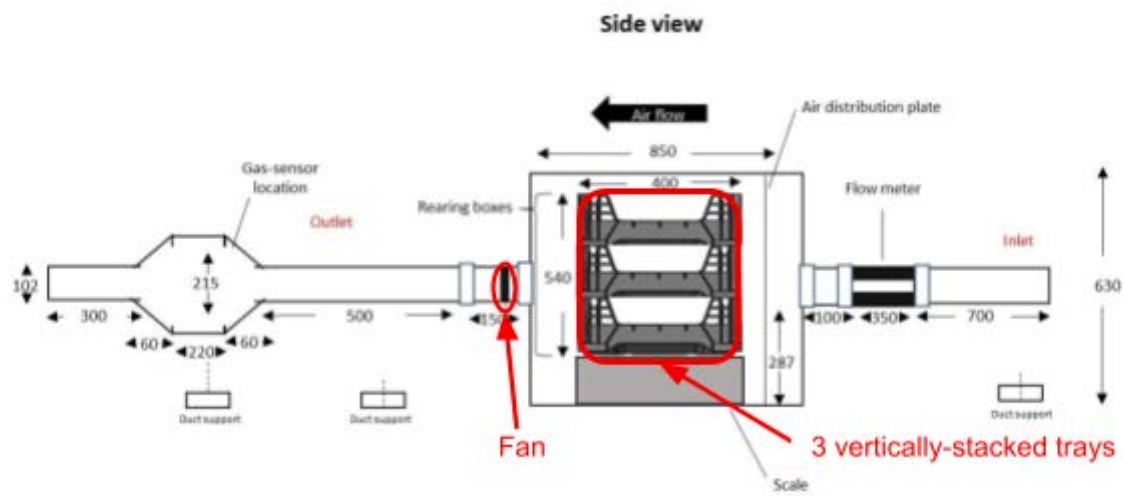


FIGURE 3b: Schematic Diagram of a SEC Reactor

3.1 Design Configurations

Five design configurations of the ventilation system were generated and evaluated using an evaluation matrix as shown in the following figures and table in this section. The evaluation matrix table of the five design configurations can be found in Appendix K.

TABLE 3.1: Summary of the 5 ventilation system configurations

Configuration Number	Number of fans	Location of Fans
Config A	6 Fans	1 fan per tray
Config B	3 Fans	1 fan for every 2 trays (with fan vent attached to each fan, for more even airflow distribution)
Config C	12 Fans	2 small fans per tray
Config D	7 Fans	1 fan per tray, and 1 fan at the top of the chimney
Config E	7 Fans	1 fan per tray, and 1 fan at the top of the reactor

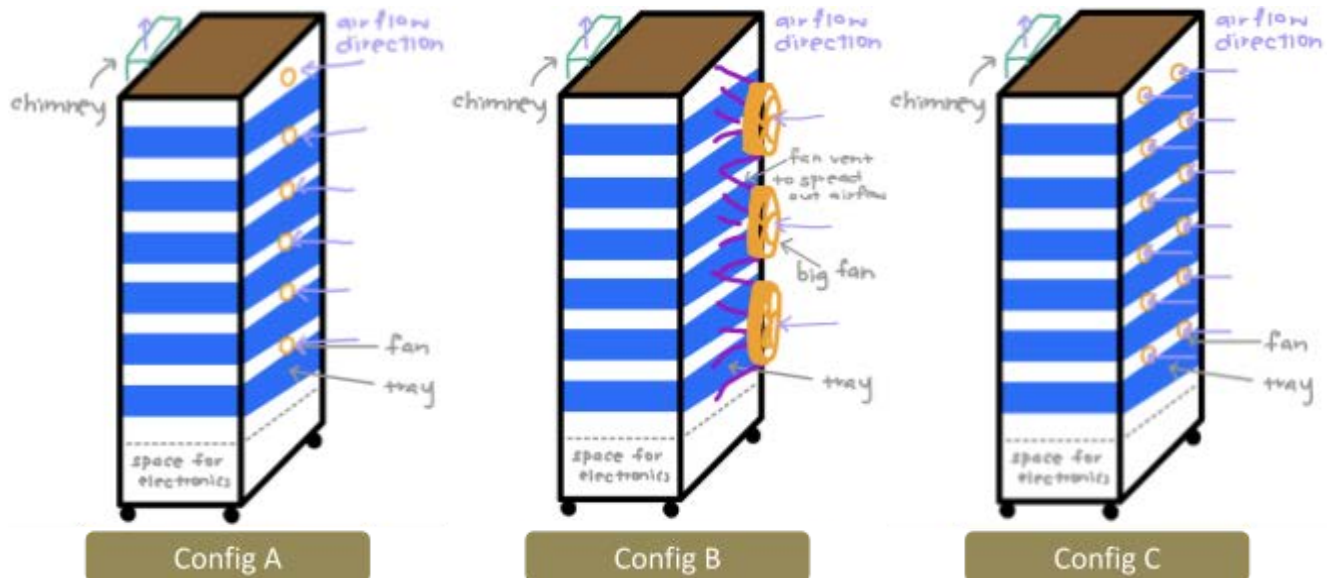


FIGURE 3.1a: Sketches of Config A, Config B and Config C

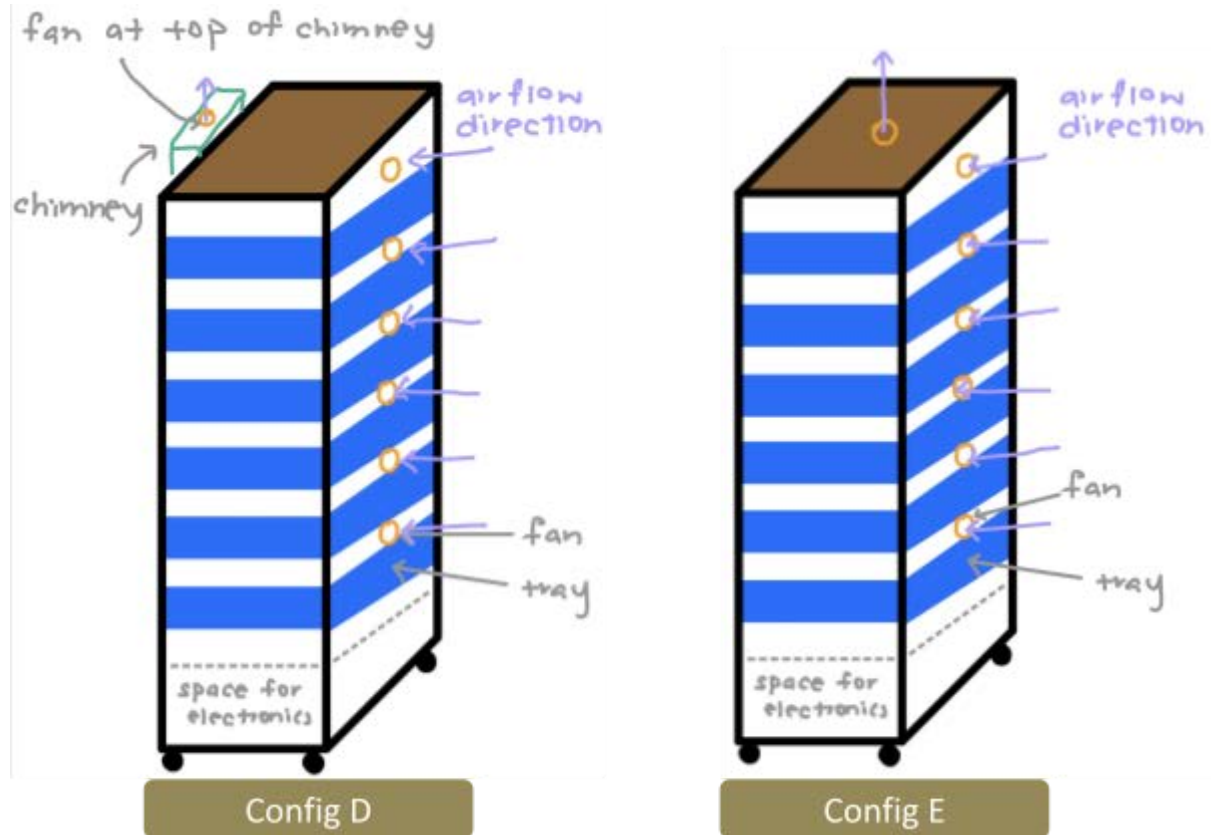


FIGURE 3.1b: Sketches of Config D and Config E

3.2 Detailed Design of Ventilation System

The air exchange requirements of our ventilation system were sized based on the SEC reactor's air exchange capabilities. Noting that the size and food waste bioconversion capacity of our reactor is significantly larger than the SEC reactor, our reactor would require a higher air exchange rate to maintain a suitable internal environment for the BSFL and bioconversion process. To estimate the required air exchange rate of our reactor, it was assumed that the required air exchange rate is

proportional to the reactor's interior body volume. Additionally, the higher end of the SEC reactor's air exchange range was used in this estimation to ensure that our selected fans would be able to cater for the higher air exchange rate should it be required.

With these considerations, the minimum air exchange capacity of $330\text{m}^3\text{h}^{-1}$ for every 1m^3 of internal reactor volume was derived, and it has been set as the air exchange design specification of our reactor. The derived air exchange capacity required of our reactor is $274.337\text{ m}^3\text{h}^{-1}$, the full derivation of the required air exchange rate of our reactor can be found in Appendix L and the key values involved in this derivation is shown in TABLE 3.2.

TABLE 3.2: Key values used in determining the air exchange capacity required of our reactor

Parameter	Value
Minimum air exchange capacity for every 1m^3 of internal reactor volume	$330 \text{ m}^3\text{h}^{-1}$
Internal dimensions of our reactor	$0.845 \times 0.56 \times 1.75 \text{ m}$
Our reactor's internal volume	0.828 m^3
Air exchange capacity required of our reactor	$274.337 \text{ m}^3\text{h}^{-1}$

3.2.1 Sizing and Selection of fan

For the sizing of our reactor's fan, the significant reduction in air exchange performance of the SEC reactor as compared with its fan's rated air exchange capability can be considered. It was observed that the SEC reactor fan's rated air exchange was four times the actual maximum air exchange rate of SEC's reactor, as shown in TABLE 3.2.1a and TABLE 3.2.1b.

TABLE 3.2.1a: Specifications of SEC reactor

(A. Fuhrmann, Research student at SEC, personal communication, August 18, 2023)

Parameter	Value
Interior reactor body volume	0.332 m^3
Interior reactor body dimensions (H x L x W)	$0.630 \text{ m} \times 0.850 \text{ m} \times 0.620 \text{ m}$
Air exchange range	$30 - 110 \text{ m}^3 \text{h}^{-1}$

TABLE 3.2.1b: Air Exchange Fan used in the SEC reactor [49]

Air Exchange Fan: San Ace 9LG Series Axial Fan, Sanyo Electric Co.	
Attribute	Value
Rated air exchange	$420 \text{ m}^3 \text{ h}^{-1}$
Supply voltage	12 V DC
Maximum current	3.2A
Dimensions	120 x 120 x 38mm
Sensor type	PWM, Tachometer

In a 6-fan configuration, our reactor would require a fan rated with $182.892 \text{ m}^3 \text{ h}^{-1}$ (equivalent to 107.646 CFM) as shown in TABLE 3.2.1c.

TABLE 3.2.1c: Air exchange requirements for 6-fan configuration

Parameter	Value
Air exchange capacity required of our reactor	$274.337 \text{ m}^3 \text{ h}^{-1}$
Number of fans	6
Actual air exchange required per fan	$45.723 \text{ m}^3 \text{ h}^{-1}$
Fan's rated air exchange (Four times actual air exchange required per fan)	$182.892 \text{ m}^3 \text{ h}^{-1}$ (in CMH) $107.646 \text{ ft}^3 \text{ min}^{-1}$ (in CFM)

However, during a rough sizing of the reactor with the placing of the fans in between the six vertically stacked trays, it was noted that the top of the top tray would potentially reach 1700 mm which may be difficult for loading and unloading, shown in FIGURE 3.2.1a. Hence, a configuration with only five trays which would correspond to having five fans per reactor was considered and the required fan rating would be $219.470 \text{ m}^3 \text{ h}^{-1}$ (equivalent to 129.175 CFM) as shown in TABLE 3.2.1d.

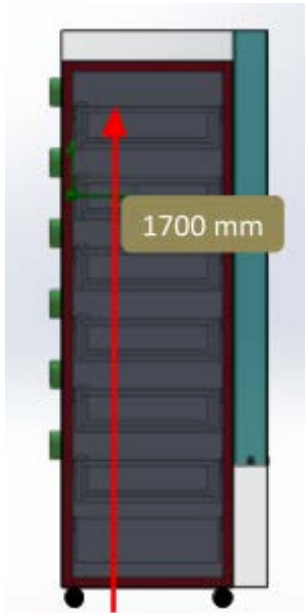


FIGURE 3.2.1a: 6-fan configuration with full-fan spacing reaches a height of 1700 mm at the top of the top drawer

TABLE 3.2.1d: Air exchange requirements for 5-fan configuration

Parameter	Value
Air exchange capacity required of our reactor	$274.337 \text{ m}^3\text{h}^{-1}$
Number of fans	5
Actual air exchange required per fan	$54.8674 \text{ m}^3\text{h}^{-1}$
Fan's rated air exchange (Four times actual air exchange required per fan)	$219.470 \text{ m}^3\text{h}^{-1}$ (in CMH) $129.175 \text{ ft}^3\text{min}^{-1}$ (in CFM)

Due to the limited budget of our project, the fan selected for purchase would need to cater for both 5-fan and 6-fan configurations, hence the rated air exchange required of the fan would need to be minimally 130 CFM. Additionally, for the integration with the other electronics system, the fan was required to have a 12V rating and termination of 4 wire leads.

Considering a compact size, lower current rating to reduce power consumption, cost and date of delivery of the fan, a 92.5 x 38 mm 12VDC Wire fan from Orion Fans was chosen and shown in FIGURE 3.2.1b and specifications found in TABLE 3.2.1e.



FIGURE 3.2.1b: 92.5 x 38 mm 12VDC Wire fan from Orion Fans [50]

TABLE 3.2.1e: Specifications of selected fan [50]

Parameter	Value
Air flow	135.0 CFM
Voltaged-rated	12VDC
External dimensions	92.5 x 92.5 x 38.0 mm
Current Rating	1.3 A
Termination	4 Wire Leads

An alternative considered to keep the food waste bioconversion capacity of our reactor at 48 kg and still have easy loading and unloading is to maintain a 6-tray configuration while reducing the vertical gap between the trays. Instead of having a full-fan spacing between the trays, a half-fan spacing would allow the top of the top drawer to be more easily accessible at 1470mm as shown in FIGURE

3.2.1c. Hence, there is a need to explore these two configurations and evaluate their air exchange performance.

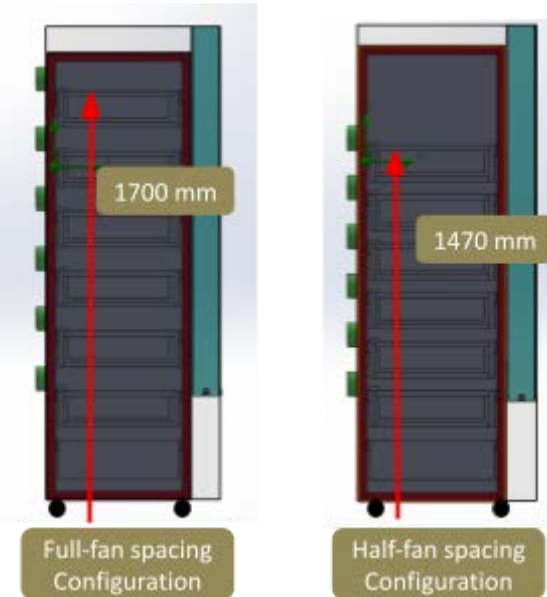


FIGURE 3.2.1c: Full-fan and half-fan spacing configurations

3.2.2 Chimney sizing

The purpose of the chimney is to direct all the outflow to a limited region for sensors to monitor the conditions and composition of the outflow air during the bioconversion process. The data collected would aid in selecting suitable fan speed and configurations within the reactor to optimise our reactor's internal environment for the bioconversion process.

The designed chimney consists of three parts shown in FIGURE 3.2.2a. The size of the chimney channel is crucial as it can affect the reactor's air exchange rate. It has to have sufficient depth and width to prevent excessive resistance from building up in the chimney that could restrict the airflow exiting the reactor. It was recommended by Mr Hamilton, a Senior Production Manager at NUS Professional Workshop, to have a depth of at least 10 to 20 mm more than the reactor's exit height

to reduce the chances of resistance in airflow through the chimney. Since the exit height from the reactor into the chimney is 92.5 mm, the depth of the chimney channel was sized to be 112.5 mm as shown in FIGURE 3.2.2b and FIGURE 3.2.2c. Additionally, it was recommended by Mr Hamilton for the width of the chimney channel to be at least 10 to 20 mm wider on each side compared to the exit width. Since the exit width is 530 mm, the chimney channel width was sized to be 570 mm as shown in FIGURE 3.2.2d and FIGURE 3.2.2e.

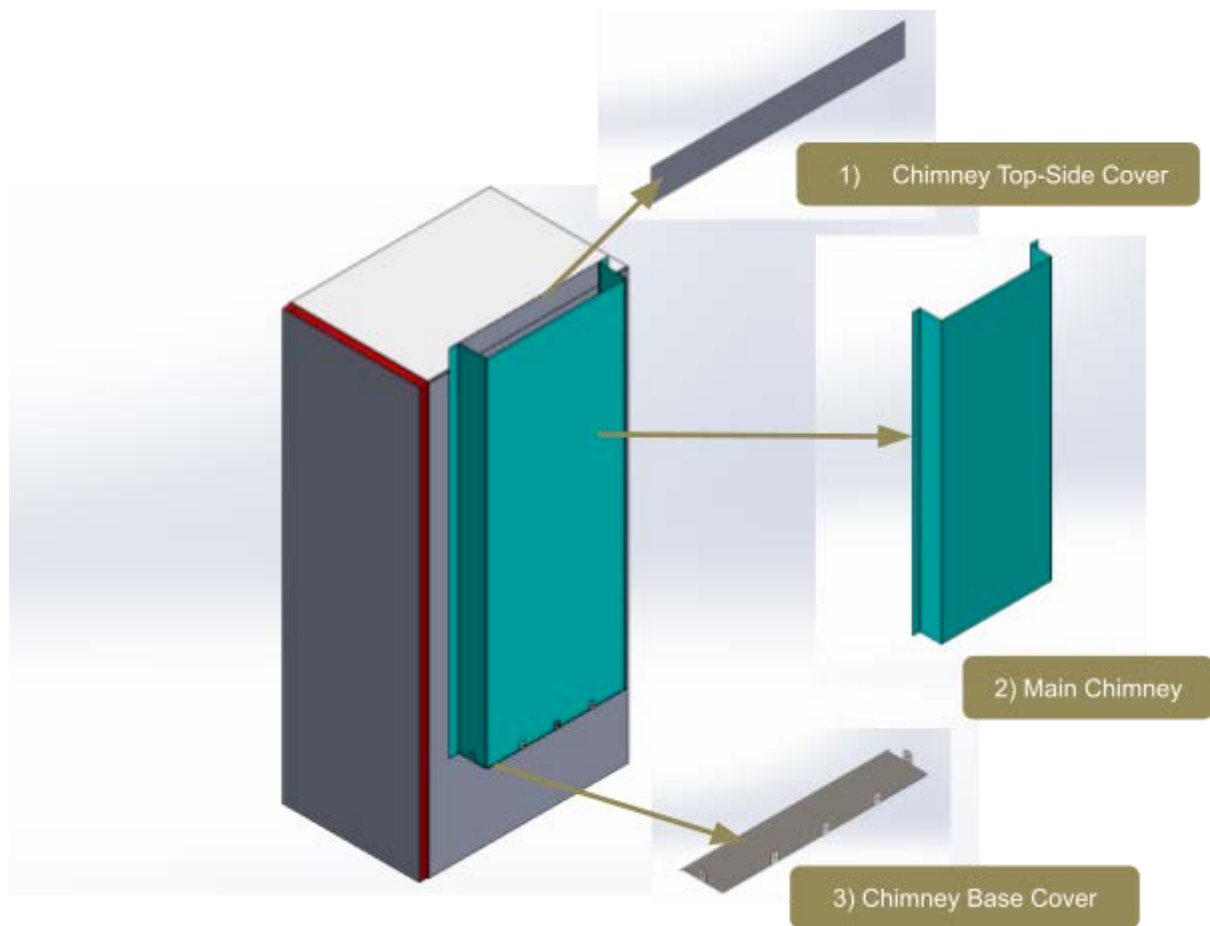


FIGURE 3.2.2a: Exploded view of the three chimney parts

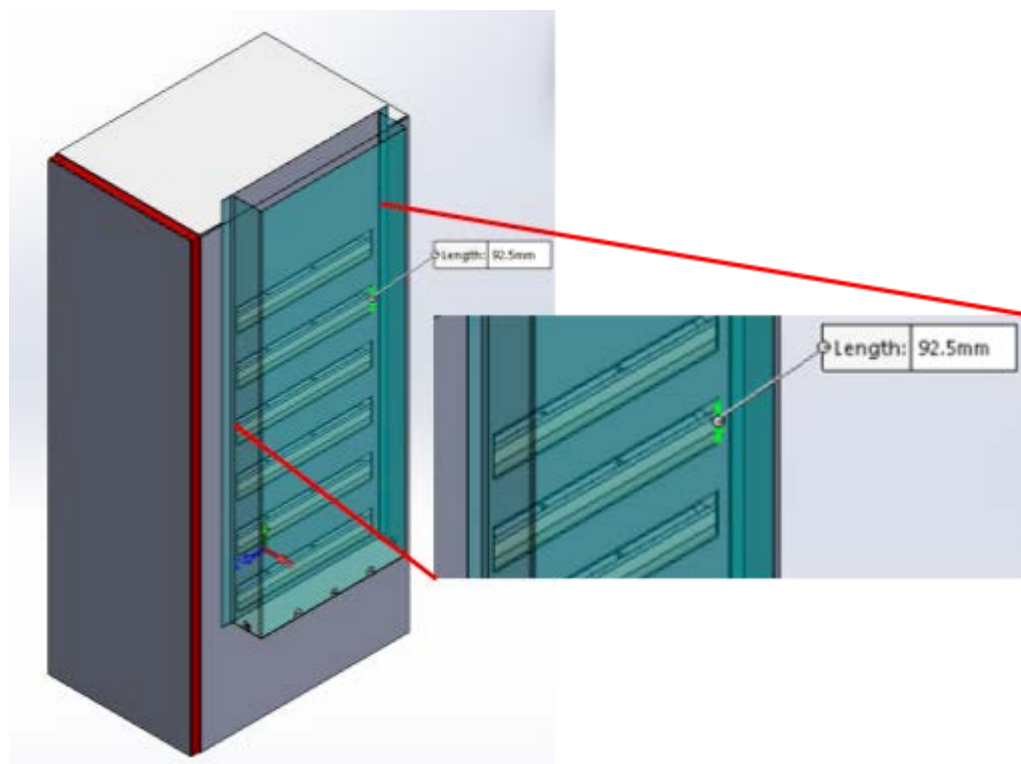


FIGURE 3.2.2b: Reactor's exit into chimney has a height of 92.5 mm

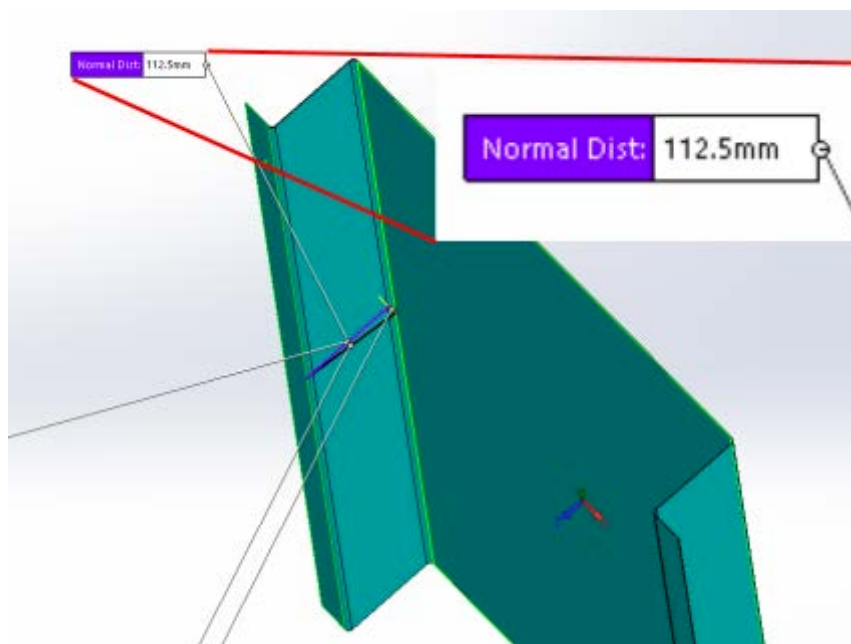


FIGURE 3.2.2c: The main chimney has a depth of 112.5 mm

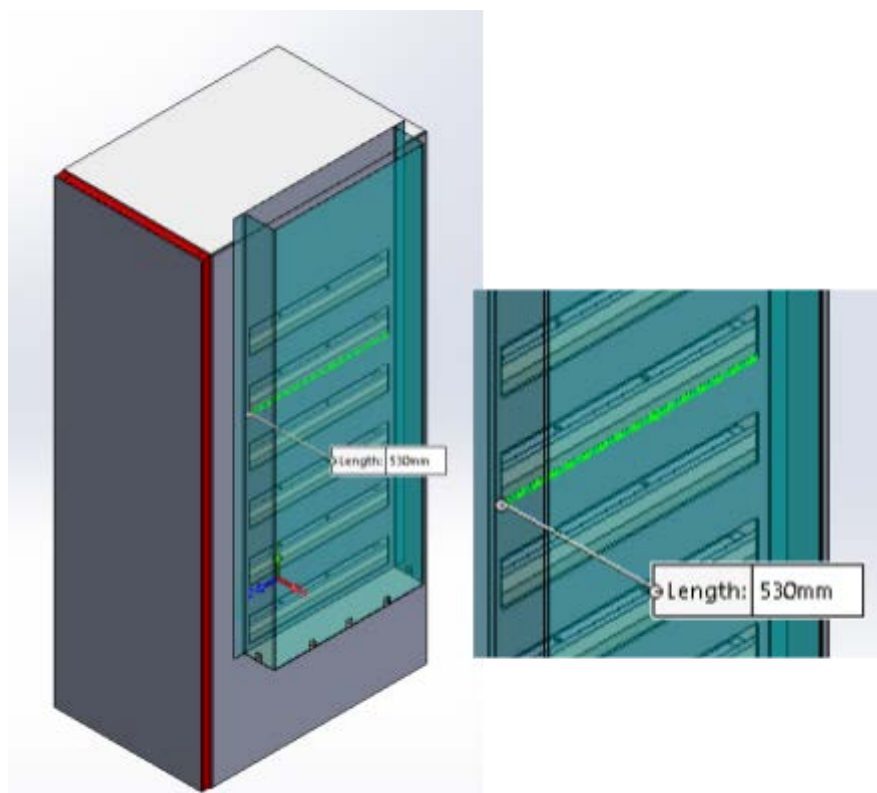


FIGURE 3.2.2d: The exit hole has a width of 530 mm



FIGURE 3.2.2e: The main chimney has a width of 570 mm

3.3 Simulations

The purpose of conducting the following simulations is to choose a ventilation system design and arrangement of trays that would enable the reactor to have sufficient air exchange, and if possible, optimise the configurations for better air exchange. Air flow simulations for a full-fan spacing and half-fan spacing with six trays would be conducted.

Solidworks flow simulation was used to conduct the simulations. The key parameters set in the following simulations are recorded in TABLE 3.3 and shown in FIGURE 3.3.

TABLE 3.3: Key parameters set in air simulations

Parameter	Selected region	Setting
Inlet	Inlet into the reactor of all 6 fans	Inlet volume flow = $274.337 \text{ m}^3\text{h}^{-1}$
Outlet	Outlet of chimney	Environmental pressure = 101325 Pa

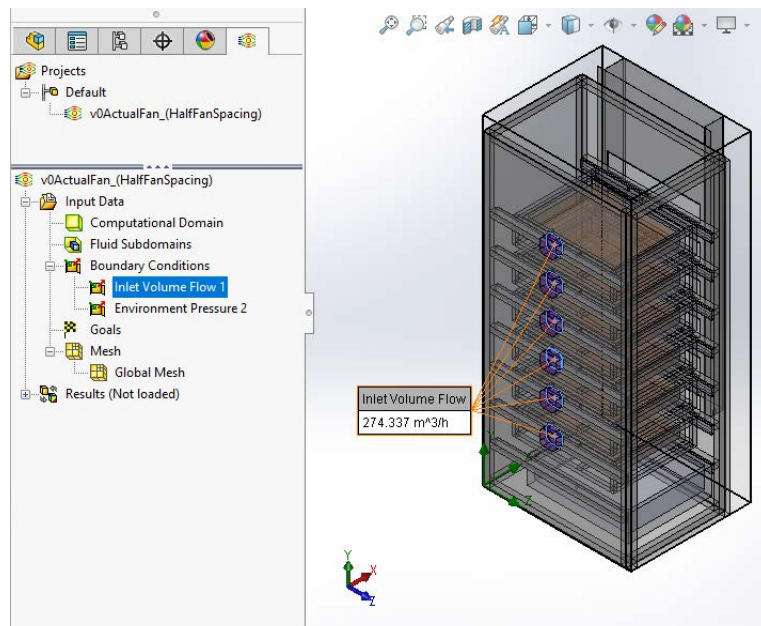


FIGURE 3.3a: Inlet of all six fans into the reactor set to a total inlet volume flow of $273.337 \text{ m}^3\text{h}^{-1}$

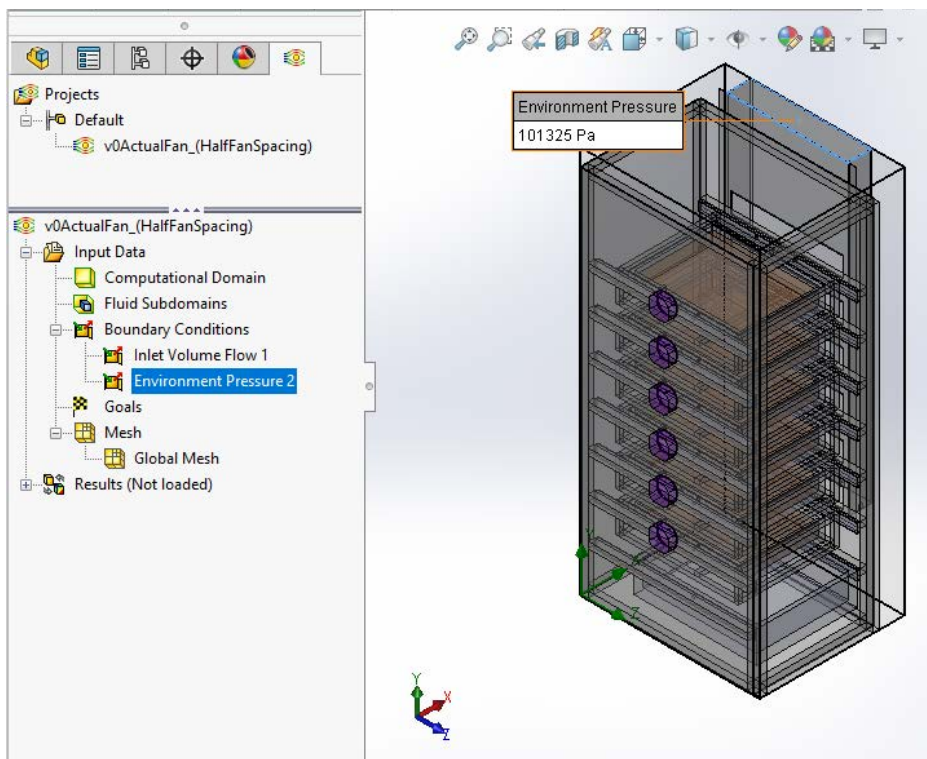


FIGURE 3.3b: Chimney outlet set to environmental pressure of 101325 Pa

3.3.1 Airflow Simulation for Full-fan spacing Configuration

FIGURE 3.3.1a shows how the full-fan spacing configuration with six trays would look like. Airflow simulations for this configuration were done following TABLE 3.3 settings and shown in FIGURE 3.3.1b, FIGURE 3.3.1c and FIGURE 3.3.1d.

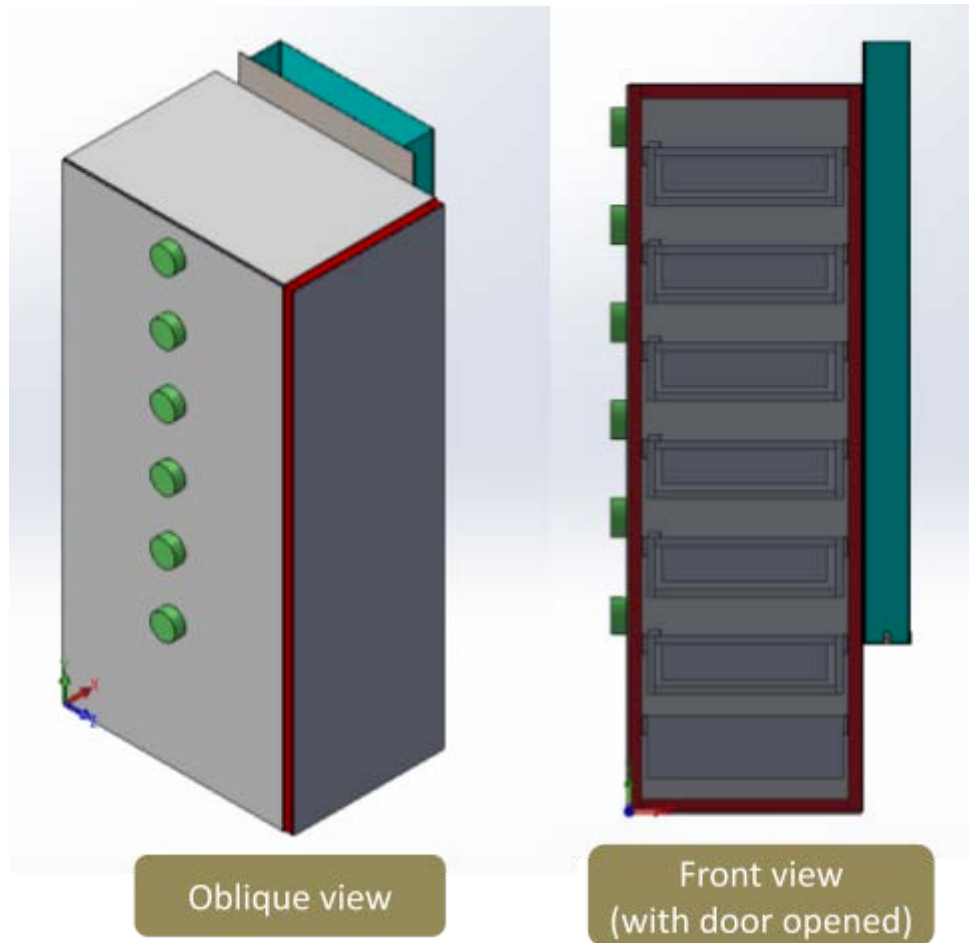


FIGURE 3.3.1a: 3D computer-aided design (CAD) of full-fan spacing configuration

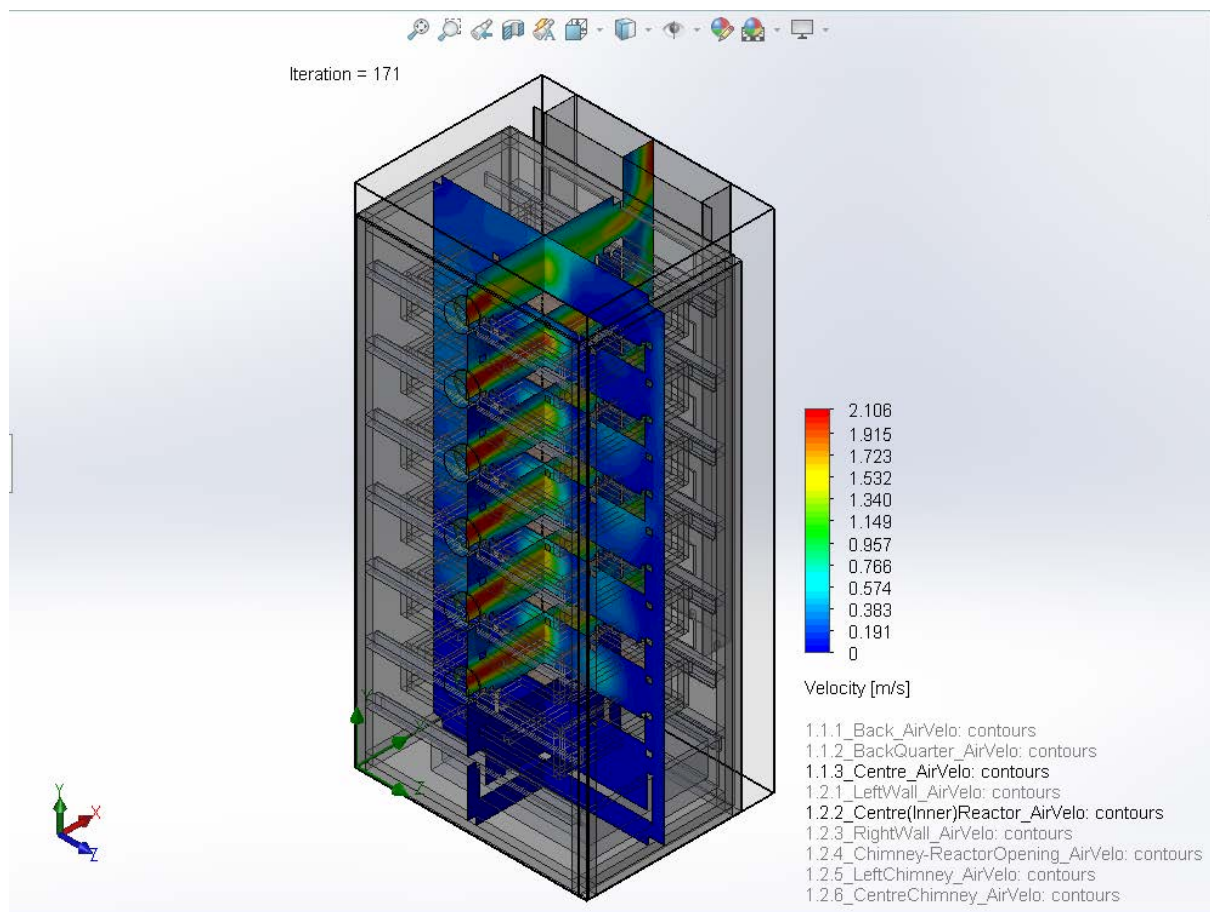


FIGURE 3.3.1b: Air velocity simulation of the full-fan spacing configuration
with the centre of the reactor in the front and right plane

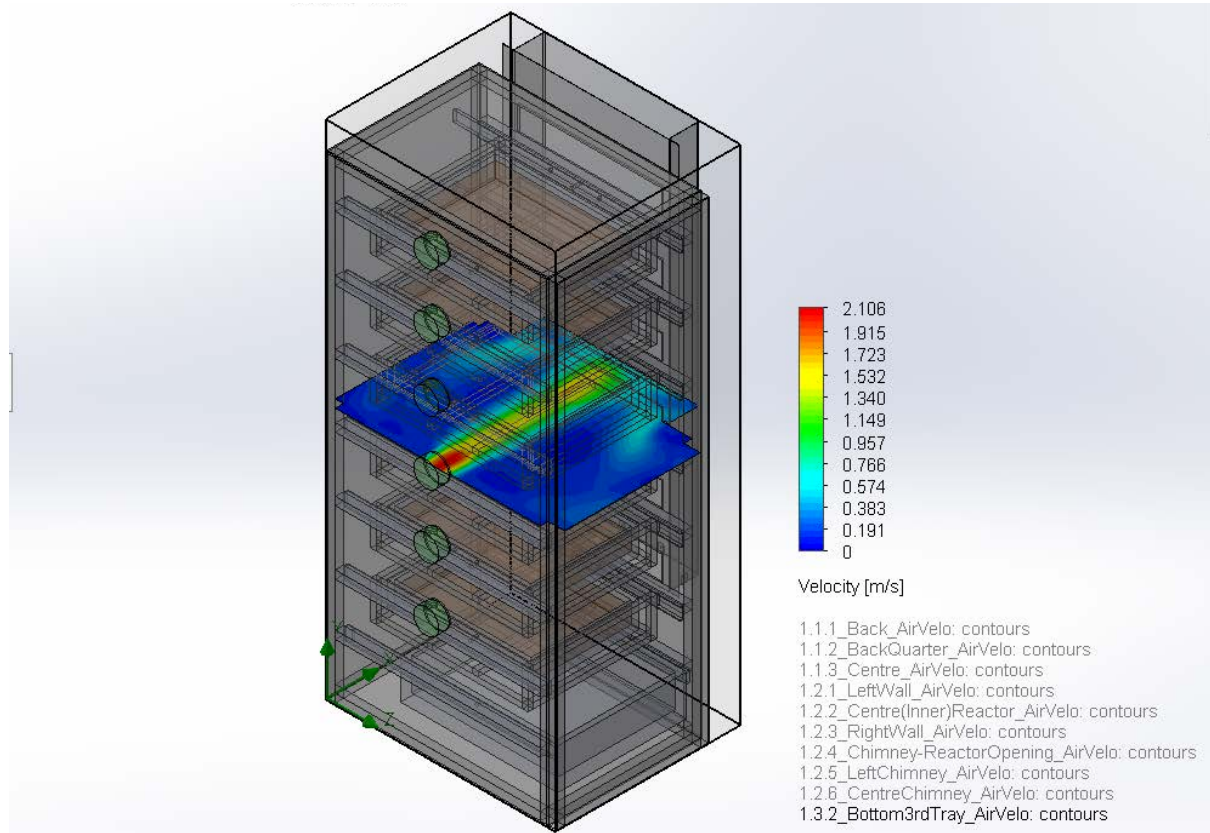


FIGURE 3.3.1c: Air velocity simulation of the full-fan spacing configuration

with the centre of one of the tray in the top plane

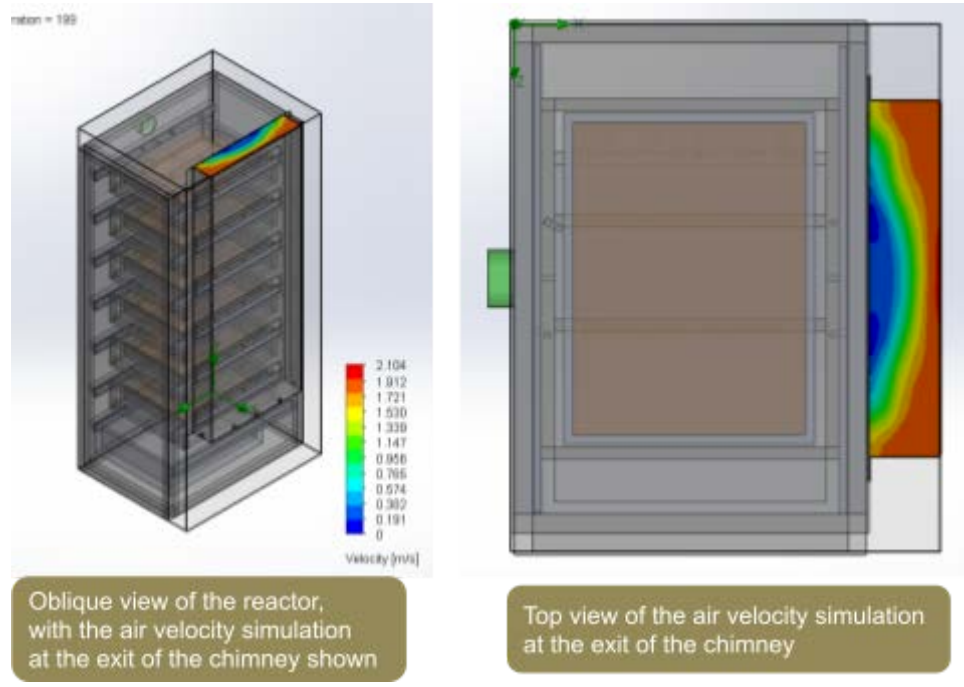


FIGURE 3.3.1d: Air velocity simulation of the of the chimney exit of the full-fan spacing configuration

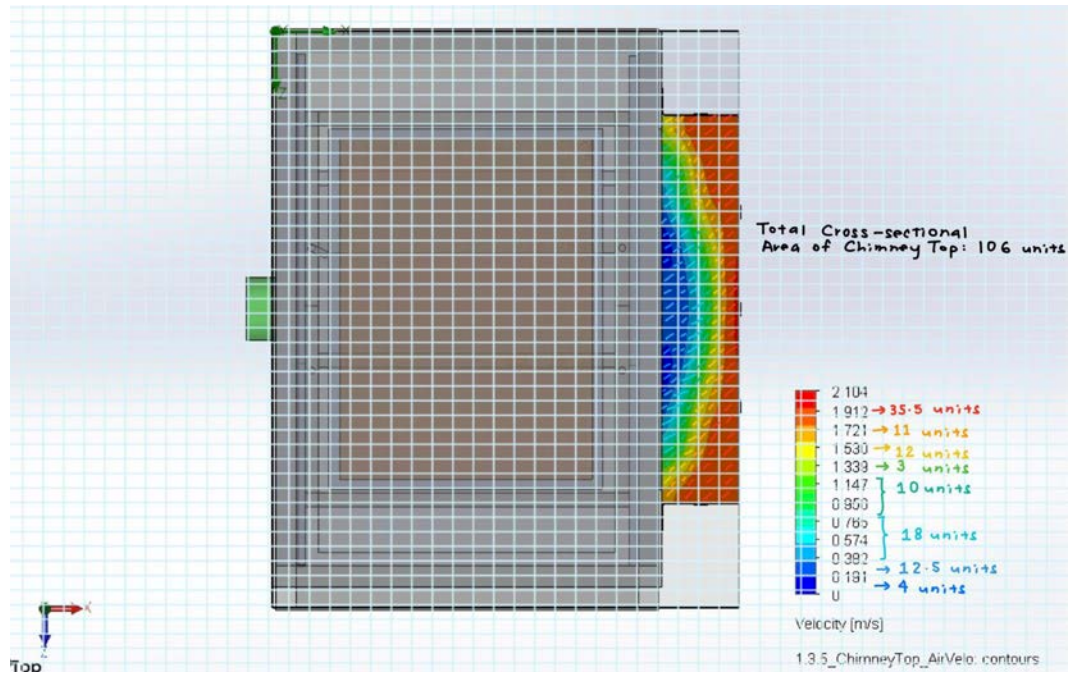


FIGURE 3.3.1e: Counting of rectangles to estimate the average velocity of the exit airflow of the full-fan spacing configuration

To determine the air exchange out of the reactor, the average velocity of the exit air was determined by counting the rectangles marked out in FIGURE 3.3.1e and tabulated in TABLE 3.3.1a.

TABLE 3.3.1a: Calculation of average velocity of exit airflow of the full-fan spacing configuration

Velocity (m/s)	Number of Rectangles	Calculations (rounded off to 3dp)
1.912 - 2.104	0	$[(1.912 + 2.104)/2] * 0 = 0$
1.721 - 1.912	35.5	$[(1.721 + 1.912)/2] * 35.5 = 64.486$
1.530 - 1.721	11	$[(1.530 + 1.721)/2] * 11 = 17.881$
1.339 - 1.530	12	$[(1.339 + 1.530)/2] * 12 = 17.214$
1.147 - 1.339	3	$[(1.147 + 1.339)/2] * 3 = 3.729$
0.956 - 1.147	10	$[(1.147 + 0.765)/2] * 10 = 9.560$
0.765 - 0.956		
0.574 - 0.765	18	$[(0.765 + 0.382)/2] * 18 = 10.323$
0.382 - 0.574		
0.191 - 0.382	12.5	$[(0.191 + 0.382)/2] * 12.5 = 3.581$
0 - 0.191	4	$[(0 + 0.191)/2] * 4 = 0.382$
		Total: 127.156
Total Number of Rectangles (Cross-sectional Area of Chimney Top)	106	
Average Velocity		127.156 / 106 = 1.200 m/s = 4320 m/h

TABLE 3.3.1b: Key values considered when determining the air exchange out of our full-fan spacing configured reactor

Parameter	Value
Dimensions of cross-section of outlet (Chimney exit)	112.5 x 570 mm (0.1125 x 0.57 m)
Area of cross-section of outlet	0.064 m ²
Average velocity	4320 m/h
Air exchange out of reactor	276.48 m ³ h ⁻¹
Air exchange required of our reactor	274.337 m ³ h ⁻¹
Conclusion from Simulation 1: Full-fan spacing configuration and current chimney size is sufficient for the air exchange required of our reactor	

Based on data from the Solidworks Flow Simulation and calculations, the air exchange out of our reactor is 276.48 m³ h⁻¹, which is larger than the 274.337 m³ h⁻¹ air exchange required for the size of our reactor, refer to TABLE 3.3.1b for the calculations breakdown. Hence, this full-fan spacing configuration and chimney size is sufficient for the air exchange required of our reactor.

3.3.2 Airflow Simulation for Half-fan spacing Configuration

FIGURE 3.3.2a shows how the half-fan spacing configuration with six trays would look like. Airflow simulations for this configuration were done following TABLE 3.3 settings and shown in FIGURE 3.3.2b and FIGURE 3.3.2c.

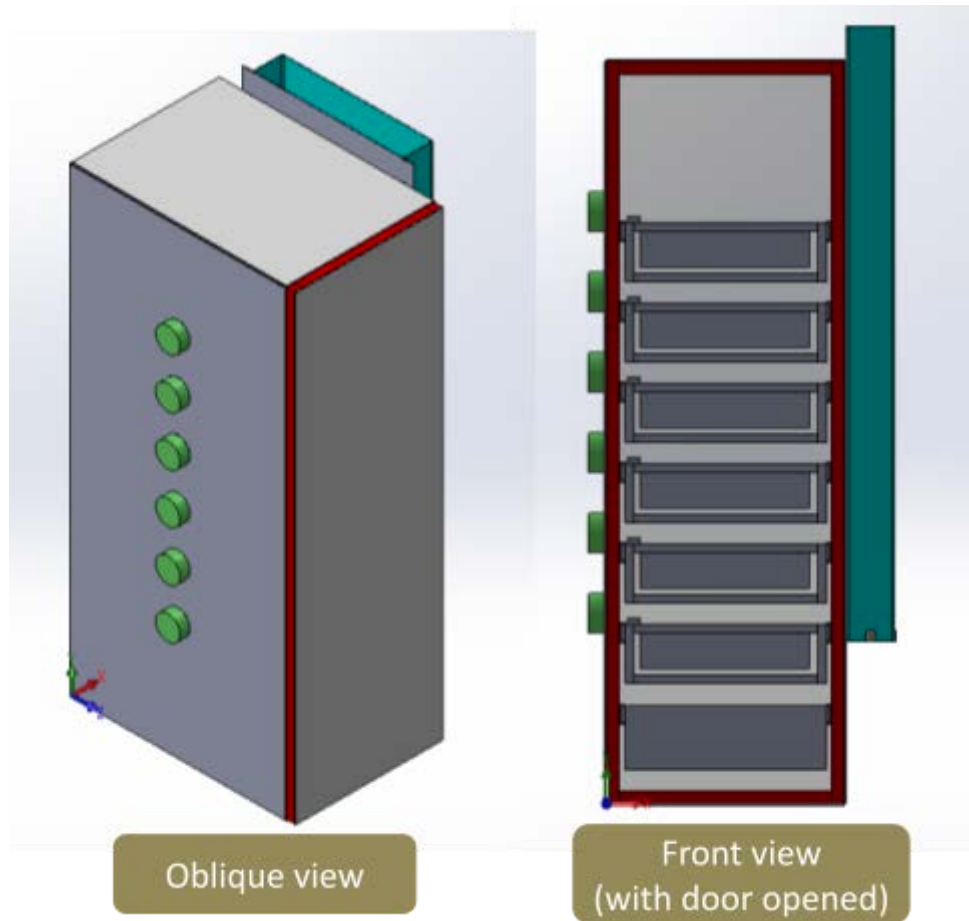


FIGURE 3.3.2a: 3D CAD of half-fan spacing configuration

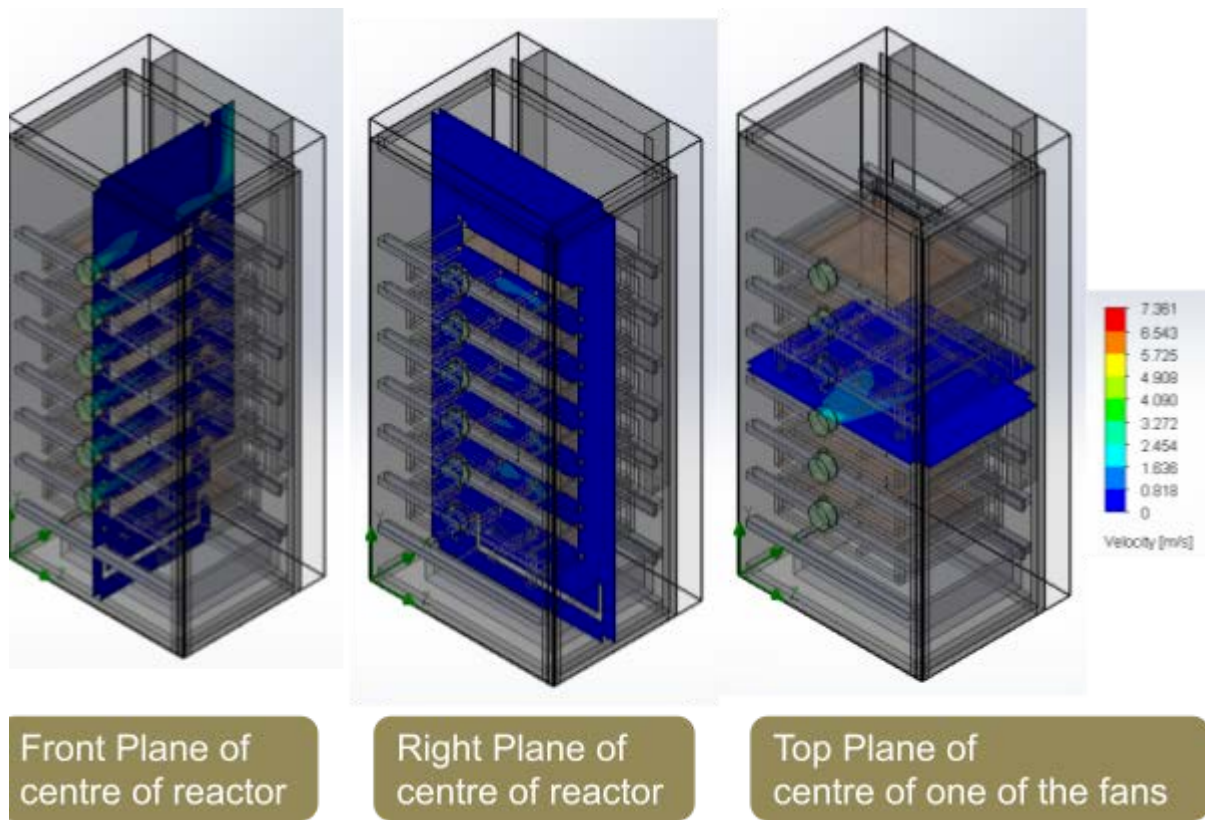


FIGURE 3.3.2b: Air velocity simulation of the half-fan spacing configuration

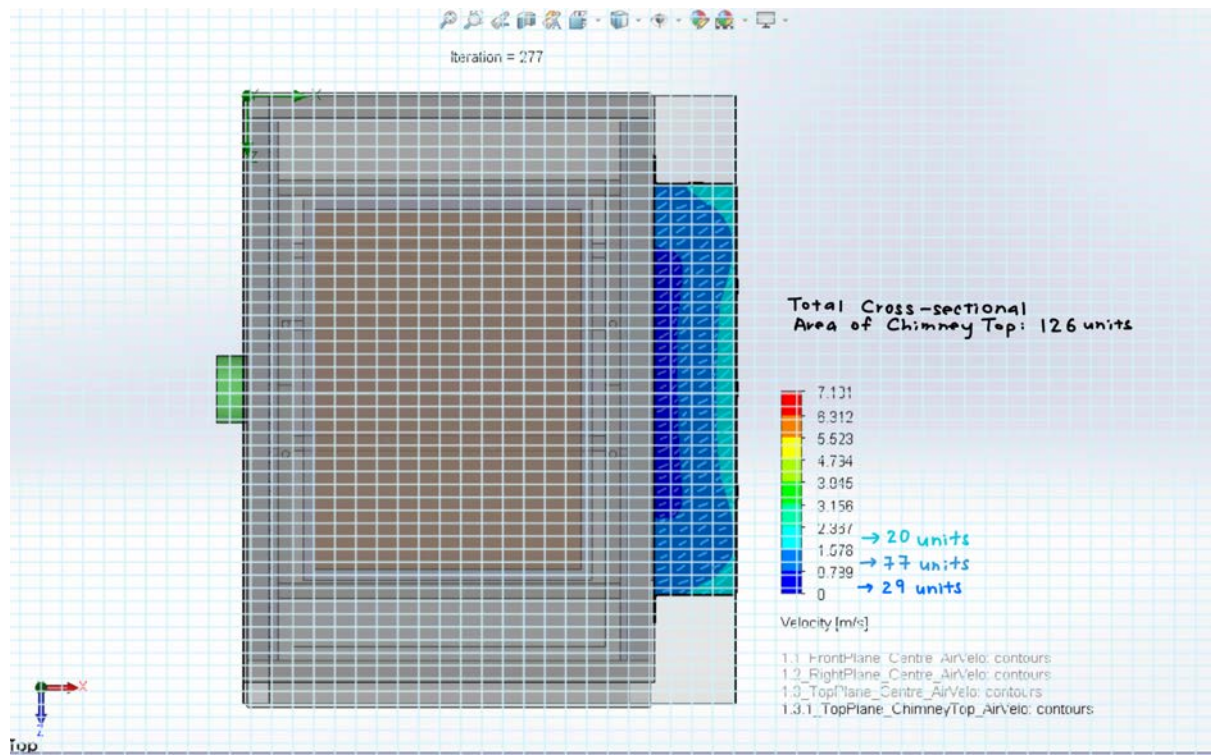


FIGURE 3.3.2c: Counting of rectangles to estimate the average velocity of the exit airflow of the half-fan spacing configuration

TABLE 3.3.2a: Key values considered when determining the air exchange out of our half-fan spacing configured reactor

Parameter	Value
Area of cross-section of outlet	0.064 m ²
Average velocity	4057 m/h
Air exchange out of reactor	259.648 m ³ h ⁻¹
Air exchange required of our reactor	274.337 m ³ h ⁻¹

Conclusion from Simulation 2: Half-fan spacing configuration and current chimney size is insufficient for the air exchange required of our reactor

To determine the air exchange out of the reactor, the average velocity of the exit air was determined by counting the rectangles marked out in FIGURE 3.3.2c and tabulated in TABLE M - 1 of Appendix M.

Based on data from the Solidworks Flow Simulation and calculations, the air exchange out of our reactor is $259.648 \text{ m}^3 \text{ h}^{-1}$, which is less than the $274.337 \text{ m}^3 \text{ h}^{-1}$ air exchange required for the size of our reactor, refer to TABLE 3.3.2a for the calculations breakdown. Based on this simulation results, the half-fan spacing configuration and chimney size is insufficient for the air exchange required of our reactor. However, the range of each colour coded airspeed is very large and may be insufficient to fully rule out the air flow exchange of this configuration. Additionally, it is noted that some parts of the fan's inlet into the reactor are directly in contact and blocked by other structures in the reactor which may have affected the results of the simulation. The method solidworks generate the simulation results in such cases is unclear and this might have led to inaccurate simulation results.

An alternative way to simulate this configuration is to edit the inlet shape of each fan as shown in FIGURE 3.3.2d and FIGURE 3.3.2e.

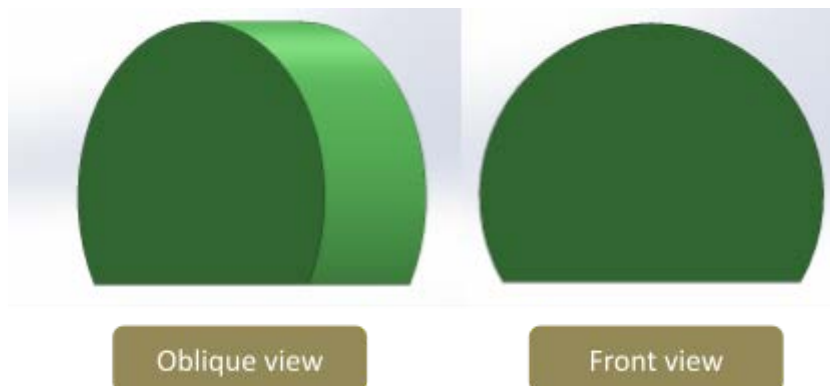


FIGURE 3.3.2d: 3D CAD of edited fan shape

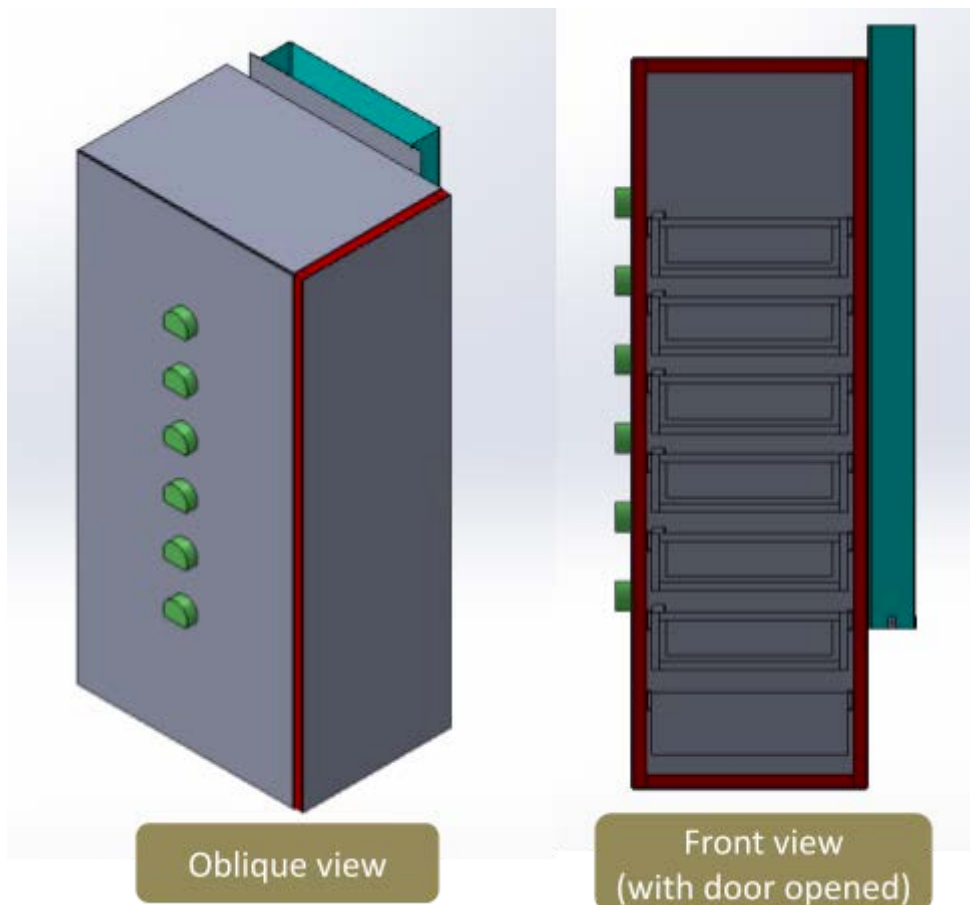


FIGURE 3.3.2e: 3D CAD of half-fan spacing with edited shape fans

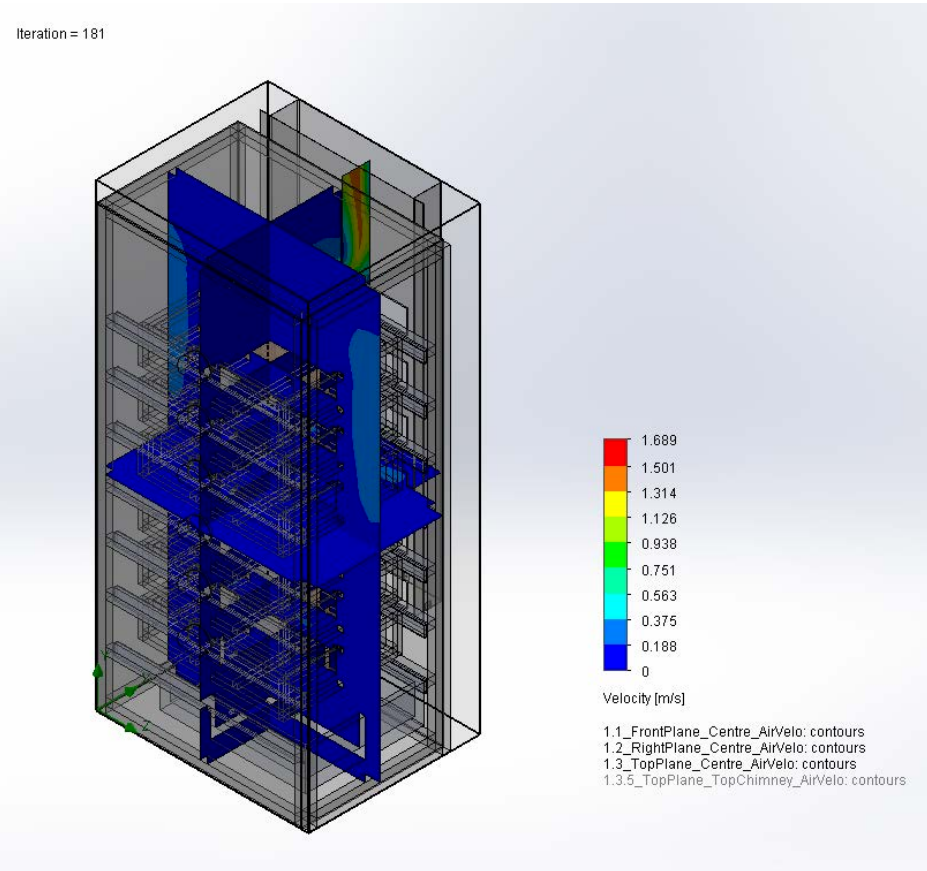
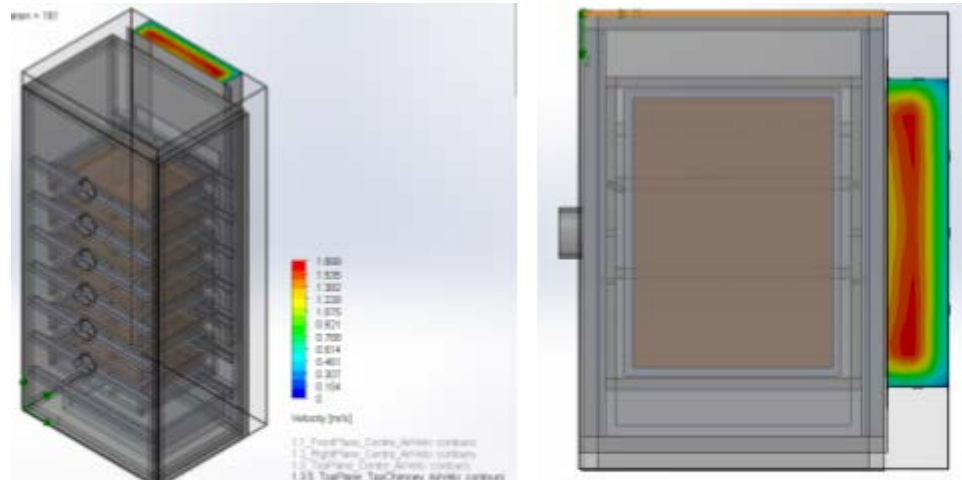


FIGURE 3.3.2f: Air velocity simulation of half-fan spacing with edited shape fans
(Results showing the centre of the reactor in the front and right plane,
and centre of one of the fan's top plane)



Oblique view of the reactor,
with the air velocity simulation
at the exit of the chimney shown

Top view of the air velocity simulation
at the exit of the chimney

FIGURE 3.3.2g: Air velocity simulation of the chimney's exit

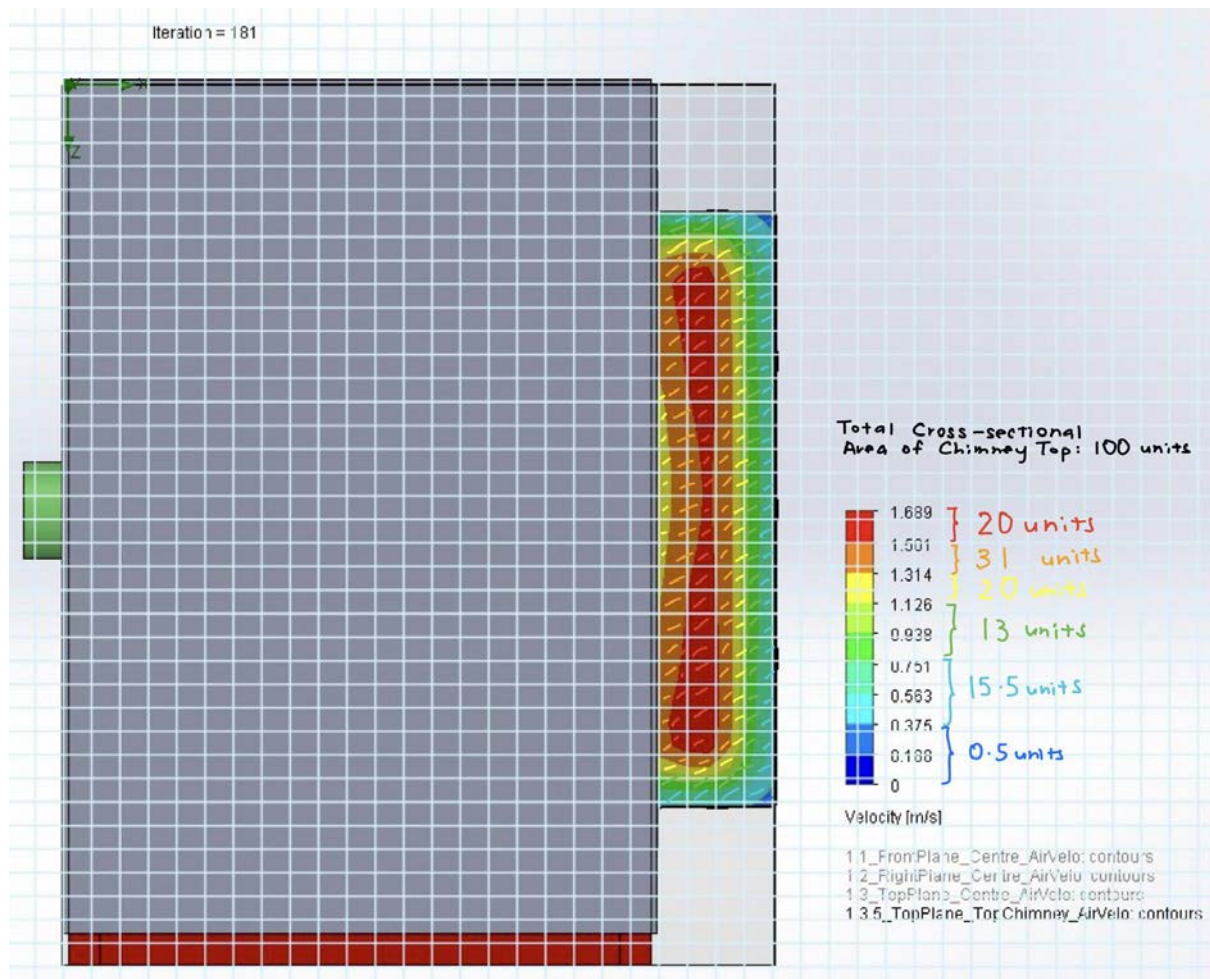


FIGURE 3.3.2h: Counting of rectangles to estimate the average velocity of the exit airflow

TABLE 3.3.2b: Key values considered when determining the air exchange out of our full-fan spacing configured reactor

Parameter	Value
Area of cross-section of outlet	0.064 m ²
Average velocity	4356 m/h
Air exchange out of reactor	278.784 m ³ h ⁻¹
Air exchange required of our reactor	274.337 m ³ h ⁻¹
Conclusion from Simulation 2.1: Half-fan spacing configuration with edited shape fans and current chimney size is sufficient for the air exchange required of our reactor	

To determine the air exchange out of the reactor, the average velocity of the exit air was determined by counting the rectangles marked out in FIGURE 3.3.2h and tabulated in TABLE M - 2 of Appendix M. Based on data from the Solidworks Flow Simulation and calculations, the air exchange out of our reactor is 278.784 m³ h⁻¹, which is larger than the 274.337 m³ h⁻¹ air exchange required for our reactor, refer to TABLE 3.3.2b for the calculations breakdown.

With the simulation results of Simulation 2 and Simulation 2.1, it is unclear whether the airflow for half-fan spacing configuration would be sufficient. Since there would be major benefits to the loading and unloading process if the half-fan spacing configuration is used instead of the full-fan spacing, there is a need to conduct actual airflow tests using our physical prototype to determine its actual airflow exchange performance.

3.3.3 Airflow Simulation for Half-fan spacing Configuration with fan tubes

The actual airflow exchange performance of the half-fan spacing configuration is unclear from the simulation results and it is potentially due to the limitations of the simulation software such as its inability to simulate the actual flow when a part of a fan's outlet is covered. Due to the benefits of using half-fan spacing configuration over full-fan spacing, it is worth exploring other ways to enable the use of half-fan spacing while meeting the ventilation requirements.

One potential method is the addition of a fan tube between the fan and the reactor. The use of a fan tube can potentially aid with reducing the speed of air that collides into the obstruction hence possibly reducing the turbulence in the airflow and eventually improving the air exchange in a half-fan spacing configuration.

To test out the fan tube idea, a 50 mm length fan tube was added to the reactor as shown in FIGURE 3.3.3a.

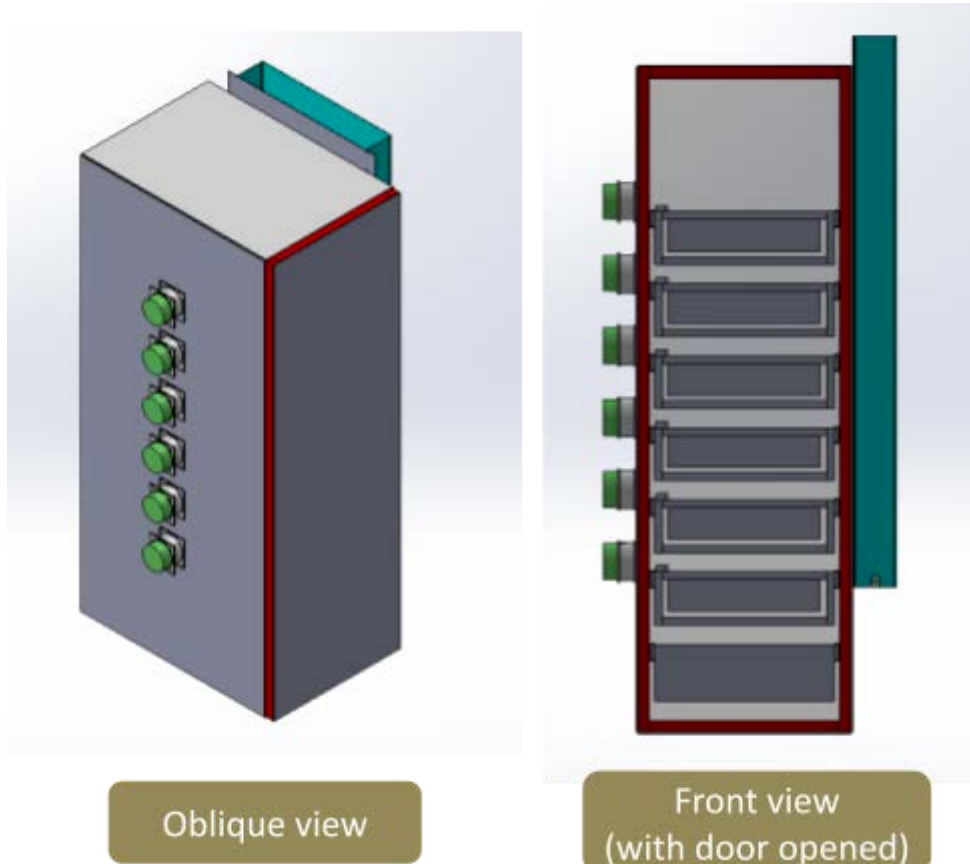
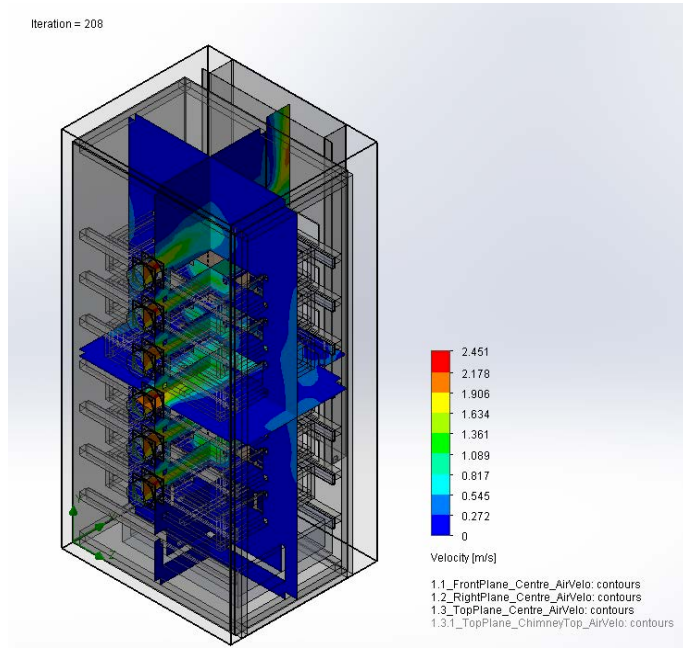


FIGURE 3.3.3a: 3D CAD of half-fan spacing configuration with 50mm fan tubes



The results of the airflow simulation are shown in FIGURE 3.3.3b. The average velocity of the air exiting the chimney is tabulated in Table M - 3 of Appendix M.

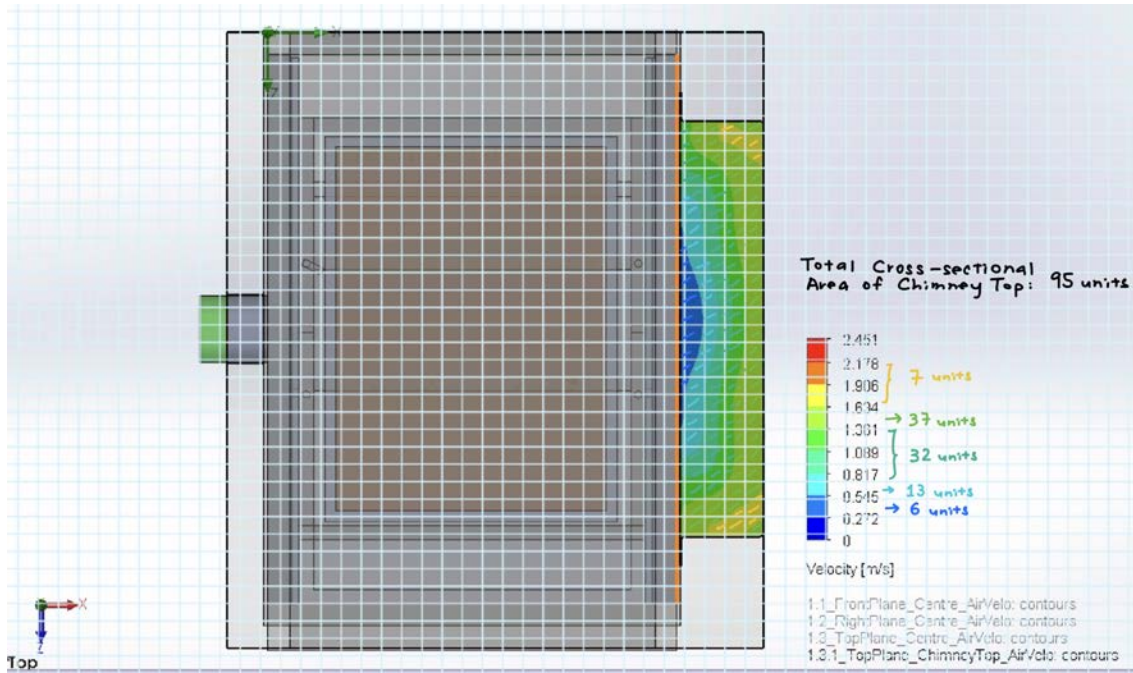


FIGURE 3.3.3c Counting of rectangles to estimate the average velocity of the exit airflow

TABLE 3.3.3a: Key values considered when determining the air exchange out of our half-fan spacing configured reactor with 50 mm fan tubes

Parameter	Value
Area of cross-section of outlet	0.064 m ²
Average velocity	4352.4 m/h
Air exchange out of reactor	278.554 m ³ h ⁻¹
Air exchange required of our reactor	274.337 m ³ h ⁻¹
Conclusion from Simulation 3: Half-fan spacing configuration with 50 mm fan tubes and current chimney size is sufficient for the air exchange required of our reactor	

Based on data from the Solidworks Flow Simulation and calculations, the air exchange out of our reactor is 278.554 m³ h⁻¹, which is larger than the 274.337 m³ h⁻¹ air exchange required for the size of our reactor, refer to TABLE 3.3.3a for the calculations breakdown. Hence, this half-fan spacing configured reactor with 50 mm fan tubes configuration and chimney size is sufficient for the air exchange required of our reactor.

3.3.4 Simulation findings

TABLE 3.3.4: Summary of simulation results of the three configurations

Configuration	Simulated air exchange out of reactor	Air exchange required of our reactor
Full-fan spacing configured reactor	276.480 $\text{m}^3 \text{h}^{-1}$	274.337 $\text{m}^3 \text{h}^{-1}$
Half-fan spacing configured reactor	259.648 $\text{m}^3 \text{h}^{-1}$	
Half-fan spacing configured reactor with edited fan shape	278.784 $\text{m}^3 \text{h}^{-1}$	
Half-fan spacing configured reactor with 50 mm fan tubes	278.554 $\text{m}^3 \text{h}^{-1}$	

A summary of the simulation results of the air exchange performance of the different configurations is tabulated in TABLE 3.3.4. From the simulations, the current sizing and configurations for the full-fan spacing and half-fan spacing with 50 mm fan tubes would provide sufficient air exchange for our reactor. However, the performance of the half-fan spacing with fans directly mounted onto the reactor wall is unclear. Given that the half-fan configuration is preferred to meet our user needs compared to the full-fan configuration and the performance of half-fan configuration is unclear, both the half-fan and full-fan configurations would be prototyped to allow actual air flow tests to be conducted. With the actual air flow test conducted on a physical prototype of our reactor, the performance of the ventilation system in different configurations can be more accurately evaluated.

4 Fabrication and Testing of Ventilation System

4.1 Fabrication of prototype

The ventilation subsystem is responsible for the manufacturing and procuring of the walls of the reactor, the chimney system and the fans and peripheral items required for the ventilation system. Hence this section focuses on the fabrication of the walls and chimney of our prototype reactor.

4.1.1 Walls of reactor

Acrylic sheets were chosen to be used as the walls of our reactor due to the ease of adding on more features on our wall should it be required after the acrylic sheet wall has been first completed. This is possible by laser cutting of the acrylic sheet when new needs arise.

Given the large walls of our reactor, as shown in FIGURE 4.1.1a, each side of the walls has to be manufactured in multiple parts to fit into the work bed of the available laser cutter machines in NUS workshops. The EPILOG LASER FUSION M2 32 laser cutter in the Professional Workshop which has a smaller work area of 812 x 508 mm was more readily available than the EPILOG LASER FUSION M2 40 laser cutter in the Fabrication Laboratory which has a work area of 1016 x 711 mm. Due to the limited time of the project, most of the items that can be easily reduced into smaller pieces without having any major impact on the structural integrity and its function were redesigned to fit into the smaller laser cutter to reduce the manufacturing time.

However, there are still sides of the reactor's walls that cannot be reduced to fit into the smaller but more readily available machine. The reactor's left and right walls have one side with 815 mm length, as shown in FIGURE 4.1.1a, to split the wall into multiple pieces in order to reduce that 815 mm length would compromise the fitting and mounting of the fans onto our left walls, as well as the mounting of the chimney on the right wall. Hence those pieces were manufactured with the larger laser cutter.

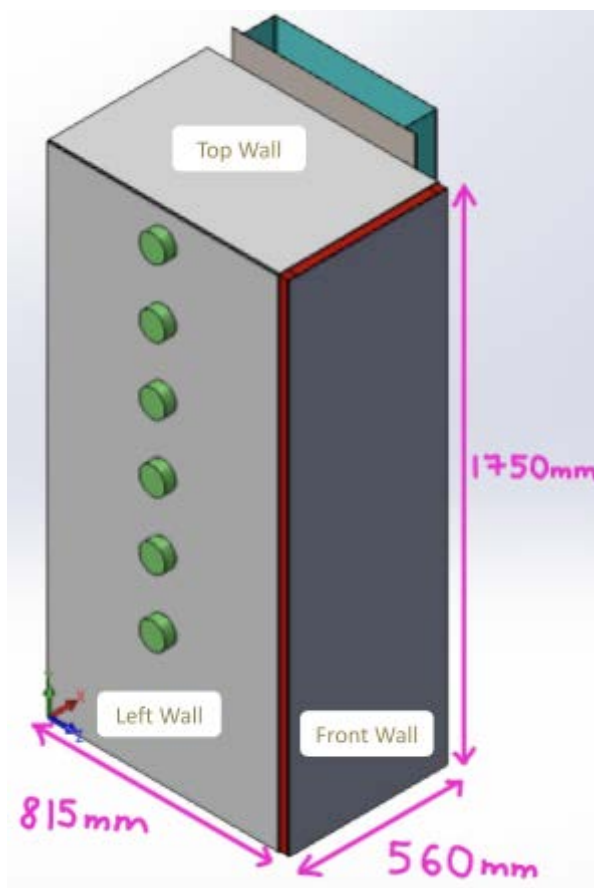


FIGURE 4.1.1a: Dimensions of the walls of our reactor

Due to the need to mount the six fans and chimney onto the walls of our reactor and the large length each piece extends to, the thickness of the acrylic sheets was chosen to be 5 mm for its rigidness.

4.1.2 Chimney

Since the purpose of the chimney is just to direct airflow and is not a load-bearing structure, the thickness of the aluminium sheet was chosen to be 1 mm thin. The base of the chimney was initially designed to have small extruded parts for mounting to the main chimney, however a more practical design from the manufacturing point of view is to have one whole continuous pieces for securing as shown in FIGURE 4.1.2a.



FIGURE 4.1.2a: Improved base cover mounting design

4.1.3 Fan tube

Various methods of manufacturing the fan tube were considered. One of which is the use of polyvinyl chloride (PVC) pipes with acrylic plates, and using adhesive to join them together. However, the PVC pipes that are readily available are often too big or too small, with the common 90 mm and 110 mm inner diameter pipes being the closest fit.

Another method is to 3D print the fan tube. The fan tube will be printed in three pieces, as shown in FIGURE 4.1.3a, and using epoxy to join the three pieces together. This method of manufacturing would be faster than 3D printing the whole fan tube as a single piece due to the excessive support material required. Additionally, using epoxy to bond the fan tube to the plates would be stronger than the joint made during 3D printing as a single piece.

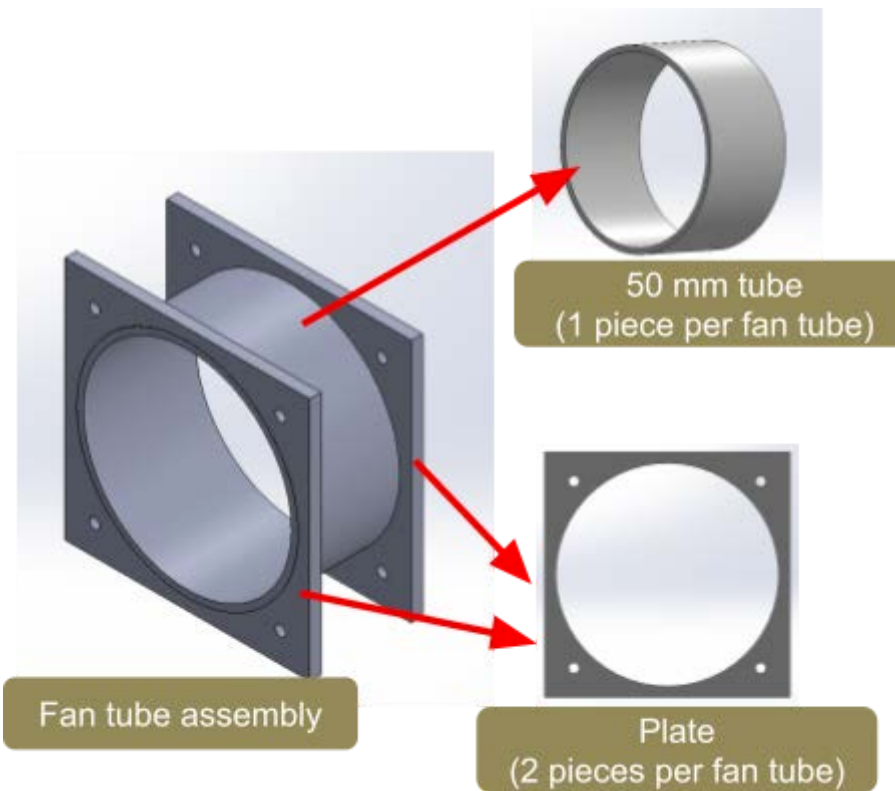


FIGURE 4.1.3a: Fan tube design for 3D printing

The school's 3D printer has both polylactic acid (PLA) and acrylonitrile butadiene styrene (ABS) filaments. PLA has low thermal resistance of around 50 °C, while ABS has a thermal resistance of up to 85 °C. Since the bioconversion process may reach around 47 °C, it would be safer to print the fan tubes using ABS [51], [52].

After printing the parts, the inner diameter of the circular plate is filed with a coarse sandpaper of 100-grit to ensure that there is a small gap between the tube and the plate, and there are some non-uniform gaps for epoxy to seep in. This would allow the epoxy to stay between the plate and tube contact compared to when the tube is forced into the plate and the epoxy gets oozed out, leaving little epoxy bonding the pieces together. The parts are left on a flat surface and screws

inserted into the four mount holes to ensure that the parts would cure in the correct position as shown in FIGURE 4.1.3b.

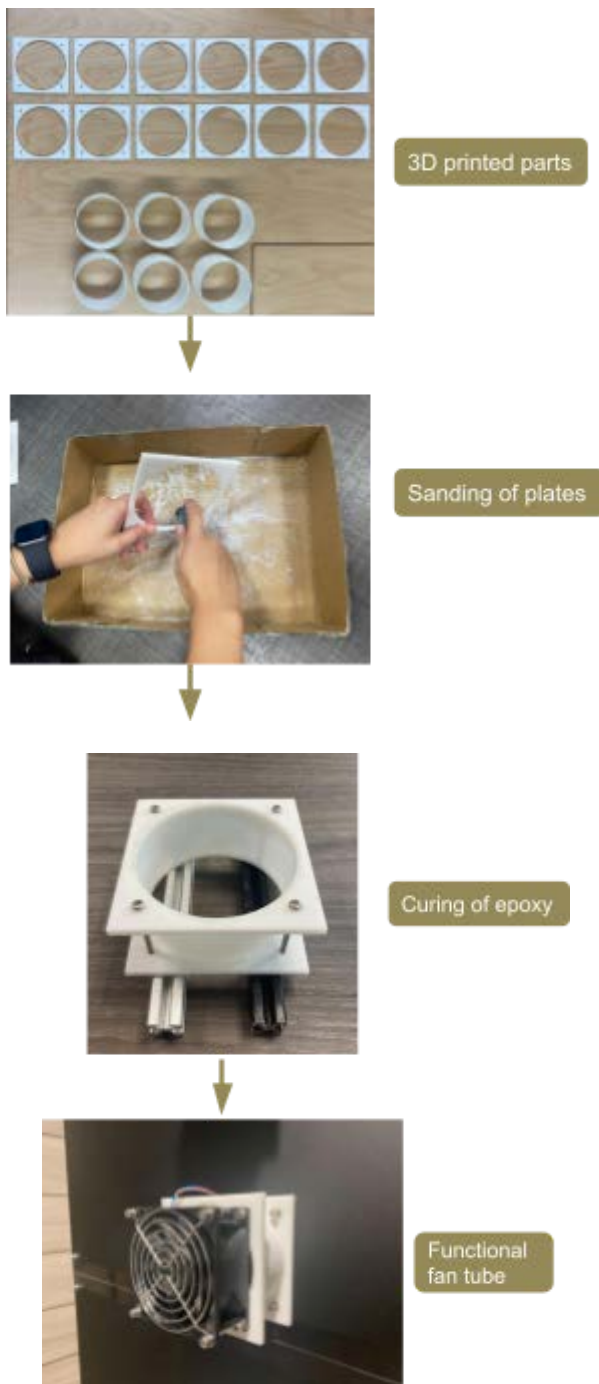


FIGURE 4.1.3b: Manufacturing process of the fan tube

4.2 Assembly

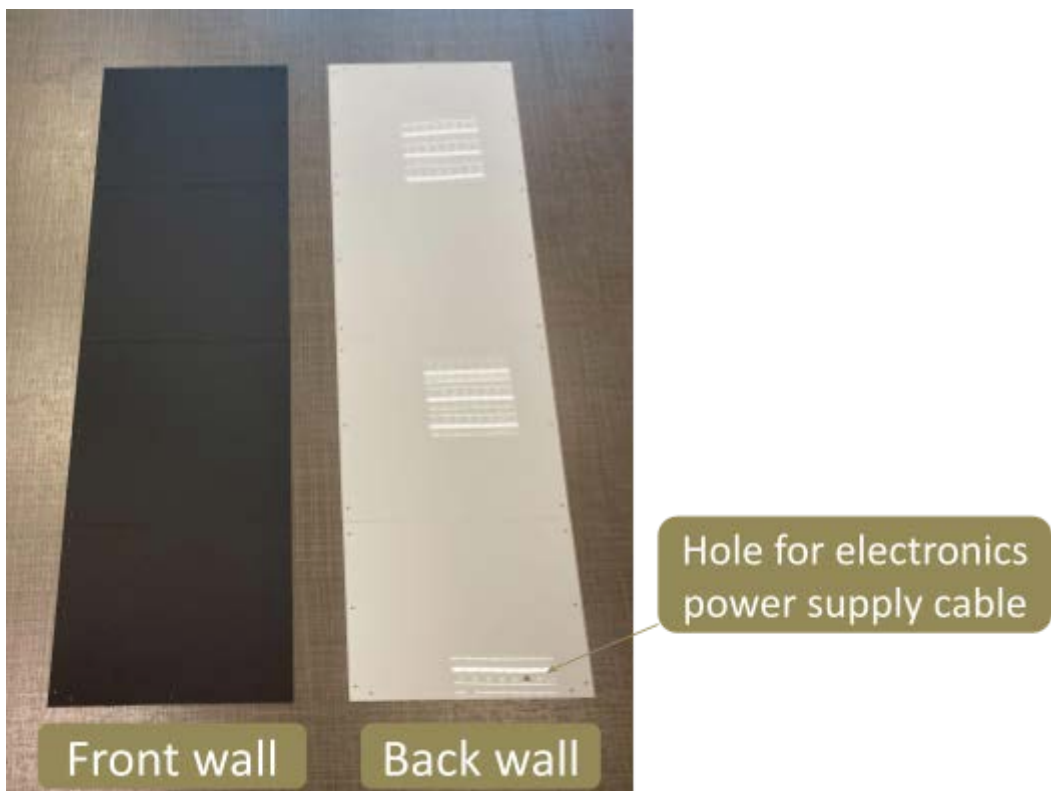


FIGURE 4.2a: Front and back walls prior to assembling

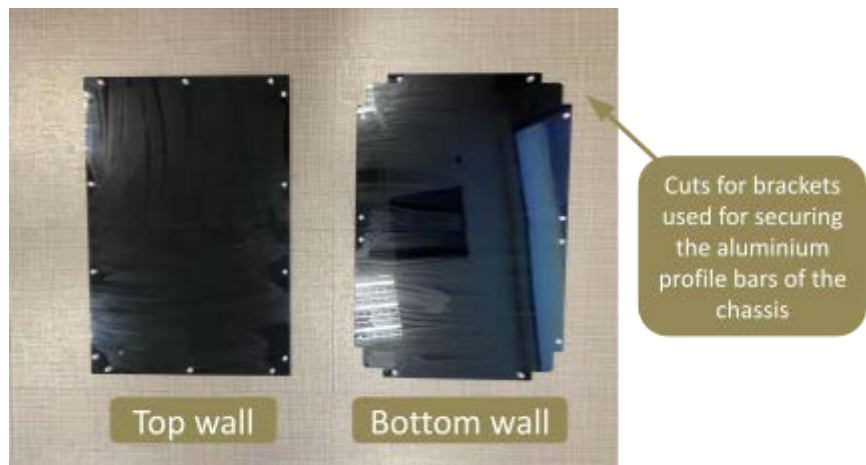


FIGURE 4.2b: Top and bottom walls prior to assembling

4.2.1 Assembly of full-fan spacing configuration

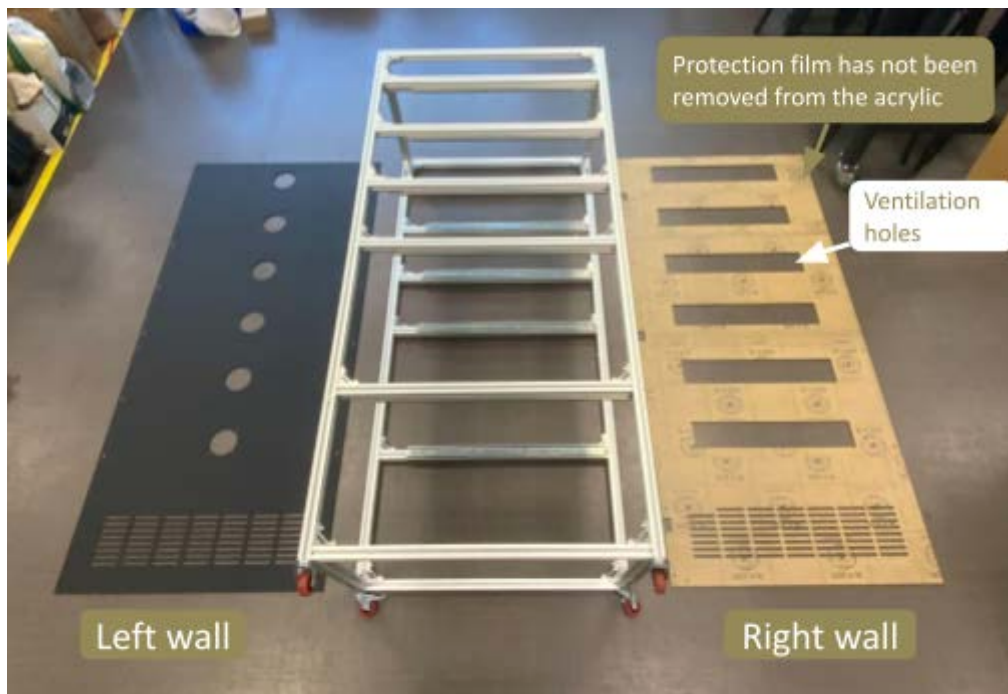


FIGURE 4.2.1a: The left and right walls of the full-fan spacing configuration prior to assembling

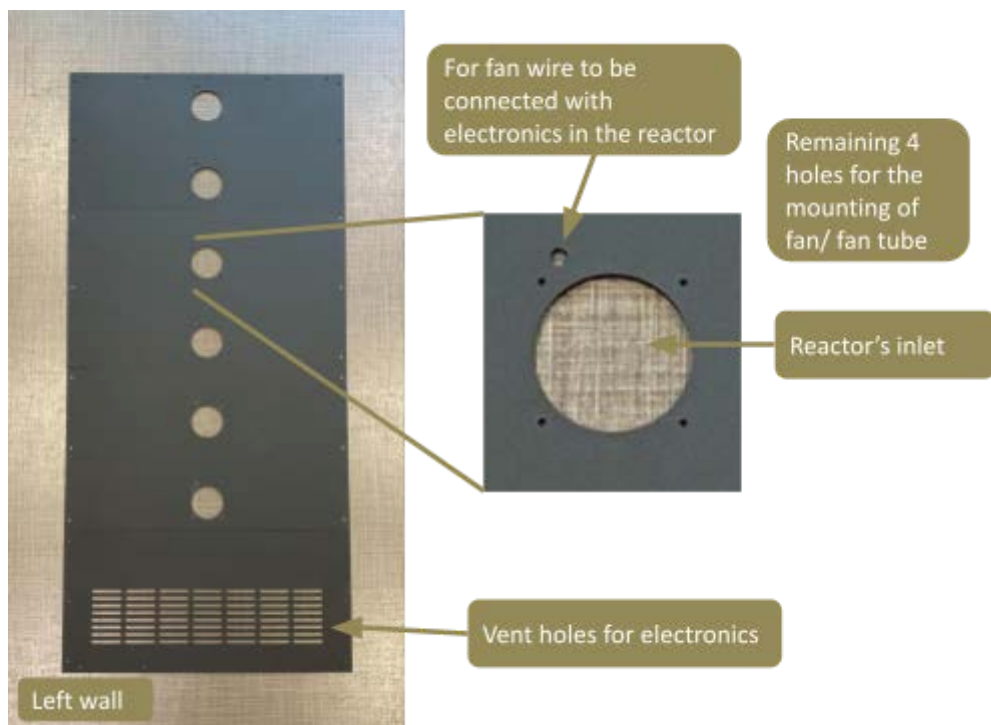


FIGURE 4.2.1b: Cut features of the left wall



FIGURE 4.2.1c: 16 mm M6 bolts and M6 rhombus nuts were used together with M6 spring and flat washers (not shown in image) for the mounting of the walls



Left wall



Right wall

FIGURE 4.2.1d: Left and right walls after mounting



With fans mounted



Door opened

FIGURE 4.2.1e: Full-fan spacing configuration

4.2.2 Assembly of half-fan spacing configuration



With fans mounted



Door opened

FIGURE 4.2.2: Half-fan spacing configuration

4.2.3 Assembly of half-fan spacing with fan tube configuration



With fans mounted



Door opened

FIGURE 4.2.3: Half-fan spacing with tube configuration

4.3 Airflow Testing

The purpose of this airflow testing is to gain a better understanding of the performance of the ventilation system in our reactor for the different configurations. This is done by conducting chimney outflow, fan inlet and outlet, as well as tray distribution tests. The purpose of the various tests has been summarised in TABLE 4.3.

The instrument used for the air velocity readings is the Testo 425 air velocity metre which was borrowed from the SEC laboratory. It has a range of 0 to 20 m/s and an accuracy of up to 0.03 m/s [53].

TABLE 4.3: Summary of the various airflow tests

Type of test	Purpose of test
Outflow	Check if the configuration is able to achieve the required air exchange of $274.337 \text{ m}^3 \text{ h}^{-1}$
	Observe the outflow distribution at the chimney outlet
Fan inlet and outlet	Observe the relationship between the inlet and outlet airspeed of the fans
	Find out if the performance of fan is affected by the location on the reactor it has been mounted to
Tray airflow distribution	Observe the airflow distribution within each tray
	Observe the effects of the tray location on the airflow distribution within each tray

4.3.1 Chimney outflow

The aim of the chimney outflow test is to check if the configuration is able to achieve the required air exchange of $274.337 \text{ m}^3 \text{ h}^{-1}$ and observe the outflow distribution at the chimney outlet.

For the chimney outflow test, the anemometer was used to take readings at six locations at the chimney exit, L1, L2, L3, R1, R2 and R3 which is illustrated in FIGURE 4.3.1a.

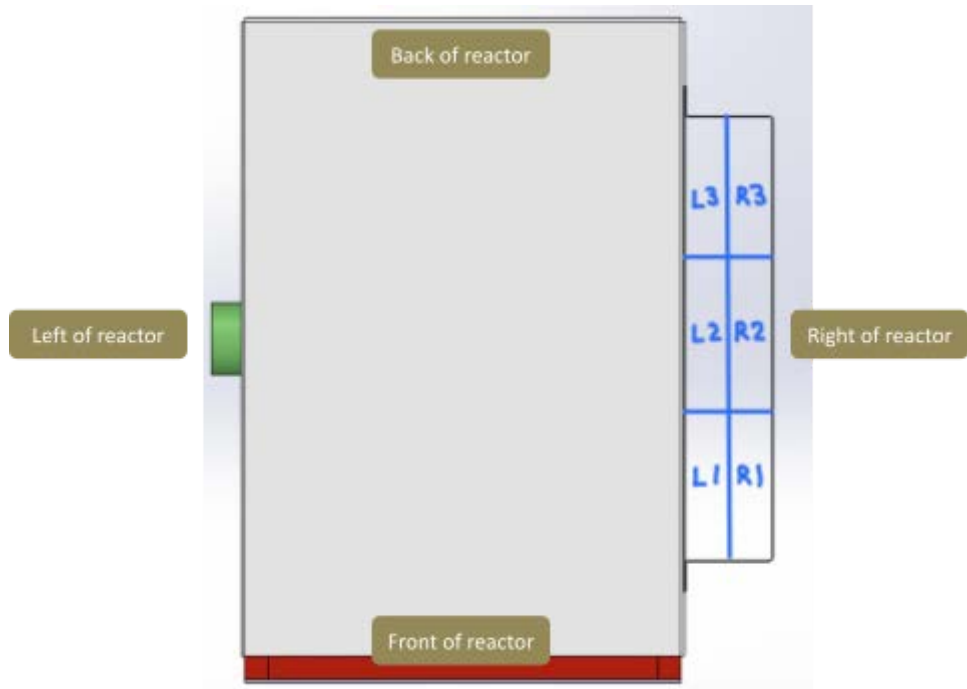


FIGURE 4.3.1a: The six locations where the chimney outflow readings were taken



FIGURE 4.3.1b: Shows the orientation the anemometer should be in when taking readings



FIGURE 4.3.1c: The setup for the chimney outflow testing

TABLE 4.3.1: Evaluation of chimney air exchange rate

Given that the cross-sectional area of the chimney = 0.064 m^2 Total required air exchange of our reactor = $274.337 \text{ m}^3 \text{ h}^{-1}$			
Configuration	Average velocity of exiting air @ PWM 20%	Actual air exchange	Simulation air exchange values
Full-fan spacing	1.803 m/s	$344.832 \text{ m}^3 \text{ h}^{-1}$	$276.480 \text{ m}^3 \text{ h}^{-1}$
Half-fan spacing	1.517 m/s	$349.517 \text{ m}^3 \text{ h}^{-1}$	$259.648 \text{ m}^3 \text{ h}^{-1}$ and $278.784 \text{ m}^3 \text{ h}^{-1}$
Half-fan spacing with 50 mm fan tube	1.497 m/s	$344.909 \text{ m}^3 \text{ h}^{-1}$	$278.554 \text{ m}^3 \text{ h}^{-1}$

It is hard to compare the results between the simulation and actual testing as the conditions are very different. Firstly, the airspeed at the inlet of the reactor in the simulation ranges from 1.915 m/s to 2.450 m/s, while the ranges for the airspeed at the inlet of the reactor in this PWM = 20% ranges from 1.497 m/s to 1.803 m/s. Despite the higher inlet airspeed in simulations, the air exchange of this actual prototype is 25% higher than air exchange in simulations. This is potentially due to the reactor being in airtight condition in all parts except the inlet and outlet chimney of the reactor, while the prototype reactor used for this testing is far from airtight. The airtight conditions in the simulation may have caused the slower airflow and hence air exchange. Additionally, in the simulation, a full circular cross section was used for the inlet airflow which is very different from an actual fan. The actual fan has blades and the trajectory of the wind may have a radial direction airflow which may aid in promoting airflow within the reactor compared to a forward travelling airflow.

FIGURE 4.3.1d shows the readings taken during the chimney outflow test for the full-fan configuration. From the outflow data collected, it is noted that air velocity at L1, L2 and L3 are lower than at R1, R2 and R3. Additionally L2 tends to have the lowest air velocity among the L locations while R2 tends to be the lowest among the R locations. Moreover, L3 tends to have a slightly higher air velocity record than L1, while R1 and R2 have similar air velocity.

PWM @ 100% (255)													
Probe Location/ Reading	Min Reading	Max Reading	Average	Reading 1	Reading 2	Reading 3	Reading 4	Reading 5	Reading 6	Reading 7	Reading 8	Reading 9	Reading 10
L1	1.46	3.43	2.56	1.88	3.41	3.31	2.27	1.60	3.05	2.75	2.94	2.65	1.77
L2	0.63	1.56	1.21	0.78	0.82	1.54	1.33	1.40	1.51	1.48	1.06	0.68	1.50
L3	1.47	3.35	2.10	2.43	2.26	1.59	3.24	1.92	1.54	2.18	2.05	2.15	1.65
R1	3.88	4.84	4.30	4.52	3.98	3.96	4.34	4.63	4.10	4.55	3.88	4.36	4.69
R2	1.78	3.64	2.43	3.21	3.01	2.32	2.71	1.82	2.42	2.03	2.23	2.61	1.92
R3	3.70	4.77	4.30	3.79	4.56	4.65	4.64	4.39	4.19	3.74	4.27	4.23	4.58

PWM @ 60% (153)													
Probe Location/ Reading	Min Reading	Max Reading	Average	Reading 1	Reading 2	Reading 3	Reading 4	Reading 5	Reading 6	Reading 7	Reading 8	Reading 9	Reading 10
L1	1.11	2.99	1.94	2.72	1.89	1.99	2.67	1.17	1.31	2.47	1.70	2.22	1.20
L2	0.39	1.91	1.01	1.40	0.82	0.99	1.32	1.14	0.71	1.71	0.83	0.79	0.40
L3	0.67	2.54	1.64	2.34	0.75	1.64	2.36	2.37	1.96	0.75	2.38	1.02	0.79
R1	2.70	3.20	2.95	2.86	3.02	2.78	3.06	2.78	3.00	3.15	2.84	2.91	3.14
R2	2.10	3.07	2.61	2.99	3.00	2.12	2.60	2.27	2.33	2.31	2.76	2.76	3.00
R3	2.87	3.27	3.04	2.92	3.20	3.11	3.00	3.16	2.90	2.92	2.91	3.19	3.13

FIGURE 4.3.1d: An example of the readings taken during the outflow testing. Refer to Appendix N for the full data, including data collected from the outflow testing of the other configurations

4.3.2 Fan test

The purpose of the fan test is to determine whether there is a relationship between the location the fan is mounted at and its performance, as well as to determine the relationship between the velocity of the airflow entering the fan and exiting the fan. To investigate these two relationships, the fans mounted at different positions must have their inflow and outflow air velocity measured.

The inflow and outflow air velocity of the fan are measured at two points, one at the top and another at the bottom, this is shown in FIGURE 4.3.2a and FIGURE 4.3.2b, respectively. The inflow and outflow test was only conducted for the six fans in the full-fan spacing configuration due to the

limited time of the project. However, from this set of data, it is clear that there is a positive correlation between the inflow and outflow airspeed.

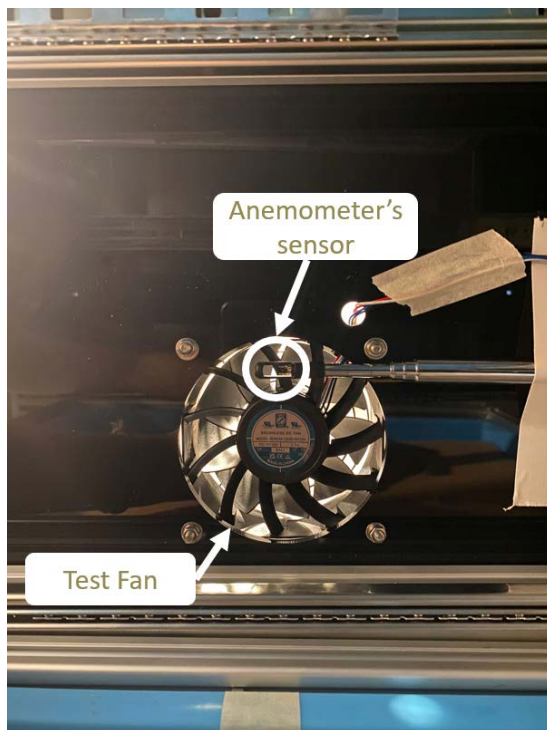


FIGURE 4.3.2a: Anemometer sensor placed at the top of the fan

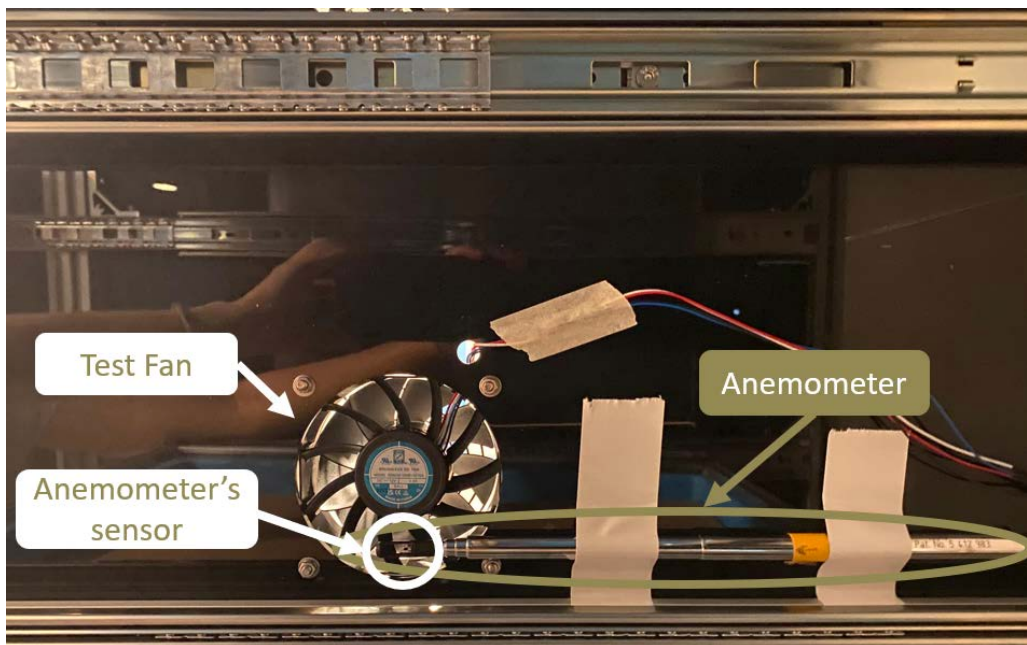


FIGURE 4.3.2b: Anemometer sensor placed at the bottom of the fan

While the investigation on the relationship between the location the fan is mounted and the performance of the fan had no clear correlation determined from the data collected.

4.3.3 Individual tray airflow distribution

To determine the individual tray airflow distribution, nine data points on each of the trays tested for the tray airflow distribution was taken, shown in FIGURE 4.3.3. From the data collected, the airflow in the middle column (C1 to C3) is consistently the highest compared to the airflow at the left (L1 to L3) and right (R1 to R3). This is possibly due to locations L1 to L3 and R1 to R3 being near the walls of the container that is perpendicular to the airflow, this perpendicular position of the walls is likely to cause a reduction in airflow near it. The left column (L1 to L3) tends to have an air velocity slightly higher than the right column (R1 to R3). This result seems reasonable given that the air travelling would tend to lose speed as the distance it travels increases. Additionally, the airflow at row 2 (L2, C2

and R2) tends to be slower than the airspeed at row 1 and 3 when compared in its own column, for example L2 tends to have a lower recorded airspeed than at L1 or L3. This is possibly due to the centre hub of the fan being located along row 2 where no airflow is generated by the centre part of the fan. These trends can be observed in FIGURE 4.3.3b where the average air velocity at the nine locations is plotted.

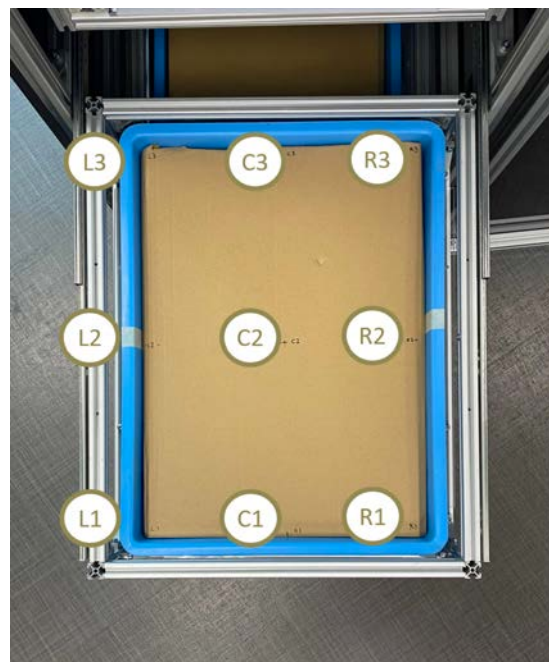


FIGURE 4.3.3a: Points where airflow is measured to determine the individual tray airflow distribution

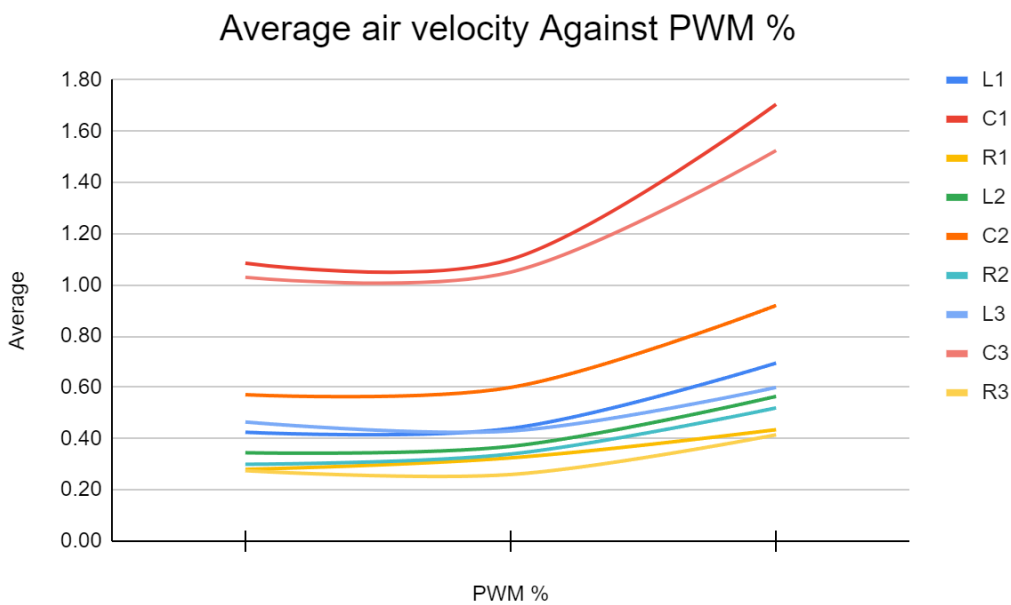


FIGURE 4.3.3b: The data of one of the trays in full-fan spacing configuration is used as an example for this Average air velocity against PWM % plot

4.3.4 Airflow testing conclusion

Through the airflow testing, the data collected has enabled a better understanding of the airflow in our reactor and the air exchange performance it has. For all the configurations, the air exchange rate at PWM 20% is higher than the requirement of $274.337 \text{ m}^3\text{h}^{-1}$. With this higher capacity, more variations on the airspeed can be done to determine a suitable airspeed that can optimise the bioconversion process and drying of the substrate. More tests would need to be done to explore the variation of PWM of the fan and its effects on bioconversion for an optimised ventilation setting.

5 Full System Testing

The aim of this first round of full system testing is to allow us to gain a better understanding of the actual change in internal environmental and substrate conditions throughout the bioconversion process that takes place in our reactor as well as to find out the effectiveness of our ventilation system. The data collected from this test would be studied and aid in determining the ventilation settings to be experimented in subsequent testings. In the long run, the data collected from the experiments would be used in determining the setting of our ventilation system for an optimised bioconversion process.

To collect useful data from the experiments, it is important to replicate the settings for the bioconversion process in our reactor to be as close to its actual deployment settings. However, a slightly smaller amount of food waste was used in this experiment, 6.5 kg of food waste was used instead of the 8 kg capacity per tray. Since this was our first full system test, the performance and suitability of our reactor's current setting for BSFL survival and the bioconversion process had not been tested prior to this test and was unknown. When BSFL are in a non-optimised environment, it has greater tendency to escape out of the trays which would be enabled if more food waste per tray was used as the feed height would increase. Therefore, a slightly smaller amount of food waste was used to reduce the likelihood of BSFL escaping in this unoptimised first full system test. Hence our reactor had a total of 39 kg of food waste in this full system testing.

5.1 Preparation of Food Waste

The preparation of food waste for our full system testing was done at the SEC laboratory where the food waste, coco peat fibre and BSFL were provided by them. The food waste used in this testing was food waste from the previous day and stored in a fridge at 4 °C and had 75 % moisture content.

For our full system testing, our reactor will be bioconverting 39 kg of food waste. The food waste was mixed with 1.23kg of coco peat fibre to bioconvert in our 6-tray configuration, key details of the test conditions can be found in TABLE 5.1.

TABLE 5.1: Key details of our full system testing

Parameters	Values
Expected duration	10 days
Number of trays	6 trays
Amount of food waste per tray	6.5 kg
Amount of coco peat fibre per tray	0.195 kg
Total food waste necessary	39 kg
Amount of larvae per tray	9280 La
Initial larvae mass	5 mg

A total of 41 kg of food waste was taken from a food waste storage pail to account for 2kg of potential food waste lost due to spillage during the preparation and the 39 kg of food waste necessary for our experiment, as shown in FIGURE 5.1a and FIGURE 5.1b.



FIGURE 5.1a: Filling of 41 kg of food waste from Food Waste Storage Pail to Mixture Pail

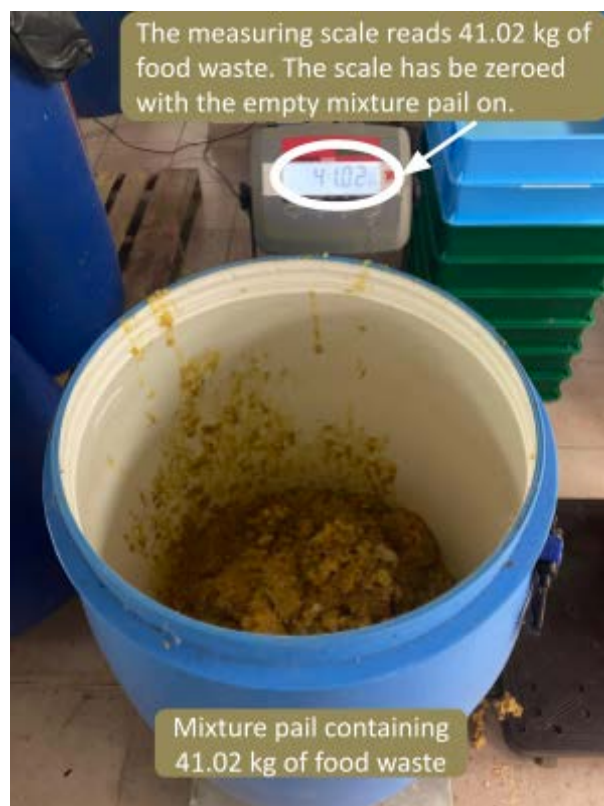


FIGURE 5.1b: 41 kg of food waste

Next, coco peat fibre was added to the food waste to reduce the moisture of the food waste. SEC has determined that 3 % of the food waste mass was the amount of coco peat fibre needed for food waste with 75 % moisture content. Hence 1.23 kg of coco peat fibre was added to the 41 kg of food waste, shown in FIGURE 5.1c.



FIGURE 5.1c: Adding coco peat fibre to food waste for moisture content reduction

Following that, the food waste and coco peat fibre were initially hand mixed using a large ladle followed by using an electric mixer, shown in FIGURE 5.1d. Although the electric mixer was a more convenient and less strenuous method for mixing, it was only used after hand mixing to prevent the light coco peat fibre from being blown away by the spinning of its mixing head. After thorough mixing, the use of a large ladle was used to visually check through the mixture for homogeneity.



FIGURE 5.1d: Mixing of food waste and coco peat fibre

After that, the trays were each filled with 6.695 kg of the food waste - coco peat fibre mixture. Due to the difference in mass of the different containers, each of them were individually weighed as shown in FIGURE 5.1e.



FIGURE 5.1e: Weighing of the mixture

After all the trays were filled with the 6.695 kg of mixture, the levelling of the mixture in each tray was done as shown in FIGURE 5.1g and FIGURE 5.1h. The height of the mixture after the levelling was consistently 3 cm for all six trays, shown in FIGURE 5.1i. Each trays were then individually securely wrapped to prevent odour contamination of the transport vehicle and transported from the SEC laboratory in NUS Science to E2A building in NUS Engineering where our reactor would be placed for this first full system test, shown in FIGURE 5.1k.



FIGURE 5.1g: Levelling of the mixture

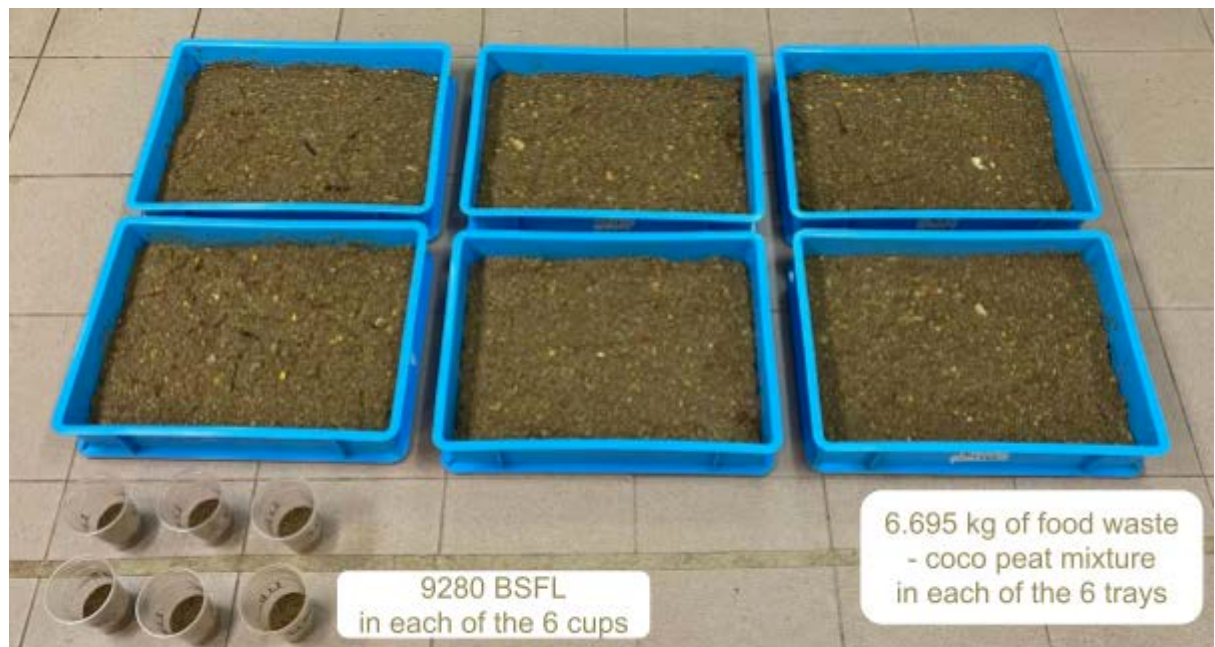


FIGURE 5.1h: 6 trays of 6.695 kg mixture and 6 cups of 9280 BSFL for our first full system test



FIGURE 5.1i: 3cm feed height



FIGURE 5.1j: Each tray was securely wrapped to prevent odour contamination of the transport vehicle



FIGURE 5.1k: Location of full system test - Level One of NUS E2A building

5.2 Characterisation of food waste

To determine the dry mass and pH of this batch of mixture, samples from the middle section of the whole 42.23kg of mixture were taken out. To determine the dry mass, three small containers of mixture were placed in a drying oven that was set at 59.4 °C, as shown in FIGURE 5.2 and details found in TABLE 5.2. The samples would be left in the oven for usually three days or until no change in mass. While the pH readings are taken by dissolving the sample in water and using the FEP20 Mettler Toledo pH sensor. The dry mass and pH readings were taken as moisture content and pH are some of

the most important parameters used to characterise the mixture used for bioconversion, and used for data analysis for the optimisation of the bioconversion process.

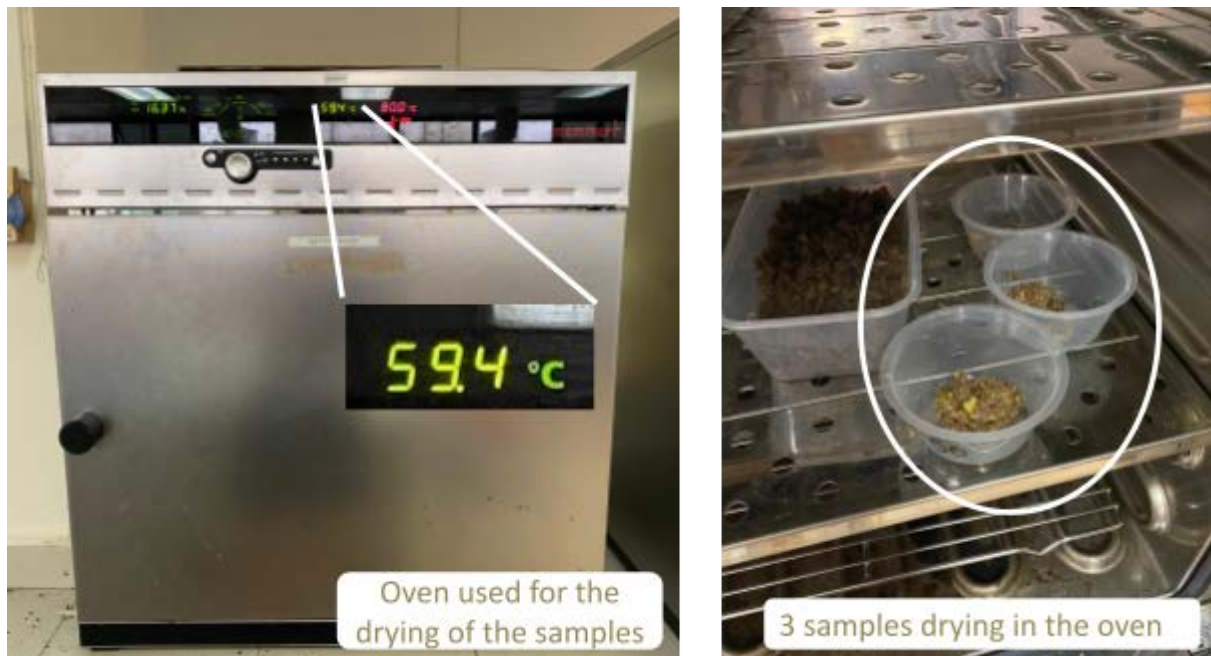


FIGURE 5.2: Drying of the three samples

TABLE 5.2: Details of the three samples

Sample Number	Mass of Cup	Mass of Cup + Sample	Mass of Cup + Dry Sample
1	5.363	17.933	(Still drying, Pending results)
2	5.343	16.510	(Still drying, Pending results)
3	5.304	23.200	(Still drying, Pending results)

5.3 Full System Test Setup



FIGURE 5.2: Full System Test Setup

The six mixture-filled six trays were loaded into our reactor, followed by putting in 9280 BSFL per tray.

Once a final electronics check that all the sensors and fans were working as expected were done, this first full system test began at 1851 on 4 April 2024.

The bioconversion of this mixture consisting of food waste with 75% moisture content and 0.3% coco peat fibre is expected to take ten days, according to A. Fuhrmann, a research student at SEC. However, apart from the composition of the mixture used, the many environmental and substrate

conditions mentioned in our design specification would affect the duration of the bioconversion process. Hence the actual end of the bioconversion would only be known via visual checks of the situation in each tray.

Our reactor will be checked daily throughout this bioconversion process to ensure that the electronics are functioning as expected and to check for any other unexpected problems for quick rectification.

5.4 Test results

At this point of writing the thesis, the full results of this bioconversion is not available yet and would be updated after the completion of the bioconversion process.

6 Conclusion and Future Work

6.1 Conclusion

Singapore generates large amounts of waste but has yet to devise an effective and sustainable solution for it, in particular its heterogeneous food waste. With the promising use of BSFL in food waste management, it is worth exploring managing Singapore's excessive food waste using BSFL. The Singapore-ETH Centre has been researching and experimenting on this food waste management method, but they are however limited to laboratory scale and setting. Hence, our project acts as a bridge, with the aim to use SEC's wealth of knowledge to apply it in Singapore's food waste problem by scaling it up.

Our solution proposes tackling the food waste produced by large food establishments as a start as larger food establishments are a big contributor to the large amounts of heterogeneous food waste Singapore generates. Additionally, these food establishments usually dispose their food waste at a nearby bin centre. Our project plans to leverage on the bin centre space to have on-site reactors which can enable a reduction in carbon footprint and reduce the need for large designated space in land-scarce Singapore as compared to when using an off-site centralised facility.

In this project, the ventilation system of the reactor has been explored via simulations and testing. From the airflow test results, a configuration with half-fan spacing between the food waste trays and six fans directly mounted on the walls of the reactor, with one fan for each tray has been selected based on its highest rate of air exchange performance among the configurations tested.

It was interesting to note that the simulation results and actual airflow test results deferred significantly. However, possible reasons such as the reactor in the simulation being in airtight condition in all parts except the inlet and outlet chimney of the reactor, while the prototype reactor used for this testing is far from airtight, as well as the difference in airflow promotion by an actual fan compared to in the simulation where a full circular cross-section of inlet airflow was set. Such simulations may be used as a rough gauge on the performance of a real-world environment, however, keeping in mind that the simplification of the conditions in simulations may lead to different actual results.

6.2 Future Work

Due to the time and budget constraints of this project, there are several limitations that could be worked on to improve the effectiveness of deploying a portable food waste reactor that uses BSFL to bioconvert for Singapore's food waste management.

Firstly, more configurations of the ventilation system can be explored. One of the possible configurations that has yet to be tested is the use of fewer fans and to distribute the airflow throughout the reactor. This has the potential benefit of reducing the power consumption for the operations of the reactor and the simplification of the electronics setup.

Additionally, due to the lack of time in this year-long project there are very limited testings done and the actual performance of our reactor in bioconverting food waste is unknown. Hence, more testing of the reactor and using the data collected from the reactor to better understand and optimise the system would improve the effectiveness of the use of portable BSFL-food waste reactors.

References

- [1] 'Food Waste'. Accessed: Sep. 16, 2023. [Online]. Available: <https://www.towardszerowaste.sg/foodwaste/>
- [2] 'Waste Statistics and Overall Recycling'. Accessed: Sep. 16, 2023. [Online]. Available: <https://www.nea.gov.sg/our-services/waste-management/waste-statistics-and-overall-recycling>
- [3] 'Food Waste Management'. Accessed: Sep. 17, 2023. [Online]. Available: <https://www.nea.gov.sg/our-services/waste-management/3r-programmes-and-resources/food-waste-management>
- [4] 'Written Reply to Parliamentary Question on the Domestic Recycling Rate by Ms Grace Fu, Minister for Sustainability and the Environment'. Accessed: Sep. 19, 2023. [Online]. Available: <https://www.mse.gov.sg/resource-room/category/2023-07-03-written-reply-to-pq-on-domestic-recycling-rate>
- [5] 'Food waste vs. plastic waste | Which is worse?' Accessed: Sep. 16, 2023. [Online]. Available: <https://www.zerowastescotland.org.uk/resources/food-waste-vs-plastic-waste-which-worse-environment>
- [6] 'Aluminium Cans vs Plastic Bottles | Wood Mackenzie | Wood Mackenzie'. Accessed: Nov. 12, 2023. [Online]. Available: <https://www.woodmac.com/news/feature/aluminium-vs-plastic-who-will-win-the-water-bottle-war/>
- [7] 'Solid Waste Management Infrastructure'. Accessed: Sep. 19, 2023. [Online]. Available: <https://www.nea.gov.sg/our-services/waste-management/waste-management-infrastructure/solid-waste-management-infrastructure>
- [8] 'Waste-To-Energy Incineration Plants'. Accessed: Sep. 18, 2023. [Online]. Available: <https://www.nea.gov.sg/our-services/waste-management/waste-management-infrastructure/se-makau-landfill/waste-to-energy-and-incineration-plants>
- [9] 'Semakau Landfill 20th Anniversary'. Accessed: Sep. 18, 2023. [Online]. Available: <https://www.nea.gov.sg/corporate-functions/resources/publications/books-journals-and-magazines/envision-lite/june-july-2020/semakau-landfill-20th-anniversary>
- [10] R. Cesaro, '50 years of waste management in Singapore - landfills', Zero Waste Consultant. Accessed: Nov. 11, 2023. [Online]. Available: <https://zerowastecity.com/50-years-of-waste-management-in-singapore-landfills/>
- [11] 'Waste-to-Energy Incineration Plants | Recyclopedia.sg'. Accessed: Nov. 12, 2023. [Online]. Available: <https://recyclopedia.sg/resources/wte>
- [12] 'Packaging & Sustainability Committee Site visit to Senoko Waste to Energy Plant', EuroCham. Accessed: Nov. 12, 2023. [Online]. Available: <https://eurocham.org.sg/event/packaging-sustainability-committee-site-visit-to-senoko-waste-to-energy-plant/>
- [13] 'News Releases'. Accessed: Nov. 12, 2023. [Online]. Available: <https://www.nea.gov.sg/media/news/news/index/tuasone---the-latest-and-most-land-efficient-waste-to-energy-plant-in-singapore>

- [14] K. Seghers, 'Keppel Seghers Tuas WTE Plant at a glance'.
- [15] 'tsip-brochure_printed-2018.pdf'. Accessed: Nov. 12, 2023. [Online]. Available: https://www.nea.gov.sg/docs/default-source/our-services/waste-management/tsip-brochure_printed-2018.pdf
- [16] '5.3 Pitch Dimensions and Surrounding Areas', FIFA Publications. Accessed: Nov. 12, 2023. [Online]. Available: <https://publications.fifa.com/en/football-stadiums-guidelines/technical-guideline/stadium-guidelines/pitch-dimensions-and-surrounding-areas/>
- [17] 'Semakau Landfill'. Accessed: Nov. 12, 2023. [Online]. Available: https://www.towardszerowaste.sg/semakau_landfill/
- [18] R. Kr, 'Food waste: digesting the impact on climate', New Food Magazine. Accessed: Nov. 12, 2023. [Online]. Available: <https://www.newfoodmagazine.com/article/153960/food-waste-climate/>
- [19] 'Car pollution facts: from production to disposal, what impact do our cars have on the planet?', Auto Express. Accessed: Nov. 12, 2023. [Online]. Available: <https://www.autoexpress.co.uk/sustainability/358628/car-pollution-production-disposal-what-impact-do-our-cars-have-planet>
- [20] 'Food Waste Management Strategies'. Accessed: Sep. 18, 2023. [Online]. Available: <https://www.nea.gov.sg/our-services/waste-management/3r-programmes-and-resources/food-waste-management/food-waste-management-strategies>
- [21] 'Why-Anaerobic-Digestion.pdf'. Accessed: Sep. 19, 2023. [Online]. Available: <https://www.epa.gov/sites/default/files/documents/Why-Anaerobic-Digestion.pdf>
- [22] 'Food waste at East Coast Lagoon Food Village to be turned into energy and fertiliser under pilot project', Food waste at East Coast Lagoon Food Village to be turned into energy and fertiliser under pilot project. Accessed: Sep. 20, 2023. [Online]. Available: <https://news.nus.edu.sg/food-waste-at-east-coast-lagoon-food-village-to-be-turned-into-energy-and-fertiliser-under-pilot-project/>
- [23] 'Chapter 4 - Optimising Infrastructure For Maximum Resource Recovery'. Accessed: Sep. 22, 2023. [Online]. Available: <https://www.towardszerowaste.sg/zero-waste-masterplan/chapter4/>
- [24] 'News Releases'. Accessed: Sep. 20, 2023. [Online]. Available: <https://www.nea.gov.sg/media/news/news/index/nea-launches-love-your-food-@-schools-project-to-encourage-youth-to-cherish-and-not-waste-food>
- [25] Y. Law, L. Wein, Y. Law, and L. Wein, 'Reversing the nutrient drain through urban insect farming—opportunities and challenges', *AIMSBOA*, vol. 5, no. 4, pp. 226–237, 2018, doi: 10.3934/bioeng.2018.4.226.
- [26] S. Ites, S. Smetana, S. Toepfl, and V. Heinz, 'Modularity of insect production and processing as a path to efficient and sustainable food waste treatment', *Journal of Cleaner Production*, vol. 248, p. 119248, Mar. 2020, doi: 10.1016/j.jclepro.2019.119248.
- [27] K. Franks *et al.*, 'The effect of *Rhodococcus rhodochrous* supplementation on black soldier fly (Diptera: Stratiomyidae) development, nutrition, and waste conversion', *Journal of Insects as Food and Feed*, vol. 7, no. 4, pp. 397–408, Jul. 2021, doi: 10.3920/JIFF2020.0033.
- [28] T. M. Fowles and C. Nansen, 'Insect-Based Bioconversion: Value from Food Waste', in *Food Waste Management: Solving the Wicked Problem*, E. Närvänen, N. Mesiranta, M. Mattila, and A. Heikkinen, Eds., Cham: Springer International Publishing, 2020, pp. 321–346. doi: 10.1007/978-3-030-20561-4_12.

- [29] I. Guidini Lopes, V. Wiklicky, E. Ermolaev, and C. Lalander, 'Dynamics of black soldier fly larvae composting – Impact of substrate properties and rearing conditions on process efficiency', *Waste Management*, vol. 172, pp. 25–32, Dec. 2023, doi: 10.1016/j.wasman.2023.08.045.
- [30] S. G. S. F. Agency, 'A sustainable food system for Singapore and beyond', Food for Thought. Accessed: Sep. 17, 2023. [Online]. Available: <https://www.sfa.gov.sg/food-for-thought/article/detail/a-sustainable-food-system-for-singapore-and-beyond>
- [31] 'Foods | Free Full-Text | Review of Black Soldier Fly (*Hermetia illucens*) as Animal Feed and Human Food'. Accessed: Sep. 21, 2023. [Online]. Available: <https://www.mdpi.com/2304-8158/6/10/91>
- [32] 'Sustainable waste management using black soldier fly larva: a review | SpringerLink'. Accessed: Sep. 24, 2023. [Online]. Available: <https://link.springer.com/article/10.1007/s13762-021-03524-7>
- [33] 'Black Soldier Fly'. Accessed: Nov. 12, 2023. [Online]. Available: <https://encyclopedia.pub/entry/7597>
- [34] A. Singh, B. H. Srikanth, and K. Kumari, 'Determining the Black Soldier fly larvae performance for plant-based food waste reduction and the effect on Biomass yield', *Waste Management*, vol. 130, pp. 147–154, Jul. 2021, doi: 10.1016/j.wasman.2021.05.028.
- [35] 'BSF_Biwaste_Processing_2nd_Edition_LR.pdf'. Accessed: Sep. 23, 2023. [Online]. Available: https://www.eawag.ch/fileadmin/Domain1/Abteilungen/sandec/schwerpunkte/swm/Practical_knowhow_on_BSF/BSF_Biwaste_Processing_2nd_Edition_LR.pdf
- [36] 'HOME', insectta. Accessed: Sep. 21, 2023. [Online]. Available: <https://www.insectta.com>
- [37] M. Chan, 'This Singapore startup is using insects to turn trash into treasure | CNN Business', CNN. Accessed: Sep. 21, 2023. [Online]. Available: <https://www.cnn.com/2021/08/29/business/insectta-black-soldier-fly-maggots-hnk-spc-intl/index.html>
- [38] 'News Releases'. Accessed: Nov. 14, 2023. [Online]. Available: <https://www.nea.gov.sg/media/news/news/index/closing-the-food-resource-loop-and-driving-sustainability-at-the-inaugural-food-resource-valorisation-awards>
- [39] TOGO, 'TOGO | Black Soldier Fly Garbage Treatment Solutions', TOGO Composting Solution. Accessed: Apr. 03, 2024. [Online]. Available: <https://totosolution.com/bsfl-waste-management/>
- [40] 'Interdisciplinary team to develop blueprint for sustainable urban food waste management and food systems using black soldier flies', Interdisciplinary team to develop blueprint for sustainable urban food waste management and food systems using black soldier flies. Accessed: Sep. 22, 2023. [Online]. Available: <https://news.nus.edu.sg/interdisciplinary-team-to-develop-blueprint-for-sustainable-urban-food-waste-management-and-food-systems-using-black-soldier-flies/>
- [41] N. F. Addeo *et al.*, 'Different Combinations of Butchery and Vegetable Wastes on Growth Performance, Chemical-Nutritional Characteristics and Oxidative Status of Black Soldier Fly Growing Larvae', *Animals*, vol. 11, p. 3515, Dec. 2021, doi: 10.3390/ani11123515.
- [42] 'Characterizing municipal solid waste component densities for use in landfill air space estimates - Carson Cline, Malak Anshassi, Steven Laux, Timothy G Townsend, 2020'. Accessed: Sep. 24, 2023. [Online]. Available: <https://journals.sagepub.com/doi/10.1177/0734242X19895324>
- [43] 'Effect of different environmental conditions on the growth and development of Black Soldier Fly Larvae and its utilization in solid waste management and pollution mitigation - ScienceDirect'. Accessed: Sep. 24, 2023. [Online]. Available:

- <https://www.sciencedirect.com/science/article/pii/S2352186422001985?via%3Dihub>
- [44] J. Y. K. Cheng, S. L. H. Chiu, and I. M. C. Lo, 'Effects of moisture content of food waste on residue separation, larval growth and larval survival in black soldier fly bioconversion', *Waste Management*, vol. 67, pp. 315–323, Sep. 2017, doi: 10.1016/j.wasman.2017.05.046.
- [45] S. A. Siddiqui *et al.*, 'Black soldier fly larvae (BSFL) and their affinity for organic waste processing', *Waste Management*, vol. 140, pp. 1–13, Mar. 2022, doi: 10.1016/j.wasman.2021.12.044.
- [46] M. Shumo *et al.*, 'Influence of Temperature on Selected Life-History Traits of Black Soldier Fly (*Hermetia illucens*) Reared on Two Common Urban Organic Waste Streams in Kenya', *Animals*, vol. 9, no. 3, Art. no. 3, Mar. 2019, doi: 10.3390/ani9030079.
- [47] 'accessibilitycode2019.pdf'. Accessed: Sep. 24, 2023. [Online]. Available: https://www1.bca.gov.sg/docs/default-source/docs-corp-news-and-publications/publications/cookies-acts-and-regulations/accessibilitycode2019.pdf?sfvrsn=ea84e8b7_0
- [48] 'How to Move a Vending Machine', The Professionals. Accessed: Sep. 24, 2023. [Online]. Available: <https://www.thepromove.com/news/how-to-move-a-vending-machine>
- [49] '9LG1212P1G001 | Sanyo Denki San Ace 9LG Series Axial Fan, 12 V dc, DC Operation, 420m³/h, 38.4W, 3.2A Max, 120 x 120 x 38mm | RS'. Accessed: Mar. 30, 2024. [Online]. Available: <https://my.rs-online.com/web/p/axial-fans/8621636>
- [50] 'OD9238_VXC.pdf'. Accessed: Mar. 22, 2024. [Online]. Available: https://orionfans.com/productFiles/datasheet/OD9238_VXC.pdf
- [51] F. Castaneda, 'PLA vs. ABS filament', UltiMaker. Accessed: Apr. 06, 2024. [Online]. Available: <https://ultimaker.com/learn/pla-vs-abs-filament/>
- [52] 'PLA vs. ABS: Which Filament Should You Use?', Dassault Systèmes. Accessed: Apr. 06, 2024. [Online]. Available: <https://www.3ds.com/make/solutions/blog/pla-vs-abs>
- [53] '425 - Air Velocity Meter, with Thermal Flow Probe, -20 to 70 °C NTC, 0 to 20 m/s Velocity'. Accessed: Apr. 06, 2024. [Online]. Available: <https://sg.element14.com/testo/425/anemometer-thermo/dp/1082992>
- [54] 'The_Year_in_Numbers_2023.pdf'. Accessed: Mar. 17, 2024. [Online]. Available: http://www.weather.gov.sg/wp-content/uploads/2024/01/The_Year_in_Numbers_2023.pdf
- [55] T. McEachern, 'Determining Heat Production of Black Solderi Fly Larvae, *Hermitia illucens*, to Design Rearing Structures at Livestock Facilities', 2018, doi: 10.13023/ETD.2018.479.
- [56] 'Free Surface - 2018 - What's New in SOLIDWORKS'. Accessed: Mar. 23, 2024. [Online]. Available: https://help.solidworks.com/2018/english/WhatsNew/c_free_surface.htm
- [57] 'News Releases'. Accessed: Mar. 23, 2024. [Online]. Available: <https://www.nea.gov.sg/media/news/news/index/2023-is-singapore-s-fourth-warmest-year-on-record>
- [58] 'News Releases'. Accessed: Sep. 18, 2023. [Online]. Available: <https://www.nea.gov.sg/media/news/news/index/tuas-nexus-singapore-s-first-integrated-water-and-solid-waste-treatment-facility-begins-construction>
- [59] 'Integrated Waste Management Facility'. Accessed: Sep. 19, 2023. [Online]. Available: <https://www.nea.gov.sg/our-services/waste-management/waste-management-infrastructure/integrated-waste-management-facility>

Appendix

Appendix A: Comparison between Food and Plastic Carbon emission when landfilled

- Landfilling a kilogram of food waste produces the same carbon emission as landfilling 25,000 500ml plastic bottles [5]
- A 500ml plastic bottle weighs about 8 to 10g [6]
 - Average mass of a 500ml plastic bottle = $(0.008 + 0.010)/2 = 0.009\text{kg}$
- 25,000 500ml plastic bottles weighs $25,000 * 0.009\text{kg} = \underline{\text{225kg}}$

Appendix B: Land Used for Singapore's Waste Management

- Singapore currently has four WTE plants [11], [12]. A total of 24.4 ha of land has been designated for WTE plants with the various plants land area breakdown in TABLE B.

WTE Plant	Land Area
TuasOne	4.8 ha [13]
Keppel Seghers Tuas	1.6 ha [14]
Tuas South	10.5 ha [15]
Senoko	7.5 ha [12]
TOTAL	24.4 ha

TABLE B: Land Area Occupied by Singapore's Currently-used WTE plants

- Semakau Landfill occupies 350 ha of land [17].

- Total Land Area of Singapore' WTE Plants and Semakau Landfill
= $24.4 + 350$ ha
= 374.4 ha
- International football fields have dimensions of 68m by 105m [16].
- Area of an International Football Field
= $68m * 105m$
= $7140 m^2$
= 0.714 ha
- Number of International Football Fields that is equivalent to 374.4ha of land
= $374.4 / 0.714$
= 524
- Therefore the 374.4 ha of land used for WTE plants and Semakau Landfill, is equivalent to
524 football fields

Appendix C: CO₂ Emission Due to Food Waste Generated

- 813,000 tonnes of food waste was generated in 2022 [2]
 - For every 1kg of food waste generated, over 2.5kg of CO₂ is emitted [18]
 - Total CO₂ emitted due to food waste generated in 2022 (in kilogram)
= $813,000,000 * 2.5$
= 2.0325 billion
- => **Approximately 2 million tonnes of CO₂ emitted due to food waste generated in 2022**

- On average, 5.6 tonnes of CO₂ emitted during a petrol or diesel car's production [19]
- CO₂ emitted due to food waste generated in 2022 is equivalent to producing 2.0325 million / 5.6 = 362,946 cars

=> CO₂ emitted due to food waste generated in 2022 is approximately equivalent to producing 363,000 cars

Appendix D: Applications of Anaerobic Digesters

Off-site Anaerobic Digesters

This technology is mainly used in off-site or centralised facilities, and one such application is the Integrated Waste Management Facility (IWMF), where food waste would be collected from numerous locations and transported to it. At this facility, the biogas generated would help with Tuas Nexus electricity generation. IWMF together with Tuas Water Reclamation Plant forms Tuas Nexus, Singapore's developing solution to solid waste management and used water treatment. At Tuas Nexus, the anaerobic digestion of food waste and used water sludge mixture would yield up to 40% more biogas than digesting the two inputs separately [58], [59].

However, having the treatment facility off-site leads to carbon emissions during the transportation of food waste from various collection points to the off-site facility and requires large land allocated to the treatment facility, FIGURE D shows the large designated land space for Tuas Nexus [23, p. 4].



FIGURE D: Artist's impressions of Tuas Nexus [23, p. 4]

On-site Anaerobic Digesters

While on-site applications of anaerobic digestion have been explored, they are still limited to pilot studies such as the anaerobic digester at East Coast Lagoon Food Village as shown in FIGURE 1.3 [1], [22], [24]. The biogas produced is used to generate electricity to power itself and has excess electricity that can power fans at the hawker. In hopes to close the food waste loop, the digestate produced is being studied by NParks for its efficacy for growing plants and landscaping [22].

This on-site solution is self-sufficient in its energy needs. However, its effectiveness in contributing to other power sources and the use of its digestate in closing the food waste loop would require further research and testing [22].

Appendix E: Food Waste Management Transportation Carbon Emission

Usual food waste disposal without bioconversion using BSF

- Transport **190kg** of food waste per hawker centre per day to centralised facility

Food waste is bioconverted at the food waste source

Before Bioconversion,

- Average mass of a 5 day old larvae (5-DOL):

0.06g [41]

- Larvae - Food Waste Density before bioconversion (larvae/cm²):

4.5 larvae/cm² (According to Adrian Fuhrmann, a research staff at the SEC project)

- Food Waste height for BSFL bioconversion in a container before bioconversion = 6cm

(According to Adrian Fuhrmann, a research staff at the SEC project)

- Hence, for food waste with height of 6cm before bioconversion,

$$4.5/6 = 0.75 \text{ larvae/cm}^3 = 0.75 * 1000000 \text{ larvae/m}^3 = 750000 \text{ larvae/m}^3$$

- Mass of 5-DOL larvae per m³ of food waste:

$$750000 * (0.06/1000) = 45\text{kg/m}^3$$

- Food waste density:

$$1.565 \text{ tonne/m}^3 [42]$$

- Volume 188kg of food waste would take up:

$$(190 / 1565) * 1 = 0.12 \text{ m}^3$$

- Mass of larvae required for 188kg of food waste:

$$45 * 0.12 = \underline{\textbf{5.4kg}}$$

After bioconversion,

- Average mass of a BSFL after feeding:

$$0.2g [41]$$

- Mass of BSFL that bioconverted 188kg of food waste:

$$750000 * (0.2/1000) * 0.12 = 18kg$$

- Food waste mass reduced by 80% compared to before bioconversion
- Mass of residue left after 190kg of food waste was bioconverted:

$$190 * 0.2 = 38kg$$

- Total mass of BSFL and residue to transport to centralised facility:

$$18 + 38 = \underline{\textbf{56kg}}$$

- Total load to be transported when using our solution: $5.4 + 56 = 61.4kg$

Assuming that the carbon emission due to transportation is only affected by the load mass and is directly proportional to it, transportation for the current food waste management method produces three times more carbon emission than our solution.

- Current food waste management method would produce carbon emission to transport a load of 190kg
- Food waste management using BSFL (Our Solution) would produce carbon emission to transport a load of 61.4kg

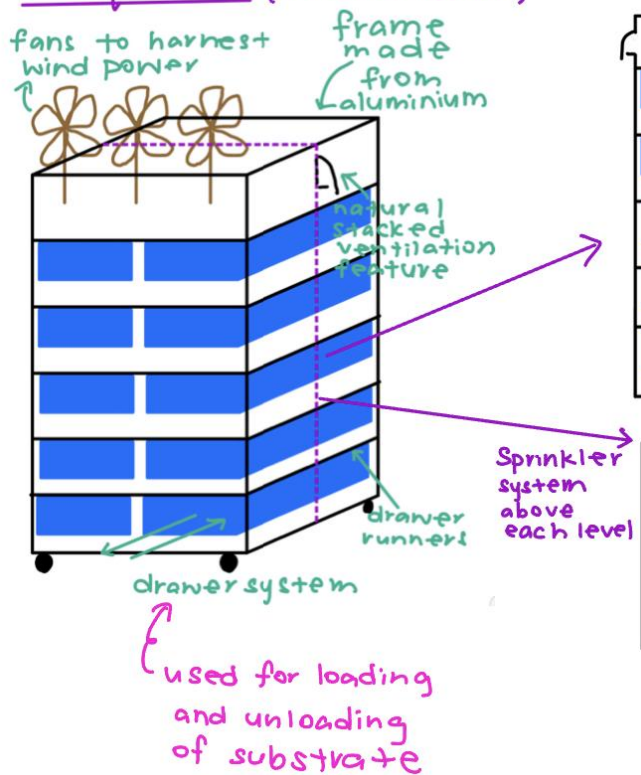
Appendix F: Concept Generation and Evaluation Matrix Table

CONCEPT A

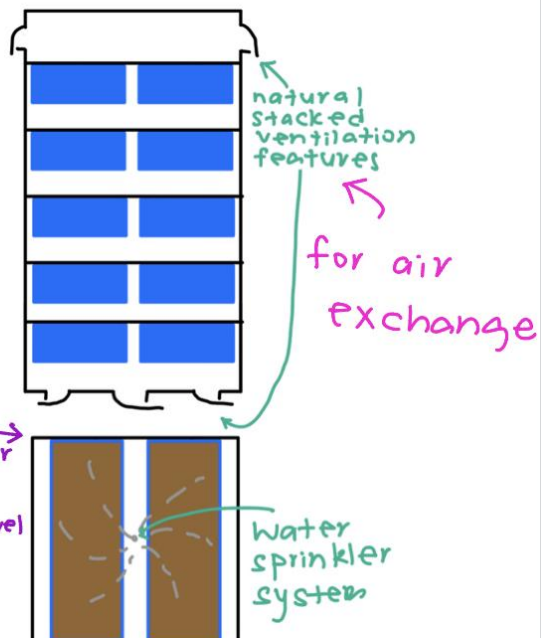
Oblique view



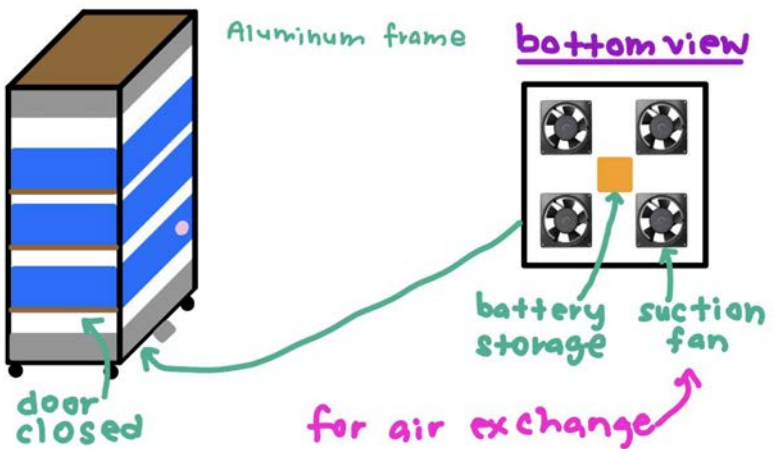
Oblique view (wo doors shown)



Cross-sectional view



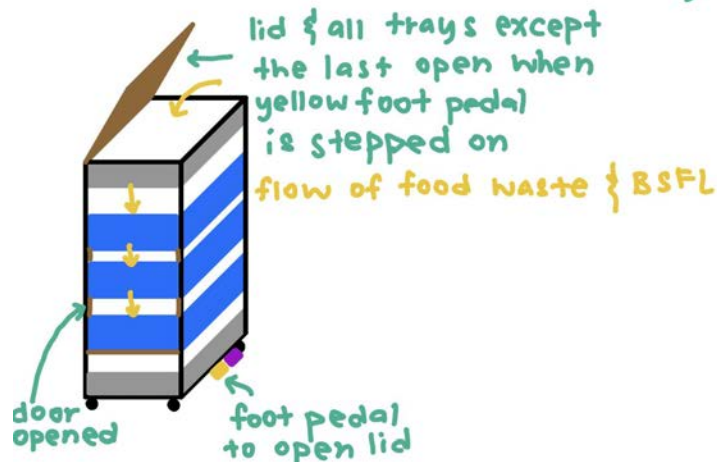
CONCEPT B



Loading / unloading of substrate



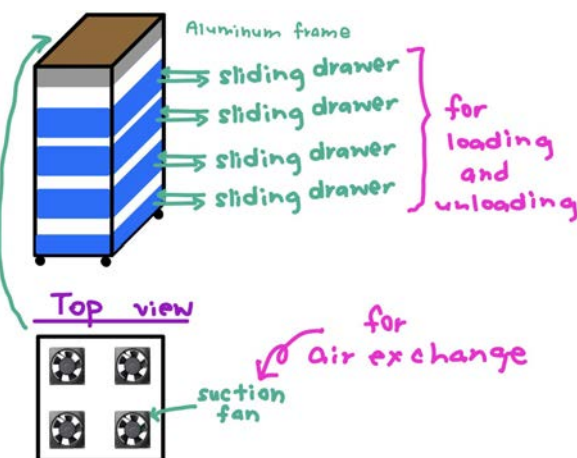
For food waste & BSFL loading



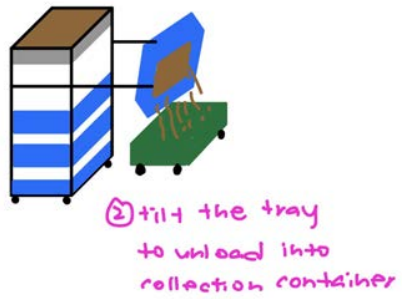
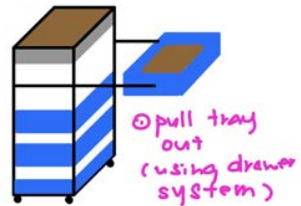
For food waste & BSFL unloading



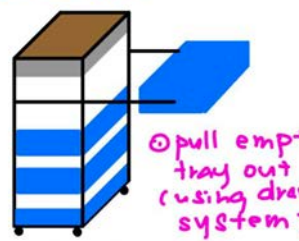
CONCEPT C



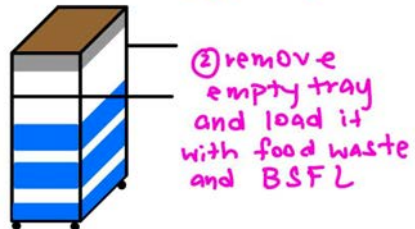
Unloading process



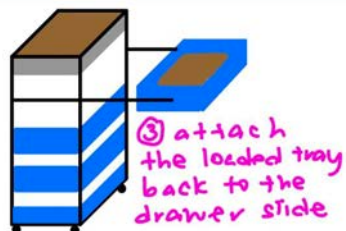
Loading process



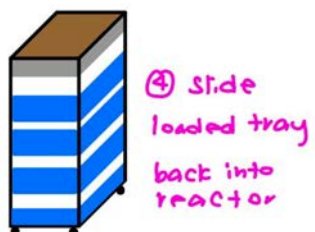
① pull empty tray out (using drawer system)



② remove empty tray and load it with food waste and BSFL

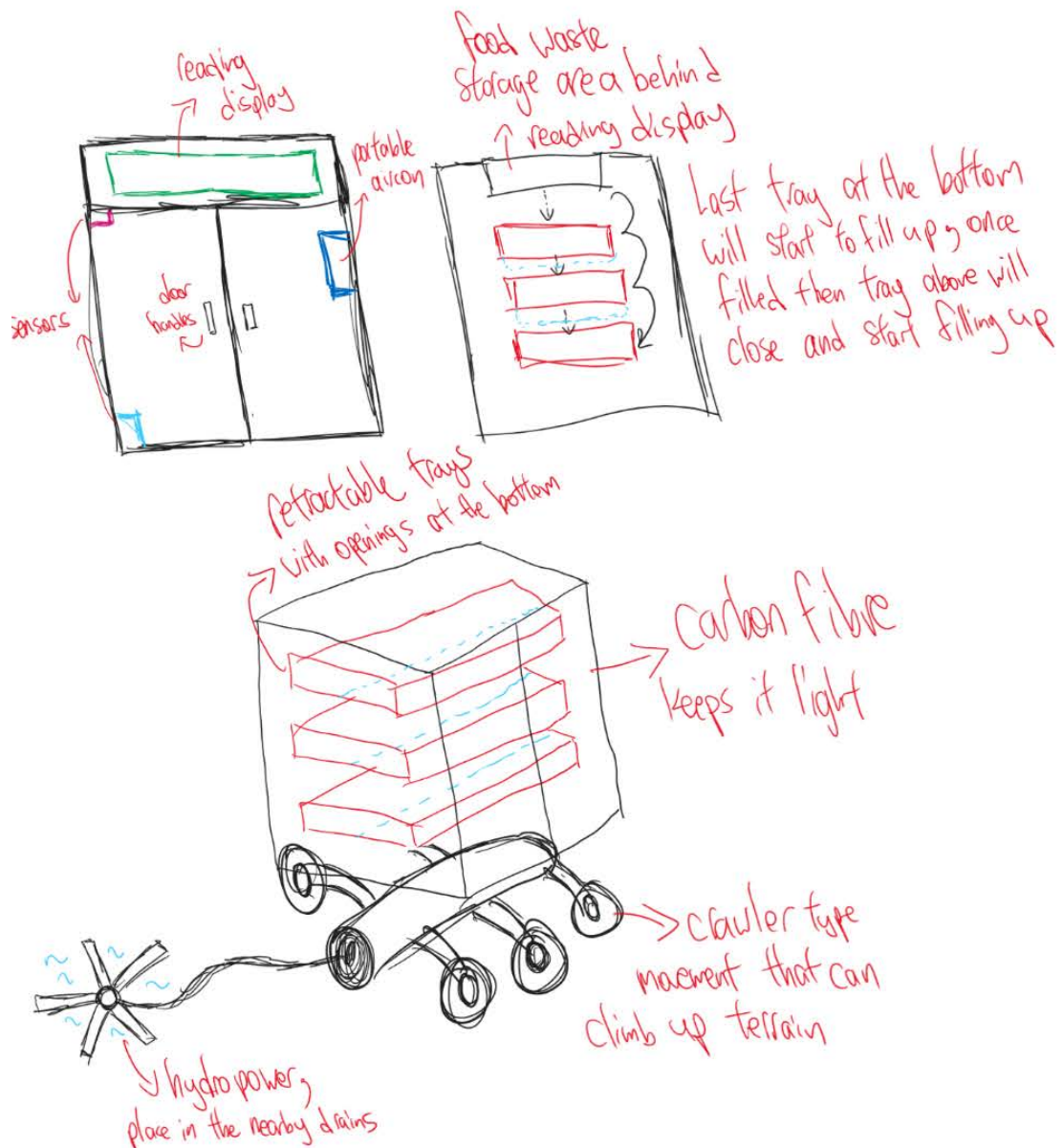


③ attach the loaded tray back to the drawer slide

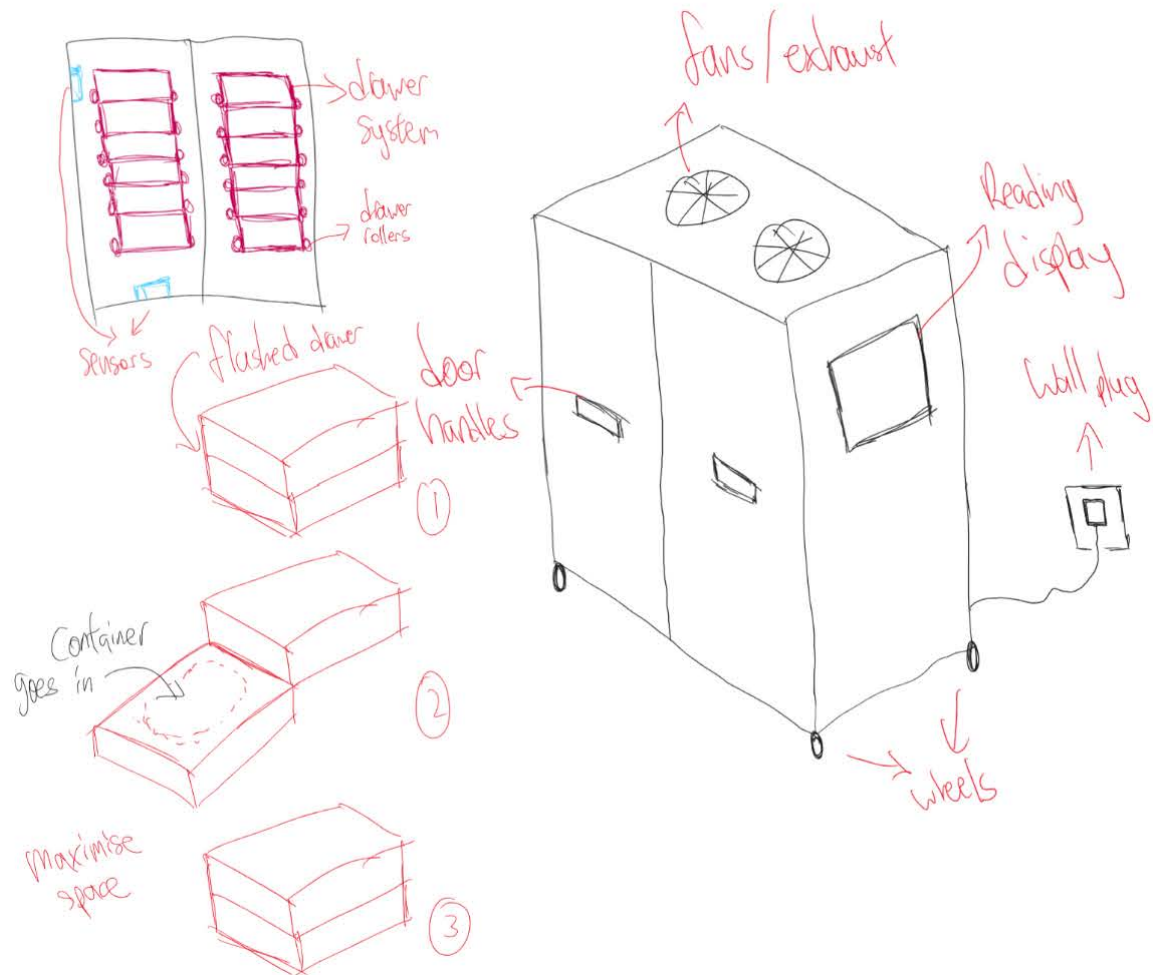


④ slide loaded tray back into reactor

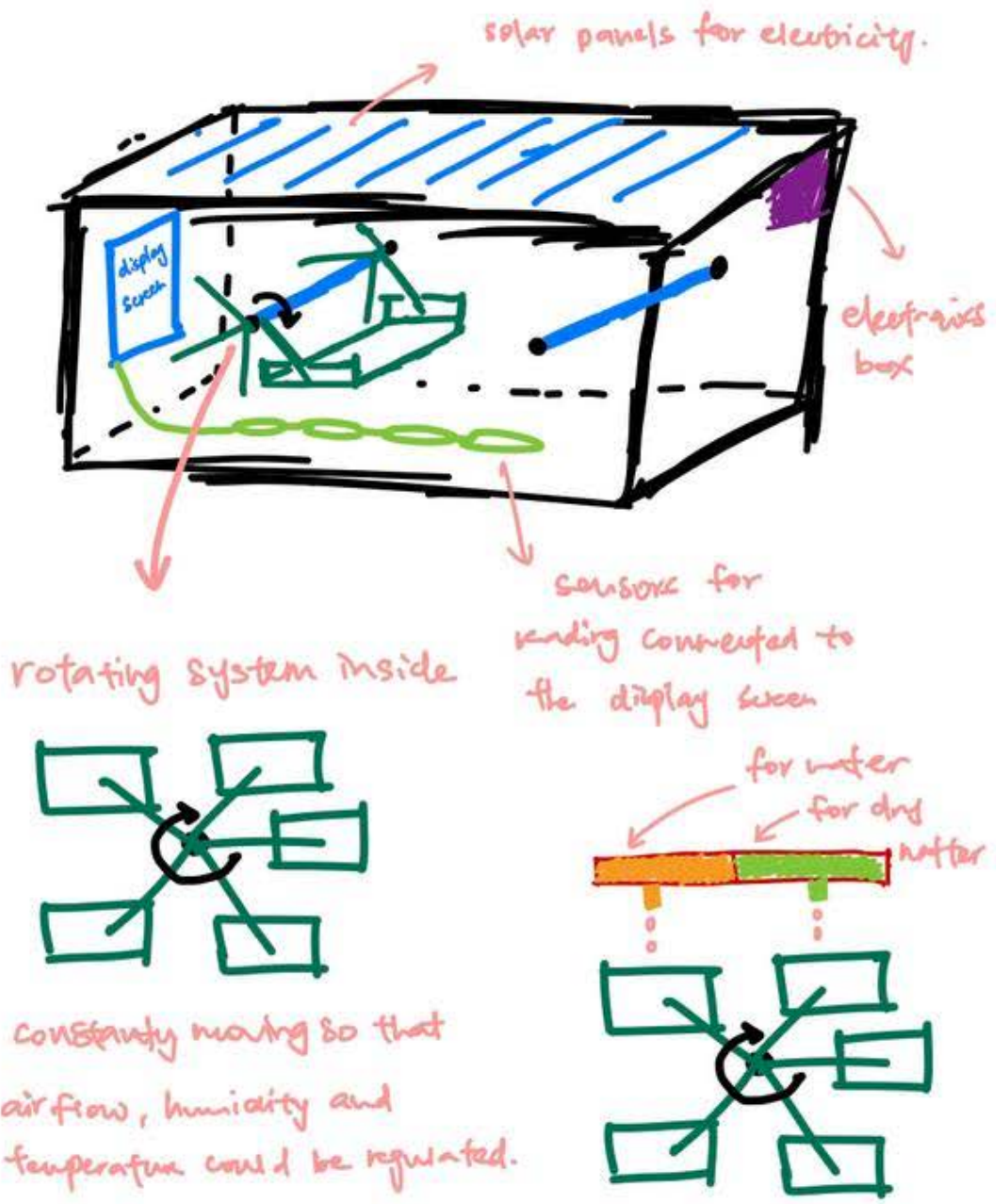
CONCEPT D



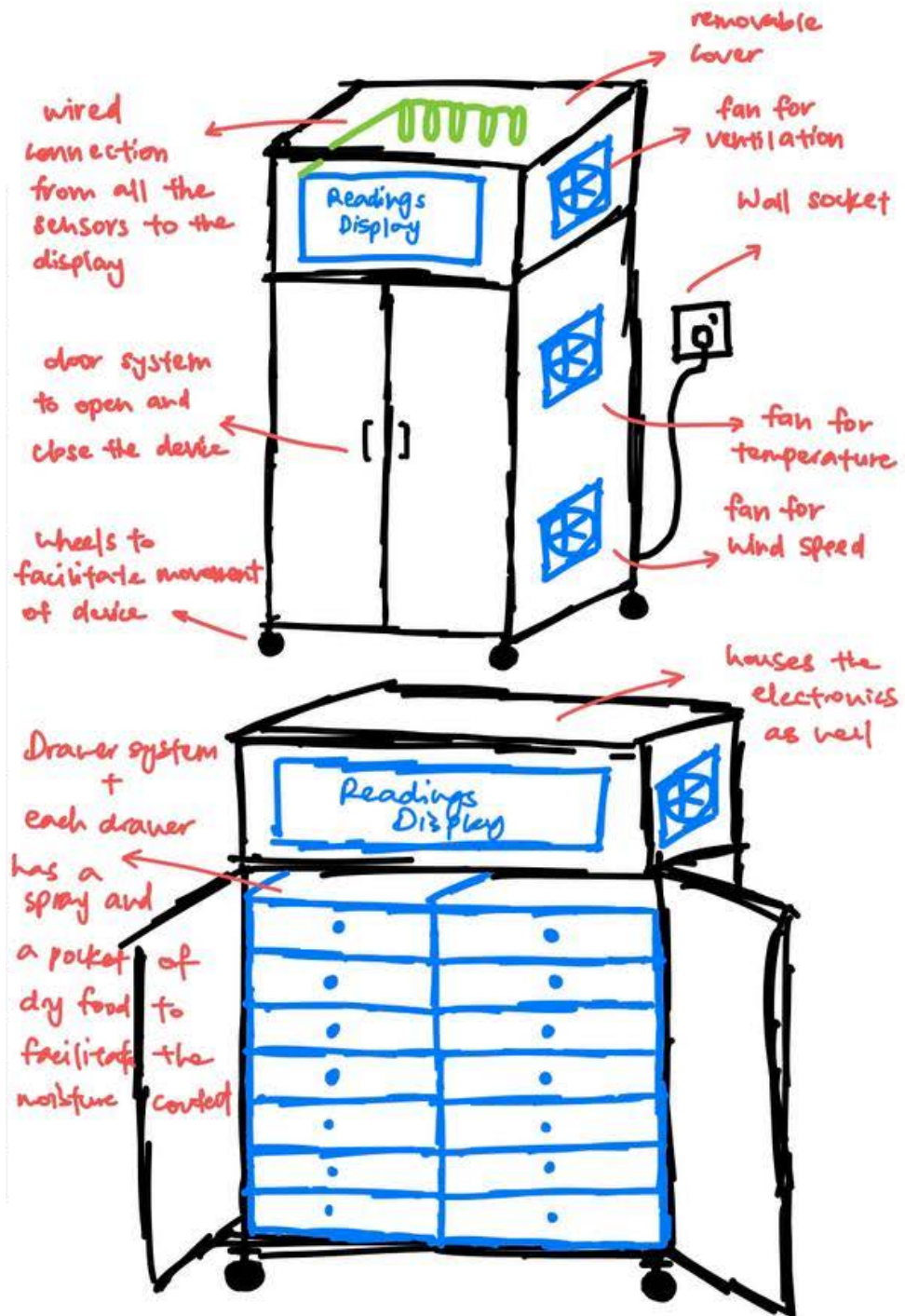
CONCEPT E



CONCEPT F



CONCEPT G



Evaluation Matrix Table for the 7 Concepts

EVALUATION MATRIX Part 1/2									
	Concepts								
		A		B		C		D	
Selection Criteria	Weight	Rating	Weighted Score						
Ease of Portability	7	9	63	9	63	8	56	8	56
Ease of Use	9	5	45	8	72	9	81	8	72
Ease of Maintenance	3	8	24	5	15	9	27	6	18
Compactability	8	8	64	10	80	9	72	7	56
Safety	6	6	36	10	60	9	54	7	42
Ease of Manufacture	4	9	36	7	28	8	32	5	20
Durability	5	8	40	6	30	8	40	6	30
Cost	1	8	8	7	7	5	5	3	3
Energy Efficiency	2	10	20	6	12	9	18	9	18
Total Score		336		367		385		315	
Rank		4		3		1		7	
Continue?									

EVALUATION MATRIX Part 2/2							
	Concepts						
		E		F		G	
Selection Criteria	Weight	Rating	Weighted Score	Rating	Weighted Score	Rating	Weighted Score
Ease of Portability	7	9	63	7	49	8	56
Ease of Use	9	7	63	8	72	9	81
Ease of Maintenance	3	6	18	8	24	6	18
Compactability	8	7	56	9	72	10	80
Safety	6	6	36	7	42	8	48
Ease of Manufacture	4	6	24	5	20	9	36
Durability	5	7	35	7	35	7	35
Cost	1	8	8	5	5	8	8
Energy Efficiency	2	7	14	5	10	8	16
Total Score		317		329		378	
Rank		6		5		2	
Continue?							

Appendix G: User Insights and Design Specifications

TABLE G: User Insights and Design Specifications

Category of User Insight	User Insight	User Needs	Design Specification	Demand/Wish
Environmental and substrate conditions	pH level in the substrate affects the survivability of BSFL and affects its growth. Larval growth performance is optimal at pH values from 6 to 10 [43]	The pH value of the substrate (feed) must be monitored and controlled for the survival of the BSFL and the optimisation of the bioconversion process.	Ability to maintain the substrate pH level to be from 6 to 10	Demand
	"the larval survival rate varied significantly for different moisture levels, with the highest rate at 40–60% moisture content" [44] "The ideal moisture content of food for BSFL is in the range of 70–80%, whereas, the lower threshold of that is likely between 40 and 55%" [45]	The moisture content in the substrate must be monitored and controlled for the survival of the BSFL and the optimisation of the bioconversion process .	Ability to maintain the substrate moisture level to be from 40% to 80%	Demand
	"when the temperature rose beyond 47 °C, the larval survival rate would fall rapidly"	The substrate temperature must be monitored and controlled for the survival of the BSFL and the optimisation of the bioconversion	Ability to maintain the substrate temperature to be within 25°C to 47°C	Demand

	<p>And “the temperature should be kept at around 35 °C because it is the optimal feeding temperature for BSF larvae” [44]</p> <p>The BSFL bioconversion worked well even when substrate temperature reaches 25°C (A. Fuhrmann, Research student at SEC, personal communication, August 18, 2023)[44]</p>	<p>process .</p>		
	<p>“Across the different phenotypes, the optimum temperature range required for the growth of BSFL has been reported between 25°C to 30°C” [32]</p> <p>“The time needed for larval development decreased gradually with the increasing temperatures and was the shortest at 30 °C for the SG-fed larvae and 35 °C for the CD-fed larvae”[46]</p>	<p>The air temperature in the reactor must be monitored and controlled for the survival of the BSFL and the optimisation of the bioconversion process.</p>	<p>Ability to maintain the internal air temperature of the reactor to be within 25°C to 35°C</p>	Demand
	<p>“with an increase in relative humidity, the mortality of the BSFL decreases. The mortality was 62, 26, and 3% at a relative humidity of 25, 40, and 70%, respectively” [32]</p>	<p>The relative humidity of the air in the reactor must be monitored and controlled for the survival of the BSFL and the optimisation of the bioconversion process.</p>	<p>Ability to maintain the relative humidity in the reactor to be \geq 40%</p>	Demand
	<p>Excessive buildup of CO₂ can be toxic and suffocating to the BSFL (A. Fuhrmann, Research student at SEC, personal communication, August 18, 2023)</p>	<p>The concentration of CO₂ must be monitored and controlled, excessive buildup of the gas can be toxic and</p>	<p>Prevent accumulation of CO₂</p>	Demand

		suffocating to the BSFL		
	Excessive buildup of CH ₄ can be toxic and suffocating to the BSFL (A. Fuhrmann, Research student at SEC, personal communication, August 18, 2023)	The concentration of CH ₄ must be monitored and controlled, excessive buildup of the gas can be toxic and suffocating to the BSFL	Prevent accumulation of CH ₄	Demand
	Excessive buildup of NH ₃ can be toxic and suffocating to the BSFL (A. Fuhrmann, Research student at SEC, personal communication, August 18, 2023)	The concentration of NH ₃ must be monitored and controlled, excessive buildup of the gas can be toxic and suffocating to the BSFL	Prevent accumulation of NH ₃	Demand
	Sufficient air exchange between the air in the reactor and the surrounding air to aid in maintaining suitable conditions for the BSFL survivability and effective bioconversion in the reactor (A. Fuhrmann, Research student at SEC, personal communication, August 18, 2023)	Minimum air exchange capacity of 330m ³ h ⁻¹ for every 1m ³ of internal reactor volume (Derivations can be found in Appendix H)	Minimum air exchange capacity of 330m ³ h ⁻¹ for every 1m ³ of internal reactor volume (Derivations can be found in Appendix H)	Demand
Mechanical Design	Current methods of loading and unloading of the food waste trays onto and off the bioconversion racks are very strenuous for the SEC researchers (A. Fuhrmann, Research student at SEC, personal	Current methods of loading and unloading of the food waste trays onto and off the bioconversion racks are very strenuous for the SEC researchers	Less strenuous loading and unloading of food waste trays onto the bioconversion racks	Wish

	communication, August 18, 2023)			
	A portable reactor will enable easier implementation of an on-site reactor for food waste bioconversion using BSFL due to the smaller space each reactor occupies on-site and the ease of transport to the food waste source	A portable reactor will enable easier implementation of an on-site reactor for food waste bioconversion using BSFL due to the smaller space each reactor occupies on-site and the ease of transport to the food waste source.	Maximum width of 0.85m [47] (Derivations can be found in Appendix I)	Wish
			Maximum depth of 1.2m [47] (Derivations can be found in Appendix I)	Wish
			Maximum height of 2m [47] (Derivations can be found in Appendix I)	Wish
			Maximum mass of 400 kg [48] (Derivations can be found in Appendix I)	Wish

Appendix H: Minimum air exchange capacity required of a food waste bioconversion using BSFL reactor

SEC's reactor specifications

- Air exchange range: From 30 to 110 $m^3 h^{-1}$
- Interior reactor body volume: 0.332 m^3

Minimum Air exchange Capacity Required

$$\begin{aligned} &= \frac{(Higher\ end\ of\ SEC\ reactor\ air\ exchange\ range)}{(Interior\ reactor\ body\ volume\ of\ SEC\ reactor)} \\ &= \frac{110\ m^3\ h^{-1}}{0.332\ m^3} \\ &= 331.325\ m^3\ h^{-1} \end{aligned}$$

The minimum air exchange capacity required of a reactor is approximately $330m^3h^{-1}$ for every $1m^3$ of internal reactor volume.

Appendix I: Derivation of Size Constraints

The sizing constraints of the width, depth and height were determined from Singapore's Building and Construction Authority's latest Code On Accessibility in the Built Environment 2019 which states the requirements of pathways, stairs, doors and lifts.

While the mass constraint was estimated based on an empty vending machine weight. This is due to the aim to develop a portable reactor and given that vending machines are heavy-weight and portable, its empty weight would be a reasonable gauge on the maximum weight our reactor can be at and to be portable. The sizing constraints considered are listed in TABLE I.

TABLE I: Summary of Sizing Constraints

Summary of Sizing Constraints			
Constraint Categories	Constraints	Details of Constraints	Overall Constraints

Width [47]	Corridors	Maximum of 1.2m	Maximum of 0.85m
	Doorways	Maximum of 0.85m	
	Lifts	Maximum of 1.2m	
	Stairs	Maximum of 0.9m	
Depth [47]	Lifts	Maximum of 1.2m	Maximum of 1.2m
Height [47]	Headroom	Maximum of 2m	Maximum of 2m
Mass	Mass	Maximum of 400kg	Maximum of 400kg

Corridor

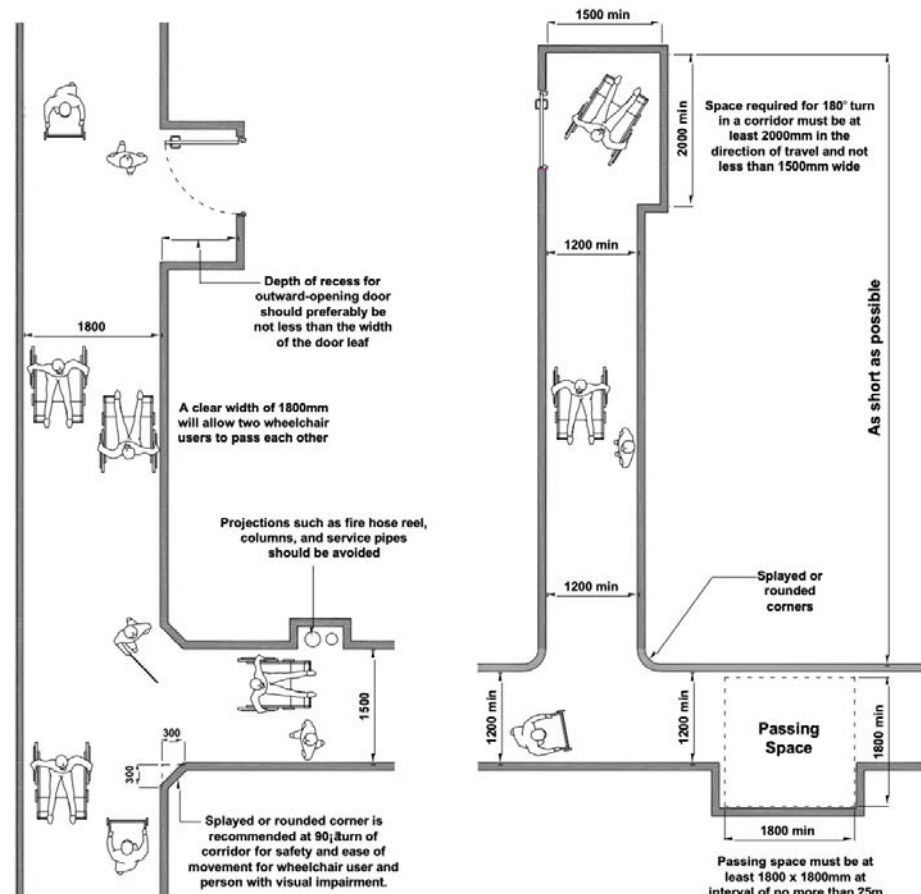
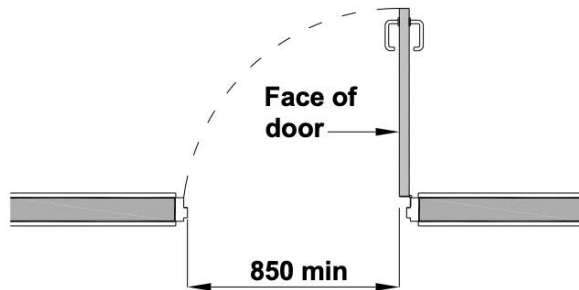


FIGURE I - 1: Singapore's Building and Construction Authority (BCA)'s Dimensional Requirements for
Corridors [47]

Doorways



(a) Sliding/automatic door



(b) Swing Door



(c) Folding Door

FIGURE I - 2: BCA's Dimensional Requirements for Doorways Width [47]

Lifts

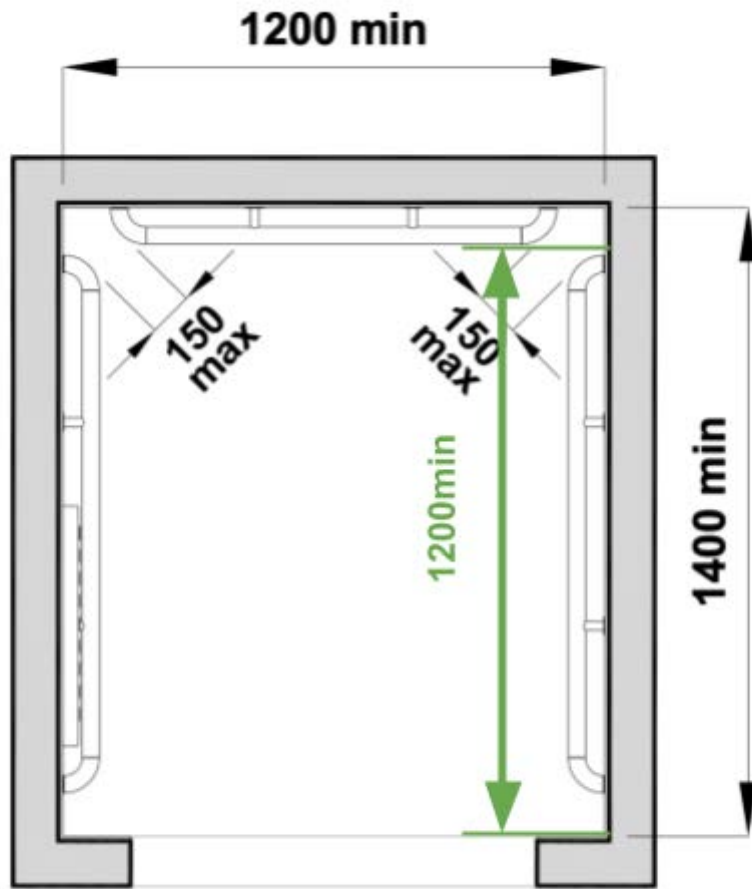


FIGURE I - 3: BCA's Dimensional Requirements for Lifts Width and Depth. Adapted from [47]

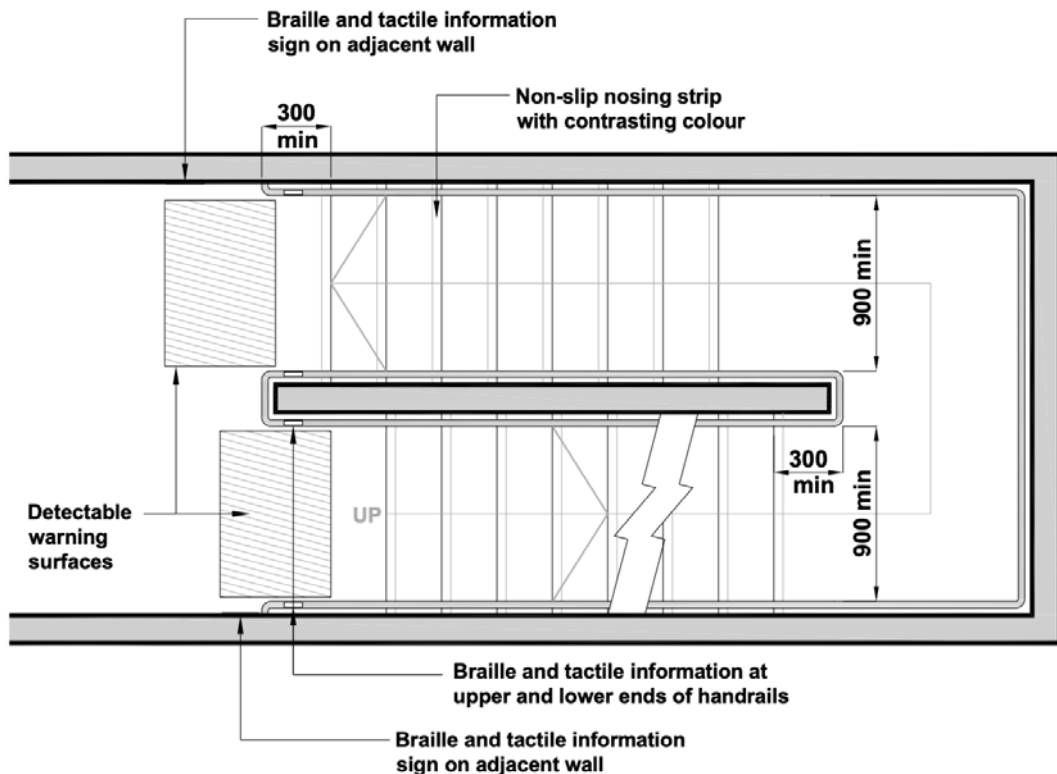


FIGURE I -4: BCA's Dimensional Requirements for Stairs Width [47]

Appendix J : Derivations used for Sizing of our reactor

Appendix J Part 1: Derivation of Amount of Food Waste

- Based on Singapore food court and hawker centre' staff, the average amount of food waste per food establishment in a day:

1 Full National Environment Agency (NEA) Mobile Garbage Bin per Food Court per Day

- According to NEA, a NEA Mobile Food Waste Garbage Bin is the 120L SS-EN840 Mobile Garbage Bin. Each bin has a 120 litres capacity.
 - Sidenote: 120 litres of food waste is approximately equivalent to 120000cm³

- Average Density of Food Waste:

$$1.565 \text{ tonne/m}^3 = \underline{1.565 \text{kg/litre}} [42]$$

Hence, the Mass of Food Waste per food establishment in a day:

$$1 \text{ bin} \times 120 \text{ litres} \times 1.565 \text{kg/litre} = \underline{187.8 \text{kg}}$$

=> Approximately **190kg of food waste per food court/ hawker centre in a day**

Appendix J Part 2: Derivation of Area of Container Base Area Required for Food Waste

- From Appendix J, an average of 120000cm^3 food waste is generated per food establishment in a day.
- 6cm food waste height is recommended by Adrian Fuhrmann, a laboratory staff at SEC.
- Hence, a container base area of $120000/6 = 20000 \text{cm}^2 = 2 \text{m}^2$ is required for food waste generated per food establishment in a day.

Appendix K : Evaluation Matrix Table of Ventilation System's 5 Design

Configurations

TABLE K: Evaluation Matrix Table of the 5 ventilation system design configurations

EVALUATION MATRIX	
	Concepts

		A		B		C		D		E	
Selection Criteria	Weight	Rating	Weighted Score								
Ease of achieving sufficient airflow	10	8	80	5	50	10	100	9	90	9	90
Ease of Use	8	5	40	7	56	1	8	4	32	4	32
Ease of Maintenance	10	5	50	5	50	1	10	4	40	4	40
Safety	6	5	30	3	18	2	12	5	30	4	24
Ease of Assembling	7	4	28	3	21	2	14	4	28	4	28
Cost	4	5	20	5	20	3	12	5	20	5	20
Energy Efficiency	4	6	24	8	32	4	16	6	24	6	24
Total Score		272		247		172		264		258	
Rank		1		4		5		2		3	
Continue?											

Appendix L: Derivation of the required air exchange rate of our reactor

Interior reactor body volume of our reactor

$$= 0.845 \times 0.56 \times 1.75 \text{ m}^3$$

$$= 0.828 \text{ m}^3$$

Required Rate of Air exchange of our reactor

$$= \frac{(\text{Higher end of SEC reactor air exchange range})}{(\text{Interior reactor body volume of SEC reactor})} \times (\text{Interior reactor body volume of our reactor})$$

$$= \frac{110 \text{ m}^3 \text{ h}^{-1}}{0.332 \text{ m}^3} \times 0.828 \text{ m}^3$$

$$= 274.337 m^3 h^{-1}$$

The required air exchange rate of our reactor is determined to be $274.337 m^3 h^{-1}$

Appendix M: Average velocity of exit airflow for various configurations

TABLE M - 1: Calculation of average velocity of exit airflow of the half-fan spacing configuration

Velocity (m/s)	Number of Rectangles	Calculations (3dp)
1.578 - 2.367	20	$[(1.578 + 2.367)/2]*20 = 39.45$
0.789 - 1.578	77	$[(0.789 + 1.578)/2]*77 = 91.1295$
0 - 0.789	29	$[(0 + 0.789)/2]*29 = 11.4405$
		= 142.02
<hr/>		
Total Number of Rectangles (Cross-sectional Area of Chimney Top)	126	
Average Velocity	1.127 m/s = 4057.197 m/h	

TABLE M - 2: Calculation of average velocity of exit airflow

of the half-fan spacing configuration with edited shape fans

Velocity (m/s)	Number of Rectangles	Calculations (rounded off to 3dp)
1.501 - 1.689	20	$[(1.501 + 1.689)/2]*20 = 31.900$
1.314 - 1.501	31	$[(1.314 + 1.501)/2]*31 = 43.633$
1.126 - 1.314	20	$[(1.126 + 1.314)/2]*20 = 24.400$
0.938 - 1.126	13	$[(0.938 + 1.126)/2]*13 = 12.201$
0.751 - 0.938		

0.563 - 0.751	15.5	$[(0.375 + 0.751)/2]*15.5 = 8.727$	
0.375 - 0.563			
0.188 - 0.375	0.5	$[(0 + 0.375)/2]*0.5 = 0.094$	
0 - 0.188			
		Total: 120.955	
<hr/>			
Total Number of Rectangles (Cross-sectional Area of Chimney Top)	100		
Average Velocity	$120.955 / 100$ $= 1.210 \text{ m/s}$ $= 4356 \text{ m/h}$		

TABLE M - 3: Calculation of average velocity of exit airflow
of the half-fan spacing configuration with 50 mm fan tubes

Velocity (m/s)	Number of Rectangles	Calculations (3dp)
2.178 - 2.451	0	$[(2.178 + 2.451)/2]*0 = 0$
1.906 - 2.178	7	
1.634 - 1.906		$[(1.634 + 2.178)/2]*7 = 13.342$
1.361 - 1.634	37	$[(1.361 + 1.634)/2]*37 = 55.408$
1.089 - 1.361	32	
0.817 - 1.089		$[(0.817 + 1.361)/2]*32 = 34.848$
0.545 - 0.817	13	$[(0.545 + 0.817)/2]*13 = 8.853$
0.272 - 0.545	6	$[(0.272 + 0.545)/2]*6 = 2.451$
0 - 0.272	0	$[(0 + 0.272)/2]*0 = 0$
		Total: 114.902

Total Number of Rectangles (Cross-sectional Area of Chimney Top)	95	
Average Velocity	$114.902 / 95$ = 1.209 m/s = 4352.4 m/h	

Appendix N: Ventilation system testing - Chimney outflow results

- 1) For full-fan spacing configuration (Tested with PWM @ 100%, 60%, 40%, 20% and 10%)

PWM @ 100% (255)													
Probe Location/ Reading	Min Reading	Max Reading	Average	Reading 1	Reading 2	Reading 3	Reading 4	Reading 5	Reading 6	Reading 7	Reading 8	Reading 9	Reading 10
L1	1.46	3.43	2.56	1.88	3.41	3.31	2.27	1.60	3.05	2.75	2.94	2.65	1.77
L2	0.63	1.56	1.21	0.78	0.82	1.54	1.33	1.40	1.51	1.48	1.06	0.68	1.50
L3	1.47	3.35	2.10	2.43	2.26	1.59	3.24	1.92	1.54	2.18	2.05	2.15	1.65
R1	3.88	4.84	4.30	4.52	3.98	3.96	4.34	4.63	4.10	4.55	3.88	4.36	4.69
R2	1.78	3.64	2.43	3.21	3.01	2.32	2.71	1.82	2.42	2.03	2.23	2.61	1.92
R3	3.70	4.77	4.30	3.79	4.56	4.65	4.64	4.39	4.19	3.74	4.27	4.23	4.58

PWM @ 60% (153)													
Probe Location/ Reading	Min Reading	Max Reading	Average	Reading 1	Reading 2	Reading 3	Reading 4	Reading 5	Reading 6	Reading 7	Reading 8	Reading 9	Reading 10
L1	1.11	2.99	1.94	2.72	1.89	1.99	2.67	1.17	1.31	2.47	1.70	2.22	1.20
L2	0.39	1.91	1.01	1.40	0.82	0.99	1.32	1.14	0.71	1.71	0.83	0.79	0.40
L3	0.67	2.54	1.64	2.34	0.75	1.64	2.36	2.37	1.96	0.75	2.38	1.02	0.79
R1	2.70	3.20	2.95	2.86	3.02	2.78	3.06	2.78	3.00	3.15	2.84	2.91	3.14
R2	2.10	3.07	2.61	2.99	3.00	2.12	2.60	2.27	2.33	2.31	2.76	2.76	3.00
R3	2.87	3.27	3.04	2.92	3.20	3.11	3.00	3.16	2.90	2.92	2.91	3.19	3.13

PWM @ 40% (102)													
Probe Location/ Reading	Min Reading	Max Reading	Average	Reading 1	Reading 2	Reading 3	Reading 4	Reading 5	Reading 6	Reading 7	Reading 8	Reading 9	Reading 10
L1	0.82	2.10	1.59	1.79	0.82	1.92	1.18	1.49	1.83	1.41	1.85	1.88	1.73
L2	0.24	0.90	0.56	0.53	0.83	0.31	0.57	0.31	0.87	0.53	0.76	0.39	0.47
L3	0.71	2.13	1.38	1.38	1.10	1.13	1.58	1.68	1.85	1.90	0.79	1.04	1.38
R1	2.57	3.01	2.80	2.94	2.82	2.73	2.72	2.59	2.92	2.65	2.73	2.91	2.97
R2	1.63	2.98	2.17	1.75	2.10	2.12	2.51	2.75	2.00	1.99	2.57	2.20	1.68
R3	2.47	3.00	2.74	2.64	2.88	2.80	2.66	2.69	2.66	2.47	2.81	2.81	2.96

PWM @ 20% (51)													
Probe Location/ Reading	Min Reading	Max Reading	Average	Reading 1	Reading 2	Reading 3	Reading 4	Reading 5	Reading 6	Reading 7	Reading 8	Reading 9	Reading 10
L1	1.48	2.34	1.80	1.57	1.66	1.76	2.01	1.68	1.75	2.34	1.57	2.01	1.68
L2	0.35	1.53	0.97	0.97	0.47	0.68	1.07	0.98	1.36	0.85	0.78	1.11	1.40
L3	0.64	2.09	1.20	1.69	1.03	1.27	1.12	0.89	1.67	0.80	0.81	1.60	1.12
R1	2.36	2.87	2.61	2.62	2.63	2.71	2.54	2.52	2.54	2.80	2.61	2.73	2.41
R2	1.43	2.47	1.78	1.58	1.72	1.55	2.23	1.97	1.50	1.88	1.52	2.02	1.86
R3	2.11	2.81	2.46	2.59	2.63	2.74	2.31	2.68	2.60	2.35	2.16	2.34	2.19

PWM @ 10% (25)													
Probe Location/ Reading	Min Reading	Max Reading	Average	Reading 1	Reading 2	Reading 3	Reading 4	Reading 5	Reading 6	Reading 7	Reading 8	Reading 9	Reading 10
L1	1.00	2.43	1.81	2.19	2.20	1.45	2.33	1.66	1.48	2.20	1.00	1.33	2.24
L2	0.24	1.11	0.62	0.46	0.50	0.72	0.61	0.45	0.91	0.59	0.36	1.10	0.54
L3	0.84	2.52	1.73	1.72	2.32	1.25	1.54	2.29	2.41	1.46	1.48	1.82	1.01
R1	2.14	2.89	2.47	2.22	2.72	2.66	2.33	2.83	2.56	2.43	2.50	2.18	2.25
R2	1.12	2.44	1.88	1.14	1.15	2.26	2.03	2.37	1.88	2.10	2.10	2.40	1.36
R3	2.47	2.87	2.65	2.75	2.61	2.74	2.61	2.61	2.68	2.73	2.51	2.66	2.62

PWM @ (15)													
Probe Location/ Reading	Min Reading	Max Reading	Average	Reading 1	Reading 2	Reading 3	Reading 4	Reading 5	Reading 6	Reading 7	Reading 8	Reading 9	Reading 10
L1	0.84	2.06	1.62	2.05	2.02	1.16	1.64	1.09	1.86	1.96	1.37	2.02	1.01
L2	0.18	1.01	0.57	0.59	0.88	0.77	0.23	0.30	0.52	0.61	0.64	0.96	0.21
L3	0.65	2.10	1.26	0.84	1.31	1.13	1.54	1.82	0.72	1.25	1.13	1.51	1.40
R1	2.48	2.97	2.70	2.63	2.66	2.67	2.72	2.85	2.78	2.62	2.56	2.93	2.53
R2	1.58	2.92	2.33	2.00	2.44	1.97	2.58	2.61	2.36	2.30	2.39	2.72	1.92
R3	2.42	2.75	2.54	2.71	2.52	2.51	2.48	2.49	2.44	2.66	2.54	2.56	2.52

PWM @ (7)													
Probe Location/ Reading	Min Reading	Max Reading	Average	Reading 1	Reading 2	Reading 3	Reading 4	Reading 5	Reading 6	Reading 7	Reading 8	Reading 9	Reading 10
L1	0.73	1.99	1.18	1.62	1.48	1.20	1.45	1.07	1.08	0.94	0.78	1.08	1.05
L2	0.22	0.91	0.63	0.65	0.88	0.36	0.83	0.78	0.75	0.34	0.55	0.69	0.47
L3	0.68	2.03	1.52	1.90	1.97	1.51	1.59	1.41	1.26	0.93	0.78	1.87	1.97
R1	2.53	3.00	2.70	2.82	2.73	2.55	2.90	2.55	2.79	2.80	2.66	2.58	2.64
R2	1.52	2.85	1.95	1.64	2.11	2.54	1.91	2.61	1.54	2.09	1.59	1.74	1.79
R3	2.41	2.98	2.64	2.70	2.72	2.85	2.77	2.55	2.46	2.59	2.75	2.51	2.48

PWM @ (4)													
Probe Location/ Reading	Min Reading	Max Reading	Average	Reading 1	Reading 2	Reading 3	Reading 4	Reading 5	Reading 6	Reading 7	Reading 8	Reading 9	Reading 10
L1	0.77	2.00	1.47	1.76	1.59	1.23	1.79	1.34	1.90	0.86	0.84	1.98	1.42
L2	0.21	0.87	0.51	0.44	0.62	0.35	0.40	0.54	0.56	0.69	0.62	0.61	0.24
L3	0.69	2.11	1.38	1.58	1.87	1.35	0.81	1.64	1.18	1.52	1.47	1.13	1.24
R1	2.40	2.99	2.78	2.94	2.95	2.88	2.66	2.81	2.66	2.60	2.91	2.59	2.84
R2	1.60	2.72	2.12	1.60	2.33	2.12	2.54	2.65	1.70	1.98	1.69	2.67	1.92
R3	2.43	2.93	2.66	2.71	2.77	2.55	2.86	2.64	2.51	2.74	2.46	2.68	2.65

2) For full-fan spacing configuration with 50 mm fan tube (Tested with PWM @ 100%, 60%, 40% and 20%)

PWM @ 100% (255)													
Probe Location/ Reading	Min Reading	Max Reading	Average	Reading 1	Reading 2	Reading 3	Reading 4	Reading 5	Reading 6	Reading 7	Reading 8	Reading 9	Reading 10
L1	1.78	3.38	2.59	2.95	3.05	2.59	2.18	1.98	2.05	1.99	2.76	3.19	3.18
L2	0.88	2.95	1.72	2.07	2.14	1.92	0.98	0.96	1.69	1.01	2.00	2.22	2.24
L3	0.86	2.81	1.83	1.32	2.36	2.28	1.83	0.96	1.08	1.66	2.61	1.70	2.45
R1	3.73	4.78	4.29	3.98	4.63	4.23	4.37	3.94	3.97	4.39	4.59	4.11	4.73
R2	3.12	4.24	3.75	4.09	4.01	3.79	3.51	3.72	3.24	3.91	3.87	4.12	3.30
R3	3.74	4.35	4.08	4.26	4.02	4.28	3.88	4.20	4.11	4.25	4.14	3.79	3.91

PWM @ 60% (153)													
Probe Location/ Reading	Min Reading	Max Reading	Average	Reading 1	Reading 2	Reading 3	Reading 4	Reading 5	Reading 6	Reading 7	Reading 8	Reading 9	Reading 10
L1	0.66	2.31	1.55	1.43	1.91	1.83	1.37	1.07	1.37	1.39	2.05	1.88	1.17
L2	0.28	1.74	1.25	1.42	1.57	1.61	1.33	1.35	1.06	1.47	0.80	1.08	0.82
L3	0.40	2.35	1.16	0.61	1.18	1.35	1.39	1.45	1.65	0.80	0.81	1.06	1.27
R1	2.50	3.16	2.74	3.02	2.58	2.61	2.73	2.82	2.86	2.72	2.56	3.00	2.50
R2	1.90	2.85	2.37	2.30	2.83	2.70	2.04	2.32	1.94	2.82	2.08	2.29	2.42
R3	2.38	3.13	2.72	2.65	2.55	2.64	2.67	2.69	2.45	3.09	2.96	2.63	2.88

PWM @ 40% (102)													
Probe Location/ Reading	Min Reading	Max Reading	Average	Reading 1	Reading 2	Reading 3	Reading 4	Reading 5	Reading 6	Reading 7	Reading 8	Reading 9	Reading 10
L1	0.92	2.09	1.47	1.50	1.16	1.86	1.79	1.77	1.27	1.34	1.18	1.27	1.52
L2	0.55	1.51	1.19	1.45	1.19	0.79	1.03	1.06	1.15	1.36	1.33	1.17	1.39
L3	0.83	2.16	1.56	1.73	2.07	1.01	2.02	1.76	1.49	1.41	1.10	1.29	1.76
R1	1.97	2.60	2.35	2.30	2.48	2.20	2.29	2.26	2.56	2.46	2.27	2.19	2.44
R2	1.49	2.64	2.01	1.86	1.88	1.70	1.53	2.20	1.74	2.16	2.17	2.57	2.27
R3	1.84	2.54	2.31	2.46	2.48	2.50	2.31	2.34	1.90	2.03	2.47	2.39	2.26

PWM @ 20% (51)													
Probe Location/ Reading	Min Reading	Max Reading	Average	Reading 1	Reading 2	Reading 3	Reading 4	Reading 5	Reading 6	Reading 7	Reading 8	Reading 9	Reading 10
L1	0.53	1.85	1.10	0.71	0.70	0.64	0.54	1.69	1.49	1.51	0.99	0.97	1.77
L2	0.44	1.66	0.96	1.04	0.45	0.91	0.64	1.01	1.19	1.26	1.12	0.94	1.07
L3	0.51	1.76	0.94	1.25	0.84	0.88	0.65	0.74	0.67	0.97	1.16	0.56	1.64
R1	2.02	2.74	2.50	2.73	2.68	2.09	2.34	2.60	2.66	2.69	2.59	2.04	2.54
R2	1.66	2.57	2.20	1.75	2.13	2.43	2.21	2.12	2.39	2.20	2.00	2.31	2.51
R3	2.06	2.62	2.33	2.12	2.19	2.57	2.20	2.47	2.07	2.44	2.35	2.37	2.48

3) For half-fan spacing configuration (Tested with PWM @ 100%, 60%, 40% and 20%)

PWM @ 100% (255)													
Probe Location/ Reading	Min Reading	Max Reading	Average	Reading 1	Reading 2	Reading 3	Reading 4	Reading 5	Reading 6	Reading 7	Reading 8	Reading 9	Reading 10
L1	1.62	3.35	2.25	2.52	2.23	1.77	2.43	1.81	2.28	2.44	2.35	2.74	1.89
L2	0.99	2.04	1.45	1.84	1.37	1.12	1.05	1.13	1.61	1.71	1.72	1.23	1.76
L3	1.34	3.27	2.52	2.26	3.16	2.86	2.18	1.98	2.35	1.83	3.02	2.33	3.20
R1	2.44	3.92	2.94	2.53	3.25	2.70	3.73	2.49	2.52	2.70	2.98	3.02	3.46
R2	1.33	3.28	2.38	2.44	2.68	1.85	2.05	1.57	2.52	3.27	2.64	3.27	1.49
R3	2.36	2.89	2.64	2.83	2.86	2.87	2.62	2.78	2.46	2.51	2.64	2.38	2.44

PWM @ 60% (153)													
Probe Location/ Reading	Min Reading	Max Reading	Average	Reading 1	Reading 2	Reading 3	Reading 4	Reading 5	Reading 6	Reading 7	Reading 8	Reading 9	Reading 10
L1	1.34	2.47	1.72	1.74	1.86	1.38	1.98	1.43	1.74	1.69	1.78	2.10	1.55
L2	0.94	1.85	1.36	1.24	1.01	1.22	1.40	1.65	1.66	1.43	1.18	1.01	1.76
L3	1.20	2.21	1.76	2.19	1.81	1.53	1.65	1.65	2.03	1.25	1.92	1.60	1.96
R1	2.14	2.38	2.27	2.29	2.32	2.31	2.23	2.25	2.30	2.24	2.21	2.36	2.16
R2	1.04	2.01	1.47	1.95	1.51	1.37	1.45	1.16	1.72	1.33	1.61	1.33	1.26
R3	1.87	2.41	2.23	2.36	2.06	2.31	2.15	2.29	2.41	2.05	2.28	2.16	2.20

PWM @ 40% (102)													
Probe Location/ Reading	Min Reading	Max Reading	Average	Reading 1	Reading 2	Reading 3	Reading 4	Reading 5	Reading 6	Reading 7	Reading 8	Reading 9	Reading 10
L1	1.29	2.10	1.55	1.50	1.48	2.08	1.34	1.37	1.40	1.51	1.79	1.37	1.69
L2	0.92	2.00	1.57	1.60	1.73	1.58	1.58	1.86	0.99	1.42	1.95	1.44	1.52
L3	0.94	2.13	1.45	1.73	0.95	2.07	1.06	1.88	1.83	1.47	1.45	1.07	1.03
R1	1.72	2.40	2.10	2.32	1.86	2.23	2.39	1.75	2.04	2.14	2.18	1.77	2.29
R2	0.98	1.96	1.42	1.36	1.31	1.17	1.03	1.56	1.63	1.87	1.44	1.49	1.37
R3	1.59	2.38	2.04	1.90	1.93	2.37	2.27	1.82	1.76	1.97	2.29	1.72	2.34

PWM @ 20% (51)													
Probe Location/ Reading	Min Reading	Max Reading	Average	Reading 1	Reading 2	Reading 3	Reading 4	Reading 5	Reading 6	Reading 7	Reading 8	Reading 9	Reading 10
L1	1.23	1.79	1.52	1.67	1.43	1.31	1.46	1.36	1.37	1.72	1.69	1.75	1.46
L2	0.95	1.62	1.28	1.34	1.62	1.15	1.10	1.28	1.47	1.35	1.18	0.98	1.29
L3	0.77	1.83	1.40	1.11	1.04	1.78	0.91	1.78	1.68	1.77	1.34	1.27	1.30
R1	1.42	1.98	1.73	1.89	1.93	1.70	1.49	1.72	1.97	1.59	1.62	1.66	1.72
R2	0.92	1.53	1.19	1.25	1.08	1.28	1.02	1.23	1.05	1.00	1.25	1.45	1.32
R3	1.87	2.20	1.98	1.95	2.11	2.01	2.10	1.95	1.97	1.97	1.91	1.99	1.88

4) For half-fan spacing configuration with 50 mm fan tube (Tested with PWM @ 100%, 60%, 40% and 20%)

PWM @ 100% (255)													
Probe Location/ Reading	Min Reading	Max Reading	Average	Reading 1	Reading 2	Reading 3	Reading 4	Reading 5	Reading 6	Reading 7	Reading 8	Reading 9	Reading 10
L1	2.40	3.45	3.08	2.96	2.93	3.08	3.31	3.03	2.49	3.38	3.45	3.38	2.76
L2	1.52	2.11	1.88	1.68	2.08	2.08	1.95	1.83	1.71	1.84	1.88	1.92	1.81
L3	1.75	3.24	2.30	2.85	1.83	2.12	2.37	1.94	1.94	2.31	2.37	2.70	2.53
R1	2.55	3.05	2.74	2.99	2.55	2.66	2.72	2.56	3.02	2.80	2.82	2.67	2.56
R2	1.40	2.38	1.83	1.70	2.24	2.06	1.54	1.51	1.69	1.86	1.64	2.02	2.08
R3	2.75	3.12	2.97	3.06	3.12	2.76	2.81	3.08	2.93	2.89	2.99	3.10	2.94

PWM @ 60% (153)													
Probe Location/ Reading	Min Reading	Max Reading	Average	Reading 1	Reading 2	Reading 3	Reading 4	Reading 5	Reading 6	Reading 7	Reading 8	Reading 9	Reading 10
L1	1.26	2.17	1.64	1.66	1.32	1.80	1.68	1.78	1.86	1.55	1.47	1.36	1.94
L2	0.83	2.06	1.38	1.77	1.48	1.31	1.49	1.38	1.15	1.24	1.10	0.95	1.89
L3	1.00	2.01	1.44	1.24	1.03	1.96	1.18	1.66	1.10	1.95	1.23	1.59	1.42
R1	1.97	2.34	2.11	2.10	2.00	1.97	1.99	2.29	2.10	2.04	2.28	2.28	2.03
R2	0.99	1.82	1.50	1.80	1.72	1.59	1.09	1.43	1.58	1.62	1.09	1.46	1.63
R3	1.43	2.35	1.95	1.91	2.24	1.87	2.27	1.53	1.96	1.96	1.60	2.09	2.08

PWM @ 40% (102)													
Probe Location/ Reading	Min Reading	Max Reading	Average	Reading 1	Reading 2	Reading 3	Reading 4	Reading 5	Reading 6	Reading 7	Reading 8	Reading 9	Reading 10
L1	1.29	2.01	1.61	1.83	1.49	1.72	1.51	1.49	1.82	1.67	1.65	1.39	1.52
L2	0.92	1.95	1.40	1.67	1.16	1.41	1.23	1.08	1.45	1.82	1.21	1.41	1.52
L3	0.94	1.88	1.54	1.27	1.62	1.83	1.37	1.60	1.15	1.68	1.61	1.60	1.68
R1	1.72	2.20	1.95	2.13	1.99	1.72	2.15	1.85	2.12	2.20	1.75	1.76	1.81
R2	0.98	1.78	1.45	1.49	1.21	1.56	1.20	1.31	1.77	1.76	1.55	1.45	1.24
R3	1.59	2.24	1.84	1.83	1.67	2.01	2.06	1.72	1.59	1.76	1.78	1.81	2.22

PWM @ 20% (51)													
Probe Location/ Reading	Min Reading	Max Reading	Average	Reading 1	Reading 2	Reading 3	Reading 4	Reading 5	Reading 6	Reading 7	Reading 8	Reading 9	Reading 10
L1	1.28	1.76	1.50	1.39	1.30	1.64	1.30	1.48	1.53	1.56	1.72	1.47	1.62
L2	1.03	1.70	1.34	1.39	1.05	1.66	1.05	1.63	1.55	1.24	1.36	1.34	1.09
L3	0.87	1.76	1.36	1.62	1.35	1.57	1.35	1.21	0.94	1.54	1.31	1.70	0.99
R1	1.30	1.81	1.54	1.38	1.42	1.67	1.75	1.81	1.32	1.34	1.58	1.48	1.69
R2	0.92	1.62	1.35	1.43	1.53	0.93	1.53	1.27	1.03	1.57	1.49	1.55	1.14
R3	1.73	2.10	1.89	1.98	1.89	1.96	1.76	2.03	1.73	1.78	1.76	1.91	2.07

Appendix O: Ventilation system testing - Fan outlet



FIGURE O: Fan numbering used in data collection

1) For full-fan configuration

FAN 4												
Probe Location: Bottom Part of Fan												
Temperature Range: 29.1 to 29.2 °C												
PWM %/ Reading	MIN	MAX	Reading 1	Reading 2	Reading 3	Reading 4	Reading 5	Reading 6	Reading 7	Reading 8	Reading 9	Reading 10
20.000%	8.13	8.52	8.35	8.37	8.18	8.14	8.27	8.36	8.37	8.30	8.24	8.14
29.803%	8.32	8.65	8.48	8.53	8.46	8.53	8.50	8.42	8.56	8.36	8.43	8.55
40.000%	8.51	8.73	8.58	8.60	8.67	8.52	8.69	8.68	8.64	8.60	8.65	8.59
49.803%	8.81	9.13	8.92	8.82	8.89	9.06	8.99	9.09	8.89	8.98	8.95	9.09
60.000%	9.44	9.81	9.60	9.48	9.45	9.63	9.63	9.59	9.79	9.77	9.65	9.72
69.803%	10.03	10.64	10.46	10.45	10.60	10.60	10.15	10.62	10.37	10.14	10.35	10.25
80.000%	10.96	11.24	11.07	10.99	11.04	11.08	11.02	11.07	11.00	10.96	11.17	11.17
90.196%	11.67	12.32	11.91	11.87	11.93	11.91	11.74	12.08	11.88	12.20	12.20	12.01
100.000%	13.24	13.81	13.52	13.44	13.29	13.63	13.76	13.74	13.70	13.77	13.37	13.76
Main switch (100.00%)	13.35	13.80	13.58	13.36	13.49	13.55	13.77	13.52	13.35	13.37	13.46	13.38
Probe Location: Top Part of Fan												
Temperature Range: 29.1 to 29.2 °C												
PWM %/ Reading	MIN	MAX	Reading 1	Reading 2	Reading 3	Reading 4	Reading 5	Reading 6	Reading 7	Reading 8	Reading 9	Reading 10
20.000%	8.12	8.32	8.14	8.27	8.21	8.28	8.20	8.13	8.16	8.18	8.16	8.16
29.803%	8.38	8.61	8.41	8.50	8.42	8.40	8.52	8.41	8.57	8.38	8.55	8.39
40.000%	8.43	8.78	8.63	8.70	8.70	8.52	8.50	8.72	8.57	8.68	8.46	8.63
49.803%	8.73	9.20	8.81	8.84	8.86	9.04	8.84	8.93	9.02	8.79	9.05	9.01
60.000%	9.38	9.83	9.70	9.48	9.59	9.81	9.59	9.80	9.77	9.38	9.82	9.53
69.803%	10.11	10.59	10.20	10.18	10.46	10.44	10.35	10.34	10.40	10.27	10.34	10.25
80.000%	10.86	11.18	11.18	11.05	10.92	10.98	11.09	11.14	10.90	11.07	11.10	11.10
90.196%	11.46	12.03	11.53	11.93	11.57	11.52	11.76	11.47	11.90	11.93	11.70	11.88
100.000%	12.74	13.64	13.36	13.02	12.81	13.45	13.20	13.50	13.23	13.21	13.64	13.44
Main switch (100.00%)	12.69	13.80	12.75	13.04	12.98	13.23	13.13	13.17	13.19	13.77	13.72	12.85

FAN 5													
Probe Location: Bottom Part of Fan													
Temperature Range: 29.9 to 30.1 °C													
PWM %/ Reading	MIN	MAX	Reading 1	Reading 2	Reading 3	Reading 4	Reading 5	Reading 6	Reading 7	Reading 8	Reading 9	Reading 10	
20.000%	8.24	8.62	8.29	8.59	8.57	8.41	8.41	8.45	8.33	8.25	8.36	8.49	
29.803%	8.47	8.70	8.56	8.66	8.63	8.66	8.52	8.61	8.61	8.50	8.66	8.65	
40.000%	8.55	8.77	8.69	8.66	8.69	8.67	8.75	8.71	8.76	8.66	8.56	8.63	
49.803%	8.94	9.22	9.02	9.00	9.07	9.01	8.98	9.03	8.98	9.09	8.95	9.01	
60.000%	9.58	9.94	9.66	9.78	9.93	9.60	9.72	9.90	9.85	9.62	9.65	9.89	
69.803%	10.56	10.79	10.57	10.59	10.75	10.77	10.74	10.67	10.75	10.61	10.75	10.74	
80.000%	11.52	11.78	11.56	11.58	11.63	11.63	11.70	11.64	11.71	11.74	11.70	11.69	
90.196%	12.49	12.78	12.76	12.60	12.63	12.73	12.62	12.62	12.58	12.55	12.66	12.73	
100.000%	13.32	13.75	13.50	13.52	13.38	13.57	13.67	13.40	13.48	13.72	13.45	13.43	
Main switch (100.00%)	13.29	13.78	13.57	13.40	13.43	13.33	13.51	13.53	13.30	13.59	13.31	13.56	
Probe Location: Top Part of Fan													
Temperature Range: 29.9 to 30.1 °C													
PWM %/ Reading	MIN	MAX	Reading 1	Reading 2	Reading 3	Reading 4	Reading 5	Reading 6	Reading 7	Reading 8	Reading 9	Reading 10	
20.000%	7.63	7.89	7.83	7.82	7.88	7.72	7.83	7.88	7.74	7.82	7.71	7.74	
29.803%	7.68	7.94	7.92	7.73	7.90	7.88	7.81	7.81	7.86	7.78	7.69	7.70	
40.000%	7.84	8.01	7.89	7.98	7.84	7.93	7.87	7.95	7.90	7.87	7.89	8.01	
49.803%	7.93	8.53	8.44	8.32	8.38	8.39	7.97	8.13	8.29	8.35	8.49	8.14	
60.000%	8.83	9.11	9.08	9.10	8.86	9.02	8.88	8.90	8.88	9.00	8.84	9.00	
69.803%	9.34	9.73	9.63	9.61	9.68	9.62	9.52	9.36	9.50	9.73	9.60	9.34	
80.000%	10.22	10.64	10.43	10.55	10.61	10.63	10.59	10.26	10.26	10.58	10.56	10.50	
90.196%	10.91	11.20	11.06	11.01	11.19	11.20	11.06	11.14	10.92	11.04	10.93	10.97	
100.000%	12.27	12.83	12.82	12.78	12.56	12.61	12.81	12.52	12.40	12.68	12.70	12.66	
Main switch (100.00%)	12.31	12.78	12.47	12.60	12.70	12.36	12.41	12.64	12.40	12.38	12.41	12.45	

FAN 6													
Probe Location: Bottom Part of Fan													
Temperature Range: 30.1 to 30.2 °C													
PWM %/ Reading	MIN	MAX	Reading 1	Reading 2	Reading 3	Reading 4	Reading 5	Reading 6	Reading 7	Reading 8	Reading 9	Reading 10	
20.000%	8.44	8.74	8.71	8.48	8.61	8.54	8.45	8.49	8.49	8.65	8.50	8.61	
29.803%	8.53	8.88	8.59	8.63	8.63	8.78	8.77	8.74	8.69	8.62	8.53	8.83	
40.000%	8.72	8.91	8.78	8.86	8.74	8.87	8.86	8.76	8.91	8.77	8.74	8.75	
49.803%	9.21	9.64	9.27	9.38	9.38	9.59	9.35	9.28	9.35	9.57	9.45	9.59	
60.000%	9.81	10.16	10.03	10.12	9.97	10.02	9.90	9.94	9.97	9.83	9.93	9.97	
69.803%	10.52	10.78	10.69	10.66	10.76	10.73	10.68	10.73	10.56	10.56	10.61	10.73	
80.000%	11.20	11.63	11.34	11.48	11.44	11.59	11.34	11.58	11.46	11.35	11.21	11.34	
90.196%	12.47	12.84	12.54	12.63	12.52	12.64	12.48	12.82	12.47	12.76	12.54	12.57	
100.000%	13.68	14.01	13.89	13.95	13.73	13.93	13.73	13.89	13.98	13.90	13.89	13.70	
Main switch (100.00%)	13.53	13.92	13.77	13.76	13.60	13.61	13.69	13.76	13.59	13.79	13.82	13.67	
Probe Location: Top Part of Fan													
Temperature Range: 30.1 to 30.2 °C													
PWM %/ Reading	MIN	MAX	Reading 1	Reading 2	Reading 3	Reading 4	Reading 5	Reading 6	Reading 7	Reading 8	Reading 9	Reading 10	
20.000%	8.29	8.73	8.71	8.72	8.39	8.30	8.60	8.52	8.31	8.32	8.46	8.54	
29.803%	8.43	8.91	8.83	8.91	8.59	8.65	8.53	8.86	8.54	8.45	8.63	8.90	
40.000%	8.64	9.01	8.97	8.72	8.71	8.74	8.96	8.72	8.78	8.73	8.79	8.65	
49.803%	8.99	9.65	9.36	9.38	9.03	9.50	9.63	9.28	9.10	9.26	9.60	9.44	
60.000%	9.78	10.23	9.91	9.83	10.17	10.13	10.10	10.22	10.11	9.96	10.01	10.16	
69.803%	10.41	10.95	10.84	10.80	10.43	10.44	10.49	10.89	10.43	10.46	10.78	10.49	
80.000%	11.22	11.54	11.33	11.35	11.36	11.34	11.43	11.42	11.41	11.43	11.35	11.48	
90.196%	12.08	12.74	12.30	12.25	12.19	12.34	12.64	12.32	12.28	12.32	12.66	12.13	
100.000%	13.59	13.86	13.69	13.79	13.70	13.80	13.75	13.77	13.72	13.80	13.64	13.78	
Main switch (100.00%)	13.33	13.79	13.36	13.34	13.47	13.46	13.43	13.37	13.35	13.35	13.57	13.65	